Tor Helge Dokka

Modelling of Indoor Air Quality in residential and commercial buildings

NTNU Trondheim
Norges teknisk-naturvitenskapelige universitet

Doktor ingeniøravhandling 2000:73
Institutt for industriell økonomi og teknologiledelse

Modelling of Indoor Air Quality in residential and commercial buildings

by

Tor Helge Dokka

Department of Industrial Economics and Industrial Management
Norwegian University of Science and Technology

Doctoral thesis
Trondheim, August 2000

List of papers

The thesis is based on the following original papers:

I: Dokka T.H., Bjørseth O., Hanssen S.O. "EnviSim; A windows application for simulation of IAQ", *Proceedings Indoor Air 96'* Nagoya, Volume 2, pp. 491-496.

II : Dokka T.H., Jørgensen R.B., Bjørseth O., Malvik B. "Comparison of field experiments in a refurbished bedroom with small chamber experiments", *Proceedings Indoor Air '99*, Edinburgh, Volume 5, pp. 93-98.

III : Jørgensen R.B., Dokka T.H., Bjørseth O. "Investigations of the interaction between different ventilation strategies and the adsorption/desorption of VOCs on material surfaces ", *Proceedings Indoor Air '99*, Edinburgh, Volume 1, pp.402-407.

IV : Jørgensen R.B., Dokka T.H., Bjørseth O. "Introduction of a sink-diffusion model to describe the interaction between VOCs and material surfaces", *Indoor Air*, Volume 10, No. 1, March 2000 : 27-38.

V : Dokka T.H., Tjeelflaat P.O., " Simplified models for prediction of vertical contaminant and temperature stratification in displacement ventilated rooms; Part 1 : derivation ", Submitted to *Energy & Buildings*.

VI : Dokka TH, Tjeelflaat P.O., " Simplified models for prediction of vertical contaminant and temperature stratification in displacement ventilated rooms; Part 2 : validation", Submitted to *Energy & Buildings*.

VII : Dokka TH, Jørgensen R., Bjørseth O., Malvik B. " The influence of substrate- and sink effects on VOC emissions from water-based paints - implication to model prediction in real rooms", Submitted to *Indoor Air*

Preface

After working some eight years as a carpenter, I started studying to become an engineer in 1989. Receiving the engineer diploma in 1992 from Trondheim Technical College, I went on to study at the Norwegian University of Science and Technology (NTNU). I received my Msc degree at the University in 1995. During these years my main interest turned from building construction to energy conservation and indoor environment in buildings.

The background for this thesis was laid in a project I had with Professor S.O. Hanssen as a supervisor, called "Mathematical modelling of Indoor air Quality". During this project I also come in contact with Olav Bjørseth and Rikke Jørgensen at the "working environment lab".

Based on the work conducted in this project there was applied for a Ph.D. grant at the Norwegian Research Council, with Olav Bjørseth and S.O. Hansson as supervisors. After receiving the grant, the work on this thesis started in 1996.

Parallel to the work with the Master degree and the doctoral thesis, I have been running a small company (ProgramByggerne ANS) with my brother Kjell A. Dokka. The main area of work has been development of software applications for energy use, building physics, and indoor environment in buildings. During the work in the company I have had a lot of contact with people in the HVAC and building industry. This contact with practising engineers and consultants has been very valuable, giving a practical basis for the work with the thesis.

Acknowledgement

This work has been conducted at the Norwegian University of Science and Technology (NTNU), department of Industrial Economy and Technology Management, with close co-operation with department of Refrigeration and Air Conditioning. The work has mainly been financially supported from the Norwegian Research Council (grant no.111372\330), but also from department of Industrial Economy and Technology Management and ProgramByggerne ANS.

Thanks to my supervisor Olav Bjørseth for professional guidance, and for always fixing both practical and financial problems. Thanks also to my co-supervisor Prof. Sten Olaf Hanssen.

Thanks to Rikke Jørgensen for all the professional and other discussions. By finishing her Ph.D. study last year, she inspired me to believe that I also could get through some day.

Thanks to Bjarne Malvik for doing all the chemical analysis in the study, and for helping me understand a small part of the intricate world of organic chemistry.

Thanks to my co-author Per Olaf Tjelflaat for professional guidance and discussions on ventilation and air flow issues.

Thanks to all my colleagues at the "working environment lab" for the many interesting political and philosophical discussions in the lunch break, and for giving me the opportunity to win the dart tournament once in a while.

I will lastly thank Hanne, David, Jakob, Alexander and Victoria for giving me something else to think about, when the work with the thesis was difficult or down right boring.

Authorship

I am primarily responsible for the scientific quality of this thesis. For the papers I hold the 1st authorship : Paper I, II, V, VI and VII, I am responsible for the quality of ideas, design of the studies, experimental accuracy and reporting of the results. In paper III and IV I share the responsibility with the first author : Rikke Jørgensen. In these two papers I was mainly responsible for the development and use of mathematical models, while Rikke Jørgensen was responsible for the experimental design and accuracy.

In paper I, II, III, IV and VII, Bjarne Malvik has conducted the chemical analysis with Gas Chromatogram and Mass Spectrometry (GC-MS).

Table of contents

1 Introduction

The indoor environment in buildings, as perceived by the occupants, is influenced by both physical conditions and psycho-social relations. It is often divided into seven different components[39], as shown in figure 1. The upper five components, which to some extent are physically measurable, are often called the indoor climate. In this thesis, the main focus is on the atmospheric environment and to some extent the thermal environment. The atmospheric environment is often also referred to as the Indoor Air Quality (IAQ), although this is given a broader meaning in some contexts. In this thesis, IAQ is used about the physically measured air quality (concentrations) and/or the perceived air quality (e.g. odour intensity).

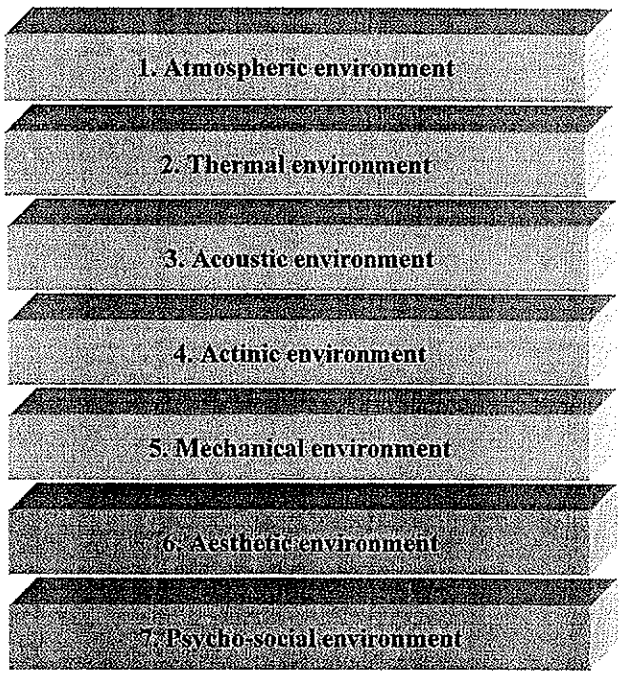

Figure 1: The working principles in displacement ventilation

1.1 Indoor air quality, health, perceived air quality and productivity

IAQ and health

The prevalence of diagnosed asthma in industrialised countries has been increasing over the last 30 years, approximately doubling every 10 to 15 years[1]. Allergies are showing a similar increase[2]. Since outdoor air pollution in industrialised countries has decreased significantly since the 1970s[1], the increase in asthma and allergies can hardly be explained by outdoor air pollution. Considering that people on average spend more than 90% of their time indoors[1], a more realistic environmental factor which can explain their increase is the change in the level of indoor pollution in the same period.

Large epidemiological surveys show that the prevalence of so-called "Sick Building Syndrome (SBS)" symptoms are common among office workers[3-6]. The sick building syndrome is defined by the WHO[7] as: "Irritative symptoms of eyes, nose, throat, lower airways and/or skin, and non-specific hyperreactivity, fatigue, headache and dizziness". High prevalence of SBS symptoms are often associated with:

- Buildings with air conditioning[3, 5, 6, 8-17]
- Buildings with sealed windows (and air conditioning)[10]
- Buildings with carpets and much fleecy material[3, 5, 17].

Most studies also show a higher prevalence of SBS symptoms in non-residential, mechanically ventilated buildings with low ventilation rates[5, 18-20] (below 10 l/s per person).

IAQ and perceived air quality

Extensive studies in non-residential buildings also show that the perceived air quality (PAQ) is reported as poor by a high percentage (30 – 50%) of the occupants[4, 21-24], even though the mean ventilation rates are high (well above minimum ventilation requirements). Studies where the PAQ in buildings has been evaluated by an external panel show that building materials and the ventilation system are the major air pollution sources, substantially greater than pollution from persons[4, 23-27]. This is in contrast to most standards and regulations where the minimum ventilation rate is calculated as a function of the number of persons in the room or zone[28, 29].

IAQ, productivity and related costs

The corporate economic and socio-economic costs due to poor IAQ are large. The Norwegian building authorities have estimated that poor IAQ costs Norway between $1.0 and $1.5 billion each year[2].

Fisk and Rosenfeld[30] have estimated the potential annual savings and productivity gains to be made in the U.S. by improving indoor environments using currently available technologies and procedures. Their estimates included reductions in respiratory diseases, allergies and asthma, and Sick Building Syndrome symptoms, and enhancement of worker performance. They estimated the total annual savings and productivity gains to be between $29 and $168 billion. Adjusted for the difference in magnitude between the U.S. population (~ 258 million) and the Norwegian population (~ 4.5 million), the Norwegian estimate lies within these estimates.

Seppanen[31] has made similar estimates for Finland. The costs of poor IAQ were estimated for the following factors: radon-related cancer, allergic diseases caused by indoor pollutants, illnesses caused by ETS, hospital infections, absenteeism from work due to airborne indoor contaminants, productivity losses due to high temperatures and sick building symptoms. The total annual cost of poor IAQ was estimated to be $3.1 billion, which is close to the upper estimate of Fisk and Rosenfeld when adjustment is made for the population in Finland (~5 million).

Possible causes of indoor air complaints

Many theories and possible causes have been proposed for the numerous complaints made about the indoor air in modern buildings:

- The energy crisis in the 1970s led to generally tighter buildings, which reduced the air flows induced by natural forces (temperature differences and wind)[1].

- Modern, non-residential buildings are often equipped with complex ventilation and air-conditioning systems which are sensitive to flaws in design, construction and maintenance. Moreover, several investigations[32-38] have shown that air treatment equipment in such systems is not easily available for maintenance and cleaning, and can be a potential source of pollution.

- Early in the 1900s, the building materials used were few and well known (brick, stone, concrete, wood, metal). Today, thousands of building materials exist, and many of them contain synthetic chemicals which can emit chemical pollution to the indoor air. The U.S. produced 15 times more synthetic organic chemicals in 1990 than in 1945[39]. The situation in Norway is probably comparable. A large proportion of these chemicals are probably used or contained in occupied buildings. It is likely that all these new materials and chemicals introduced during recent decades can influence the health and well-being of occupants in buildings.

- Due to new building methods and the capital costs involved in the building process, the construction time for new buildings has decreased considerably, especially since World War II. This has led to a reduction in the time allowed for drying and hardening, and a greater risk of encapsulating humidity in the construction. High humidity in constructions is associated with growth of mould and other micro-organisms, enhanced chemical emissions from building materials and decomposition of building materials, all of which can have a deleterious effect on the IAQ.

- Modern architecture and building methods have changed radically during the last 50 years, including lower ceiling height, acoustic ceilings, vapour barriers, highly insulated constructions in cold climates (as in Norway), lighter constructions in commercial buildings and more use of glass in buildings. All these factors can have an influence on the IAQ and climate in buildings.

- More use of glass as an architectural feature has increased the need for air conditioning in buildings. As indicated above, air conditioning in buildings has proved to increase the risk of SBS symptoms.

1.2 Indoor air quality versus energy use and the external environment

It is a common belief that increased air-flow rates result in better IAQ, because they dilute the sources of pollution in the building. Lower concentrations of pollutants result in lower occupant exposure to the components of indoor air pollutants, which again will lower the risk for health effects and poor perceived air quality. However, increased air-flow rates can lead to draught and noise problems (especially low frequency noise). Another problem often encountered by building planners is the large space needed for the ducting and air-handling units of a modern ventilation and air-conditioning system.

High air-flow rates also lead to a high demand for energy to condition (heat, cool and perhaps humidify and/or dehumidify) and move (fans) the air. More complex conditioning of the air (coils, filters, dampers, silencers, heat exchangers) and more complex air-duct systems lead to higher pressure losses and the need for more fan energy. Higher energy use in buildings also leads to higher emissions of greenhouse gases and other pollutants to the external environment, if the energy supply does not come from entirely sustainable energy resources (e.g. waterfalls, solar energy). It is therefore necessary to make a compromise between IAQ and the external environment, when determining the required air-flow rates to buildings. A better strategy for the "total environment" (the external and the internal) is therefore to reduce the sources of indoor air pollution instead of increasing the air-flow rates to high levels. Smart ways to supply fresh air to the occupants (e.g. displacement ventilation[40, 41] and task ventilation[42]) can also reduce the ventilation rate required.

However, from the viewpoint of corporate economics, energy costs are often of minor importance. In a typical office building in Norway, each employee has approximately 20 m^2 each, and the specific energy use is around 225 kWh/m^2 per year[43], energy costs around NOK 0.5/kwh ($ 0.0625/kWh) and a typical yearly salary (including social costs) is NOK 350,000 ($ 44,000). With these figures, the energy cost is only 0.57% of the salary and social costs. Even though energy costs more in other European countries, the figures there are, in magnitude, the same as estimated here. Measures to reduce the energy use in buildings are therefore mostly induced by building regulations or ethical considerations. Measures to improve the indoor climate are therefore generally much more profitable than energy efficiency measures. However, most businesses today want to have an environment-friendly image, where so-called "green buildings" with low energy use and low emissions of pollutants to the external environment can be important for the corporate image. The results from the large European audit project[4] also show that it is possible to plan, construct and run buildings which have both low energy use and good IAQ.

1.3 Design of the atmospheric environment

The thermal environment in buildings is often designed and analysed with advanced simulation software. These software applications are based on detailed mathematical models of solar radiation, transmission of radiation through windows, heat accumulation and heat transmission in the building constructions, long-wave radiation exchange in rooms, convective heat transfer at surfaces, handling of air in air treatment units, and so forth. The heat sources such as lighting, computers and occupants, and their variation with time, are given as input to these programs. Climatic files for a whole year for different locations often accompany the programs. In the hands of competent persons, such tools can be used to predict the thermal environment fairly accurately. They also allow the possibility for optimising between low energy use, low heating and cooling loads, low investment and running costs, and good thermal comfort.

In contrast to the rational and detailed thermal design of a building, the design of its atmospheric environment is generally done superficially, based on standards and building regulations describing the minimum fresh air supply per person in a building[28, 29]. Such design neglects important factors shown in figure 2, including pollution sources from building materials and equipment, sink effects on material surfaces, contaminant gradients, inter-zonal air flows, infiltration and so forth.

The olf/decipol method developed by Fanger[44], which is also the basis of the European CEN report (CR 1752[45]), is an attempt to take more of the factors shown in figure 2 into account. It is based on the philosophy that other pollution sources are counted in "person equivalent" units, where one olf is the pollution rate from a standard person and one decipol is the perceived odour intensity in a room polluted with one olf and ventilated with 10 l/s of clean air. This method takes into account outdoor air quality, pollution from the building and its ventilation system and the ventilation efficiency. By choosing the desired air quality in the premises (in decipols), the air flow rate required to achieve this air quality can be calculated by a simple equation. This method does not take into account sink effects, and it is assumed that steady-state conditions prevail. Other disadvantages of the method are:

- there is no easy way to translate the sensory evaluation of single building materials into an evaluation of a whole room[46]
- there are problems with large variability in the rating of the sensory perception of the air for different persons, and between trained and untrained panels[46, 48, 49]
- there is seldom any correlation between the perceived air quality of the external panel (trained) and the perceived air quality of the occupants of the investigated building[4, 48, 49]
- there is no clear association between the prevalence of SBS symptoms in buildings and the rating of IAQ by trained sensory panels[4, 11].

The European Collaborative Action Report 20[47] also questions the philosophy that a common dose–response relationship exists for different indoor air pollution sources (persons, polluting equipment, material emissions), as the method implies.

An alternative to the olf/decipol method is to measure or model the concentration of relevant contaminants in a building. Figure 2 shows factors that can influence the concentration of contaminants in a building. These factors are briefly discussed below.

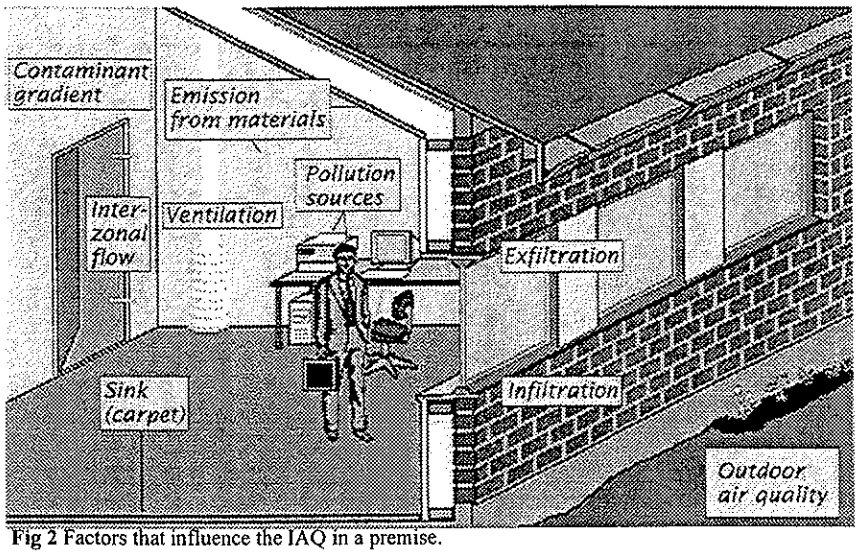

Fig 2 Factors that influence the IAQ in a premise.

Emission from building materials

Emission from building materials and furniture is now recognised as one of the major pollution sources in the indoor air. The problem was first addressed in the 1970s due to high emission of formaldehyde from particle boards, adhesives and insulation foam[2]. The emission of formaldehyde from building materials has decreased dramatically since then, and focus has been turned to the many other volatile organic compounds (VOCs) emitted in "small" amounts from building materials. Several countries have introduced voluntary labelling of building materials[50-53] to reduce emission of VOCs and enable users to choose indoor-air-friendly materials. Emission of VOCs from building materials often decays exponentially[54-57]. A distinction is frequently drawn between wet sources like paint and stain, which are often limited by surface evaporation, and solid materials like wood products, vinyl and linoleum floorings, emission from which is often limited by internal diffusion. Wet sources often have high emission initially, but decay fast if no sinks are present (see below). Solid sources often have lower emissions initially, but decay more slowly than wet sources.

Pollution from occupants

Pollutants emitted from people are considered to be a major pollution source in occupied spaces. Many standards and building regulations still set ventilation requirements according to the number of occupants of a space[28, 29], indicating that people are the dominant polluter in many premises. The production of CO_2 by occupants is often used as a measure of the pollutant rate from people, as first proposed by Pettenkoffer[58]. However, CO_2 is not toxic at concentrations found in occupied buildings, but is just an easily measurable "substitute" for the many organic compounds emitted from people[59].

Emission from equipment and processes

Emissions from equipment, such as printers and photocopiers, can also be of importance. Such equipment often emits ozone, which is known as an irritant gas[7]. Photocopiers can also emit substantial amounts of VOCs[60]. Field investigations have also revealed an association between an increased prevalence of SBS symptoms and photocopying

machines[3, 5]. Little attention has been given to chemicals in cleaning and polishing products used in buildings; these can be regarded as periodical sources, especially in commercial buildings. A few investigations have shown that processes using such products can result in rather large emissions of VOCs[61, 62].

Sink effects

Sink effects are another of the factors that can significantly influence the concentration levels of pollutants in premises[63-72] . In this thesis, the term "sink effects" is used for sorption effects on material surfaces (adsorption/desorption) and/or diffusion and absorption into materials. Such sorption effects can reduce the peak concentration levels (e.g. during painting), but also prolong the period when the concentration of contaminants is rather high, thereby exposing the occupants to harmful and/or irritating compounds for an unnecessarily long time. A few indoor environment surveys have also associated fleecy materials (e.g. carpets and curtains) with the prevalence of SBS symptoms[3, 5, 17]. Sorption effects in such materials can be measured by controlled chamber experiments, and modelled with theoretical or empirical sink models.

Ventilation

Ventilation is the most common method of controlling contaminant levels and improving IAQ. There are many types of ventilation systems, but they are often grouped into natural systems, mechanical systems and air-conditioning systems. In natural systems, the air is driven by wind and/or buoyancy (temperature differences) through more or less controlled openings in the building envelope. Mechanical systems can be divided into those with just a supplying or an extracting fan, or supplying and extracting systems often called balanced ventilation. Balanced ventilation often has air-treatment equipment such as filters, coils, heat exchangers, silencers, etc. Air-conditioning systems are systems that cool the air mechanically (refrigerative cooling) to the desired temperature, and many such systems also humidify or dehumidify the air if necessary. Since balanced ventilation is often equipped with cooling coils, the difference between balanced ventilation and air conditioning is sometimes diffuse. As there is generally a higher prevalence of SBS symptoms in air-conditioning, and to some extent mechanically balanced, systems (see above), there has been renewed interest in natural ventilation systems[73], and what are referred to as hybrid ventilation systems[74]. Hybrid ventilation systems are, in short, ventilation systems that use natural forces as far as possible, and fans when necessary.

All the systems mentioned above can supply air to premises by the mixing ventilation principle, the displacement ventilation principle, or the task ventilation principle. Using the mixing ventilation principle, air is supplied to the room outside the occupation zone with high momentum, ideally inducing full mixing of the air in the premises. With the displacement principle, cool air (a few degrees below room temperature) is supplied at a low level (near the floor) with low momentum. Heat sources in the room heat the air so that it rises to the ceiling where it is extracted. The displacement principle should ideally give cleaner and cooler air in the occupation zone, compared to mixing ventilation[40, 41]. Task ventilation supplies air more or less directly to the breathing zone of the occupants of the premises[42].

Infiltration
Infiltration and exfiltration is air flow through cracks and unintended leakages in the building fabric. The air flow rate due to infiltration is often of minor importance for contaminant transport in newer commercial buildings, but can be important in residential buildings, old (leaky) buildings and high-rise buildings where the buoyancy forces can be large. Infiltration can be measured by tracer gas techniques or modelled by simplified empirical or theoretical models[75, 76]. Infiltration can also be modelled by more comprehensive models, often called network models[75, 77, 78].

Inter-zonal air flow
Inter-zonal air flow is air exchange between rooms and zones in a building, due to temperature or pressure differences. Opening of doors or other large openings between rooms with small temperature differences (1-2 °C) can result in air flows that are 5-10 times higher than the mechanically supplied air flow to the room[79]. This exchange of air can of course influence the contaminant dispersal in a room. Inter-zonal air flows can be measured by tracer gas techniques, or be modelled by simplified theoretical models. It is also possible to model them with the network models mentioned above.

Contaminant gradients
When measuring or modelling their concentrations, it is common to assume that contaminants in premises are fully mixed. In many cases, this assumption is not valid, since significant gradients may exist in the contaminants in a room. This can lead to wrong exposure scenarios for the occupants of the premises. The distribution of contaminants in a building depends on the location and strength of pollution sources, air supply (location, momentum and temperature), air extraction (location), convective air flows due to heat sources (plumes) and cold surfaces (draughts). An uneven distribution of contaminants in a building is often described with different indices, such as ventilation efficiency and air exchange efficiency[80]. Concentration gradients can be measured by measuring the "real" contaminants (e.g. CO_2 or VOCs) in a building, or by using tracer gas techniques. If tracer gas is used, it should have approximately the same location, strength and density as the sources of real contaminant. Concentration gradients can be modelled by simplified zonal models[81, 82], or detailed Computational Fluid Dynamics (CFD) simulations[83-86].

Outdoor air quality
Even though outdoor air in most locations is cleaner than indoor air, pollution sources in the outdoor air can be substantial. Typical outdoor air contaminants are carbon dioxide (CO_2), carbon monoxide (CO), nitrogen oxides (NO_x), sulphur dioxide (SO_2), ozone (O_3), hydrocarbons, VOCs including benzene (toxic substance), particulates and pollen. The most common pollutant sources outdoors are traffic and industrial emissions. The quality of outdoor air in cities has large spatial and temporal variations, and must be evaluated individually for each building.

Air cleaning
It is common in balanced ventilation to filter the incoming air for particulates. Few ventilation systems are, however, equipped with air cleaning systems for gaseous contaminants, even though this option is available. Air cleaning devices for gaseous contaminants are mostly based on activated charcoal or similar sorbents for sorption of

gases in the incoming air. Gaseous air cleaners can either be placed in the ventilation system, or as local air cleaners in the occupied space. Local air cleaners equipped with both particulate and gaseous air cleaning devices are sometimes used in premises where smoking is allowed[87]. The effectiveness of an air cleaner is usually measured by its efficiency, which is the proportion of the incoming contaminant removed by the air cleaner (measured in mass units). Biofiltration of air using plants and trees for uptake of VOCs and CO_2 and production of O_2 is perhaps an alternative to ordinary air cleaning. Recent research has shown promising results for biofiltration[88]. Biofiltration in the form of plants and trees could also have other beneficial effects on the indoor environment[89].

1.4 The aim of this study

The main aim of this study has been to develop and validate mathematical models which can be used to predict concentrations and personal exposure in residential and commercial buildings, mainly for chemical pollution in the vapour phase. Partial aims to reach this goal have been to:

- develop and validate practical source models, mainly for VOCs in the vapour phase
- develop practical sink models which can be used to describe the sorption effects of VOCs on and in materials
- develop simplified models to describe contaminant gradients in premises without full mixing conditions
- provide sub-models to be employed in a user-friendly IAQ computer model that can be used to estimate exposure scenarios and evaluate comfort and health in occupied spaces.

2 Summary of individual papers

2.1 Paper I : The IAQ model "Envisim"

This paper describes a prototype of an IAQ model, implemented into a user-friendly software application (called EnviSim). This computer model is capable of simulating variations in the concentration of TVOC, CO_2 and single VOCs during a day.
The model in EnviSim is based on a single-zone, dynamic, mass balance for the contaminant in question. The mass balances (one for the room air and one for the sink) are described by two coupled differential equations, which are solved analytically within each time-step. The input data (emission, sink, air-exchange data) are assumed to be constant during each time-step (variable between 5 and 60 minutes). The model used is the well-known sink model of Tichenor[66]. The emission from building materials is assumed to remain constant during the design day (assumed steady state emission), but that from occupants and equipment can be described with time schedules (on/off sources). The air exchange is given as input for mechanical ventilation and/or through windows used for airing. Air flow from the latter is calculated using the empirical model developed by de Gids and Phaff[90]. Infiltration and exfiltration are simulated with the well-known LBL model[76].

A database of building tightness, climatic data, data for air cleaners and active filters, etc., is implemented in the program. Examples of data for emission rates, sink-rate data and outdoor air conditions are also included in the database.

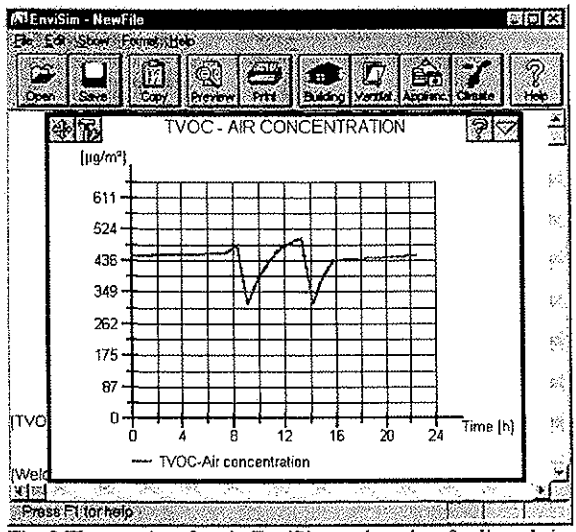

Fig. 3 The user interface in EnviSim, and results of a diurnal simulation of TVOC in a premise.

2.2 Paper II : Field experiments versus chamber experiments

The aim of this study was to determine whether testing of materials in small chambers, together with mathematical models, could predict concentrations in real rooms. A water-based paint used for refurbishing a bedroom was tested for VOC emission in a small steel chamber (100 litres). The emission from the paint was rather high. The emission profile was curve fitted to an exponentially decaying emission (source) model. The bedroom was carpeted, and this floor covering was regarded as a significant sink surface. Tichenor's sink model[66] was used to describe the sink effect from the carpet, together with sink data for a carpet from an earlier sorption (sink) experiment[64]. As shown in figure 5, the prediction was substantially higher than the measured concentration of TVOC in the bedroom. The hypotheses proposed to explain the discrepancy were:

1. Substrate effects, that is diffusion or "soaking" of paint, or compounds in the paint, into the painted wallboard, with possible chemical bindings.
2. Strong surface adsorption with very slow desorption.
3. Scaling effects, since the chamber and the bedroom are completely different in size.

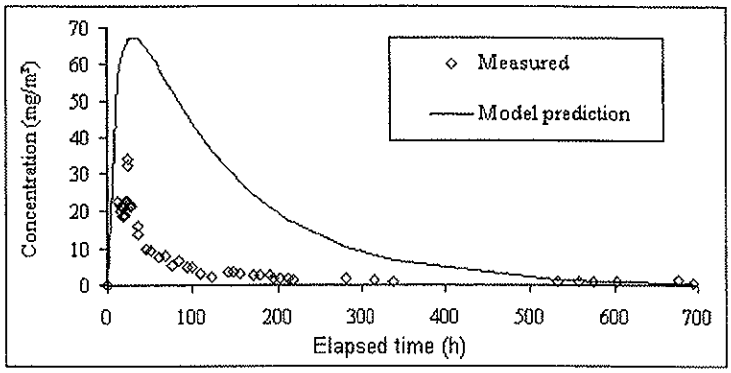

Fig. 4 Predicted and measured concentration in the bedroom.[1]

[1]In the paper the predicted concentration in the bedroom, was based on data from chamber experiments where the air change rate was set at 1.0 h^{-1}. The real air change rate was only 0.5 h^{-1}, resulting in a lower predicted concentration in the bedroom. The prediction based on the correct air change rate (0.5 h^{-1}) is shown in Fig.5

2.3 Paper III : Ventilation & sorption

The purpose of this study was to investigate the interaction between different ventilation strategies and sorption effects of VOCs on material surfaces (also called sink effects). Tests were done in small, glass chambers. Nylon carpets were used as sink surfaces, and a mixture of (-pinene and toluene (common in indoor air) was used as the indoor air pollutant. The source strength was set to be twice as high in working hours (08.00-16.00) as in non-occupied hours. The ventilation was set to mimic the condition in real buildings, with approximately two changes in air (2.0 h-1) during the day, reduced to 1/3 at night (0.67 h-1). Three time schedules were tested for the ventilation: one with the high air-flow rate (2 h-1) in phase with the occupancy (08-16), one with the high air-flow rate extended 2 hours before and after occupancy (06-18), and one with the high air-flow rate extended 3 hours before and 1 hour after occupancy (05-17). EnviSim was used to simulate (predict) the variation in concentration during the day (see summary of paper I).

The results show that sink effects significantly influence the variation in concentration (Fig. 6). The no sink curve in figure 6, showing what the variation in concentration would have been if there had been no sorption effects, does not describe the variation in concentration adequately. The model prediction based on Tichenor's sink model[66] gives an acceptable description of the variation in concentration, but the measured sink effect seems to be even stronger than predicted with this model.

Based on the results from the three ventilation strategies, it is recommended that the ventilation system is "turned" up to its high air-flow level a couple of hours before occupants arrive in the morning. Keeping the air flow at a high level after the occupants have left the building seems to have little effect on occupant exposure.

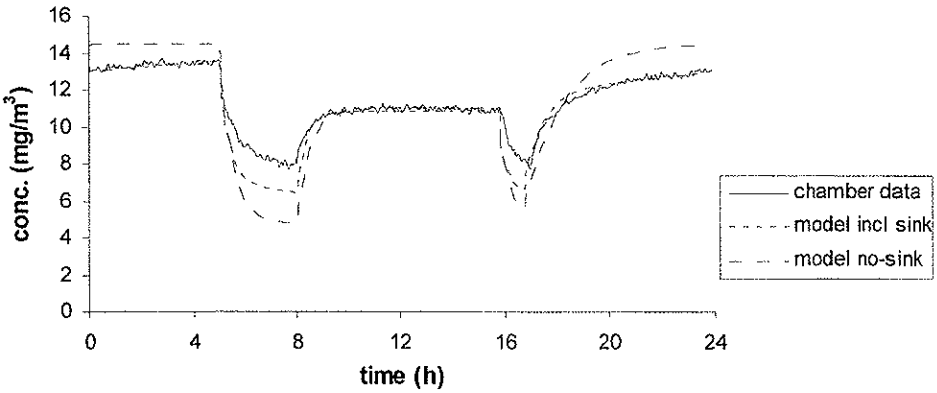

Fig 5 Ventilation strategy 3: day vent. rate: 5.00-17.00, night vent. rate: 17.00-5.00.

2.4 Paper IV : Sink models

This paper first discusses criteria which a sink model should ideally comply to:

1. It should have a sound physical and chemical foundation.
2. It should preferably be as mathematically simple as possible.
3. It should be validated against measured data.

Specific issues discussed for sink models are adsorption isotherms, mass diffusion in the interior of the material, irreversibility contra reversibility and coupling of sink models to general IAQ models.

A new sink model has been developed that complies with the above criteria. It is based on Langmuir's adsorption isotherms (as Tichenor's model) on the surface and Fickian diffusion in the interior of the material. This model can be seen as an extension to Tichenor's sink model[66], to improve the description of the tail of the concentration curve.

The new sink model is validated against measured data from chamber experiments and is also compared with Tichenor's sink model. It fits the measured data very well, and better than Tichenor's model for all cases. However, the regression coefficients of the two models differ little, so Tichenor's model also describes the measured data well for the combination of materials (carpet and PVC flooring) and compounds (α-pinene and toluene) tested here. The main advantage of the new sink model compared to Tichenor's sink model is that it describes the tail of the concentration curve substantially better for rough materials such as carpets.

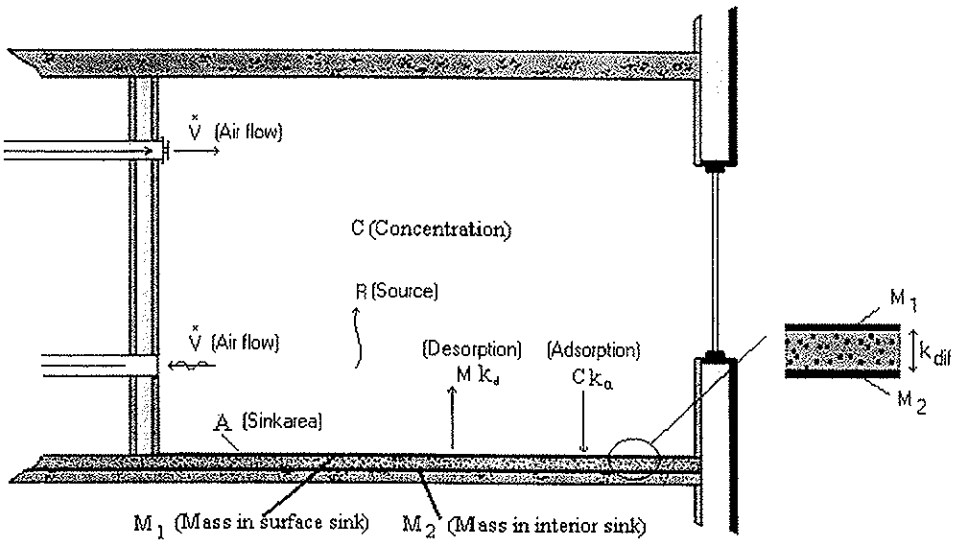

Fig. 6 Schematic figure of the new sink-diffusion model, with Langmuir adsorption and desorption on the surface, and Fickian diffusion into material

2.5 Paper V : Vertical gradient models; derivation

Displacement ventilation is an alternative to conventional mixing ventilation in various types of rooms. Displacement ventilation is superior to mixing ventilation when it comes to removing contaminants and surplus heat from a room. This paper proposes models to predict the vertical contaminant and temperature distribution in displacement ventilated rooms. Simplified steady-state models that can be used in a pre-design phase, and more detailed transient models suitable for implementation in building simulation tools, have been developed. The paper also describes and discusses different sub-models needed, such as plume models, down-draught models, radiation-exchange and radiation-distribution models.

The proposed models can be used for designing displacement ventilation and to evaluate the efficiency of ventilation and temperature.

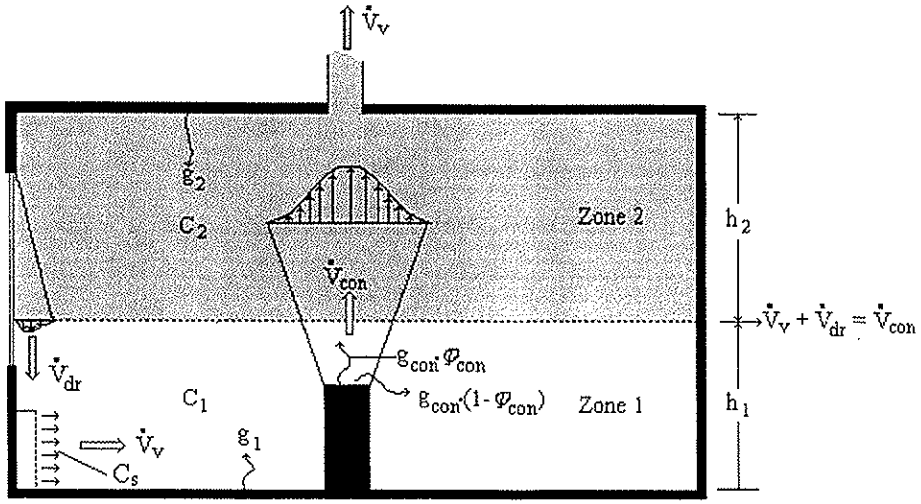

Fig. 7 Principles and variables in the contaminant two-zone model

2.6 Paper VI : Vertical gradient models; validation

In this paper, the vertical gradient models presented in paper V are validated against empirical data sets found in the literature. The steady-state temperature stratification model is also compared with three other simplified models. Seven empirical cases have been used to validate the steady-state thermal model, but only one has been found to validate the transient thermal stratification model. Fourteen empirical cases have been found to validate and evaluate the contaminant gradient models (steady state and transient).

As indicated in figure 9, the prediction of the steady-state thermal model is good, and the model is superior to the other three models for temperature stratification.
The prediction of the transient thermal model is very promising, but should be compared to more transient empirical cases before a final conclusion can be drawn about the validity of the model.

The evaluation of the contaminant models is also very promising for most of the compared parameters. However, the model under-predicts the indices related to the air quality in the inhalation zone. This under-prediction is, however, conservative when the models are used to determine required ventilation air-flow rates.

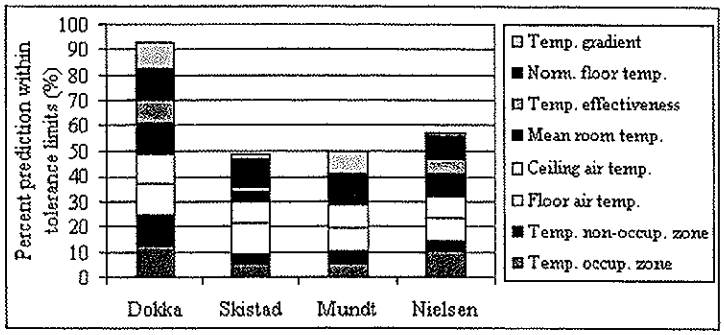

Fig 8 Percent prediction within the proposed tolerance for the steady state thermal models

2.7 Paper VII : Sink & substrate effects

This study investigated whether strong substrate and/or sink effects can explain the discrepancy found between small chamber experiments and field experiments. As reported in paper II, the modelled concentration of TVOC based on data from chamber experiments was substantially higher than the concentration measured in the field. Two of the hypotheses put forward to explain the discrepancy were strong substrate effects from the painted wallboard and/or strong sink effects on surface materials in the room.

To investigate substrate effects, emission experiments were performed in steel chambers using both a spruce panel and an aluminium sheet as substrates for a water-based paint. The emission from the aluminium substrate was substantially higher than that from the spruce substrate, but the substrate effects varied greatly for different VOCs emitted from the paint.

To investigate the sink effects, another experiment was performed in steel chambers. One chamber contained only an aluminium sheet painted with water-based paint, and the other contained, in addition, a piece of carpet (sink surface). The emission when the carpet was present was considerably less than without the carpet, but here, too, the sink effect differed greatly for different VOCs. The sink effect found was also much stronger than the sink effects found in earlier sorption experiments. The theoretically derived model of Tichenor[66] failed to describe the strong sink effect found.

The concentration of VOCs in the bedroom (field experiment) was reanalysed using data from the sink and substrate chamber experiments, along with the newly developed mathematical models. The prediction (concentrations) was now in good agreement with the measured concentrations in the bedroom (Fig. 10). This indicates that strong substrate and sink effects can explain the often reported discrepancy between field and chamber experiments.

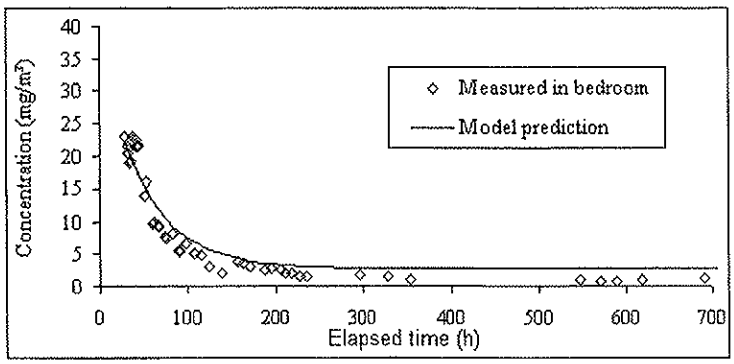

Fig. 9 Comparison between measured TVOC concentration in the bedroom and model prediction.

3 Discussion and conclusions

This chapter discusses the following topics:

1. Various models that are available for an integrated IAQ model.
2. The necessary and available input data for the various sub-models in an IAQ model.
3. How an IAQ model can be implemented into a user-friendly software application.
4. The practical application of an integrated IAQ model/software application.
5. The originality of the study presented.

The chapter closes with conclusions.

3.1 Mathematical modelling

The purpose of this study was to develop a practical and usable IAQ model, primarily for chemical pollution in indoor environments. Such a model has to be based on sub-models for different chemical and physical processes influencing the IAQ in a building. Important processes that must be modelled are:

- Emissions from building materials and also from pollutant sources such as occupants, equipment (e.g. photocopiers) and processes (e.g. polishing of floors).
- Sink effects due to sorption on and in materials.
- Air entering and leaving the analysed space from the external environment and other connected zones. Air flows due to both natural and mechanical forces must be modelled.
- Air flow patterns and contaminant dispersal inside the analysed space must also be modelled, especially if contaminant gradients in the premises significantly influence the exposure of occupants.

Existing models for the different processes, and models developed in this study are discussed below.

3.1.1 Source models

Emission of VOCs from building materials often decays exponentially. The simple model for exponential decay applied in paper II can then be used to describe the emission profile. This model is also used in the Danish indoor climate labelling method[50, 51]. However, emissions from building materials often end at a quasi-steady-state level after some time, i.e. the emission rate from the material seems to be relatively constant. In such cases, the emission/source model proposed in paper VII can be used.

Other authors have proposed more complex, double exponential models (two exponential functions) to describe the "slow" emission after a long time has elapsed[56, 57]. The drawback with such models is that more model parameters have to be estimated and reported, compared to the simpler models. There also exist source/emission models derived from general mass diffusion theory[91, 92]. The model of Claussen et al.[91] is quite simple and is an alternative to the simple exponential models proposed above. That of Little[92] is mathematically very complex, and is probably interesting for theoretical purposes only.

If long-term exposure is to be estimated, it is also possible to model the emission from building materials as a steady-state source, as was done in paper I (EnviSim). The steady-state emission must then be based on measurement of the emission rate after, for example, 3 months, or after 6 months as in the Swedish trade standard for flooring materials[52].

Emission from occupants, equipment and processes is often modelled as on/off sources. This means that they are assumed to emit at a constant rate when on (or present in the space). It is, however, doubtful whether emission from floor-cleaning products or polish wax can be modelled as an on/off source[62]. Such sources can perhaps be described better by the exponential decay models proposed above.

3.1.2 Sink models

Various models to describe the sink effects of VOCs on building materials were proposed in papers I, IV and VII. The sink model of Tichenor[61], implemented in Envisim (paper I), is relatively simple (mathematically) and is derived from general adsorption theory (the Langmuir adsorption isotherm). It seems to describe the sink effects on non-fleecy materials with rather low concentrations (below 1 mg/m^3) rather well. However, for very fleecy materials and/or high concentrations Tichenor's model does not seem to describe the sink effect acceptably.

The new sink model proposed in paper IV, which also takes into account diffusion into the material, describes the slow desorption from fleecy materials better than Tichenor's model. It is, however, more mathematically complex, and the parameter estimation procedure is more cumbersome than for Tichenor's model. Moreover, it would not be able to describe the strong sink effect found in paper VII very well, since it is based on the same surface adsorption kinetics as Tichenor's model, which failed to describe the strong sink effect found there.

The sink model derived in paper VII adequately describes the strong sink effects found there. Its drawback is a lack of a sound theoretical basis (empirically derived), even though the various parameters in the model can be given a physical meaning. Moreover, three parameters in the model have to be estimated compared to two for Tichenor's model.

Other, more complex, sink models also exist[66-70, 72, 92]. Most are so complex that they should not be used in an integrated IAQ model. The exception is the modified model of Tichenor[66], where the term describing desorption from the sink is modified with a non-linear empirical expression. This modified model describes the slow desorption from rough materials better than Tichenor's original theoretical model. It is also implemented in the IAQ/Exposure computer model EXPOSURE[55].

3.1.3 Air flow models

No air flow models have been developed or validated in this study, except that simplified infiltration and window-airing models have been implemented in the EnviSim program (see paper I). However, since air flow modelling is an important part of an integrated IAQ model, existing models appropriate for implementation in an IAQ model will be discussed below.

Modelling air flows in a multi-zonal structure such as a modern office building is a very complex task[75]. Substantial simplification is therefore often applied to model air flows in such structures. The simplest way of determining the air flow entering and leaving a space is to assume that the mechanically supplied air flow is constant and that inter-zonal air flows, airing through windows and infiltration are negligible. These assumptions are, however, seldom fulfilled in real buildings.

Simplified models

A further refinement is to assume that the mechanical air flow is fixed, and to use simplified models to model infiltration and airing through windows. Examples of such simplified infiltration models are the LBL model[76], the British standard BS 5925[93] and the proposal for a new CEN standard to calculate air-flow rates in dwellings[94]. These are models based on the single zone assumption, but simplified infiltration models for multi-zonal structures have also been developed[95, 96]. An example of a simplified model for airing through windows is the empirical model of de Gids and Phaff[90]. If wind effects are negligible, a simplified expression for buoyancy-driven air flow through large openings can be derived from Bernoullies equation[79]. This expression can also be used for inter-zonal air flows, if temperature differences between zones are the main driving force. Such simplified models are relatively easy to implement in an integrated IAQ model.

Network models

A more comprehensive and accurate way is to use network models to model all air flows entering and leaving a space. In such models, each analysed space or zone is assigned a pressure node, and each air flow pathway (crack, opening, vent, duct) between pressure nodes is denoted as air flow resistance. The association between pressure differences, the air flow resistance and the air flow is described by coupled non-linear equations. This non-linearity means that the resulting equation sets have to be solved numerically, by iteration. A distinction is often made between the infiltration network representing the natural porosity of the building fabric and the purposely provided network of openings comprised of stacks, grills, air vents, and open windows and doors. It is often more difficult to describe the infiltration network than the purposely provided network[75]. Several well-documented network models exist[75, 77, 78], the most used ones, COMIS[77] and CONTAM[78], being implemented into programs with a Windows® user interface. In network models, difficulties may be experienced in describing large openings with bi-directional flow (air flow taking place in both directions) and in handling air flow in openings with vertical temperature gradients. Network models are well suited for integration into an IAQ model.

CFD models

The most detailed way of modelling the air flow in a building is to use computational fluid dynamics (CFD) models, which analyse the air flow (velocity), temperature and contaminant field in a space. CFD models are numerical methods which divide the space into a series of small volumes (finite volume methods) or elements (finite element methods). The governing equations for conservation of momentum, mass and energy, together with governing transport laws of momentum, heat, mass and turbulence must be satisfied for each volume or element. Typically, in a 3D simulation of a room, the space is divided into 30,000 to 50,000 control volumes[75]. To solve such large systems of equations considerable computing power is required. User input to CFD codes are[75]: location of openings, mass flows in and out of the analysed space, type of flow boundary, level of

turbulence of flow through diffusers or mixing fans, thermal boundaries (temperatures, fluxes), heat sources and sinks, boundary obstacles, locations of contaminants, emission characteristics and properties. This means that a great deal of user input is required and a good understanding of the physics behind air flow is needed to achieve realistic results from these CFD codes. Further disadvantages with the use of CFD are[75]:

1. Due to the large computer power and storage capacity needed for simulation, CFD analysis is often restricted to stationary conditions, 2-dimensionality and single-space analyses. It is also very difficult to present the immense number of results from a three-dimensional and transient CFD analysis.
2. Difficulties in representing the flow fields generated by natural ventilation and infiltration.
3. Difficulties in specifying heat-transfer characteristics at boundaries (radiation, convection and conduction).
4. Some codes have difficulty solving problems where free convection dominates (e.g. in displacement-ventilated rooms).

CFD models are mostly used by specialised consultants and research institutes, and seem too costly and complex for the average consultant and architect. Even though CFD models theoretically can model both source and sink effects, this would be too complex and time consuming to do in most building projects. Hence, in the author's opinion, CFD is not suitable for integration into or with a general IAQ model. CFD can, however, be a valuable tool for temperature, contaminant and air-flow analysis of large enclosures such as atria, shopping precincts, airports, concert halls and so forth. Examples of commercial CFD codes that are available for tackling problems in the physics of buildings are FLOVENT[83] and VORTEX-2[84].

3.1.4 Gradient models

As mentioned in the introduction, it is common to assume full mixing (no contaminant gradients) when modelling or measuring contaminants in a space. However, vertical contaminant gradients can be substantial, especially in displacement-ventilated rooms where contaminant gradients are intended, and in rooms with high ceilings. For such rooms, the two-zonal contaminant models presented in paper V and evaluated in paper VI can be used. These are, however, based on the assumption that the movement of the occupants is moderate. In spaces with substantial movement (e.g. shops, walking areas), the models have to be further refined and validated against measured data.

In spaces with complex geometry and/or uneven sources of contaminants, horizontal contaminant gradients can be of importance. The models presented in paper V cannot handle such cases. To take into account both vertical and horizontal contaminant gradients, resort has to be made to CFD codes (described above). Zonal models which model both horizontal and vertical temperature gradients have been developed[97, 98], but so far they do not handle contaminant gradients.

The contaminant-gradient models developed in paper V are well suited for implementation in an integrated IAQ model. Both the source and sink models described above can relatively easily be coupled to the two-zonal contaminant model. A problem can, however, arise if the vertical temperature gradient model also presented in paper V is to be coupled with an air-

flow model. Most air-flow models (simplified and network models) are based on the assumption that the temperature remains uniform. However, work being performed by IEA Annex 35 Hybvent[74] is aimed at developing air-flow models which also handle rooms and spaces with vertical temperature gradients.

3.2 Input data for mathematical models

3.2.1 Chemical source data

Even though emission testing of building materials has been going on for some years, relatively few data on emissions from building materials have been published[52, 99-101, 103]. Moreover, some of these data are probably out-of-date due to changes in the composition and manufacture of the tested materials (e.g. to reduce emissions[53]), or the procedures and analysis methods for testing the emissions.

Several Nordic countries have introduced voluntary indoor climate labelling of building materials[50-53, 102]. A European collaborative effort has also resulted in a report[99] which describes a method for testing emissions from, and labelling of, flooring materials. The problem with most of these methods[50, 51, 99] is that they focus upon giving an indoor climate label that fulfils certain requirements, rather than giving relevant emission data for use in an IAQ model. A better approach, in the author's opinion, is to allocate the materials to three (or more) classes depending on their emission rate, as proposed by the Scandinavian HVAC organisation, SCANVAC[100], in 1991. This proposal was based on TVOC as a measure of the health and/or comfort effects arising from the emissions. However, there now seems to be consensus that the TVOC metric is not a good measure of health or comfort effects[104, 105]. Hence, the labelling methods of the European Collaborative Action[99] and the Danish indoor climate labelling[50, 51] weight the different VOCs emitted with their respective odour or irritative thresholds. This approach is based on the assumption that the health and comfort effects of a VOC mixture are equal to the sum of each weighted component. Few data exist which verify this assumption[99]. However, Brinke et al.[106] tested different VOC metrics against the prevalence of SBS symptoms in several investigated buildings. They found that a VOC metric using irritative thresholds to weight different compounds was statistically significantly correlated with the prevalence of SBS symptoms in the buildings.

Even though few emission data exist at present, the "new" Norwegian building code[107, 108] lays down requirements for labelling emissions from building materials. It also takes into account the emission from building materials when ventilation air-flow requirements are stipulated. Hopefully, these demands will lead to more readily available emission data for building materials in the near future.

Only limited data exist regarding VOC emissions from occupants, equipment and processes. To the author's knowledge, Bluyssen[59] is the only one who has published VOC emissions from persons. Brown[60] has recently published data concerning VOC emissions from photocopiers, but emission data from both photocopiers and laser printers have been published earlier[109]. Vejrup[62] has published VOC emission data for several cleaning and polishing products. Eatough[110] give examples of VOC contents in environmental tobacco smoke (ETS).

3.2.2 Chemical sink data

For Tichenor's theoretical sink model, also referred to in papers I, II, III, IV and VII, there exists a considerable amount of published data[63-66, 111] in addition to those given in papers II and III. These data are, however, mostly for single VOCs, and must be used with caution for other components and VOC mixtures.

For other models than Tichenor's theoretical one, there seldom exists more published sink-rate data than those used to validate them. This is also true for the two sink models developed in this study (papers III and VII).

3.2.3 Input to air flow models

Input data required for air-flow models are:

1. The distribution and air flow characteristics of cracks and gaps in the building envelope. In simplified models, this is often described using the standardised air tightness measured at a reference pressure of 50 Pa (n_{50}), together with an estimated distribution of leakage between floors, ceilings and facades. In network models, this is described with the flow coefficient (C) and flow exponent (n) for each flow path (at least two for each face), and for internal air-flow paths between rooms and zones.
2. The frequency of purposely provided areas and openings such as chimneys, air vents, open doors and windows, both in the building envelope and internally between rooms and zones.
3. Climatic data in the form of temperature, wind velocity and wind direction for the location.
   The characteristics of the terrain and shielding from nearby buildings and obstacles have to be known to calculate the local wind velocity from the wind velocity at the nearest weather station. Wind pressure coefficients (C_p) around the building are needed to estimate the external pressure caused by wind. The indoor air temperature and the height between openings are needed to calculate the stack pressures (caused by differences in air density).

The distribution and air flow characteristics of cracks and gaps can be difficult to estimate. However, air leakage characteristics for different building components have been published by the Air Infiltration and Ventilation Centre (AIVC)[75, 112]. Data for air tightness, measured with the n50 value for different building types and building constructions are given in CEN TC 156/WG2[94]. In Norway, the n50 value is usually in the range of 2-6 h^{-1} for residential buildings[113].

How frequently purposely provided openings are opened may also be difficult to estimate with certainty. A way of overcoming this problem may be to perform a sensitivity analysis, i.e. vary the frequency of opening within a probable range and see what effect this has on the results for the model (e.g. air flows, IAQ).

Climatic data for a typical year with a time resolution of 1 hour are often available for larger cities. However, for smaller towns and rural districts reliable climatic data, especially wind velocity and wind direction can be hard to find.

Data on the distribution of wind pressure on facades, described by the Cp value, can be taken from AIVC publications[75, 112]. Models also exist which calculate the local distribution of wind pressure on buildings[77].

Indoor air temperature is input in air flow models (both simplified and network models), and a design value (e.g. 22 °C) is most often used. An alternative is to use thermal simulation tools to estimate the indoor air temperature. A more comprehensive and accurate way is to couple a thermal simulation program to an air-flow model, since the air flows influence the indoor air temperature, and the temperature influences the air flows. Work being done by IEA Annex 35 Hybvent[74] is aimed at coupling thermal simulation models and air-flow models (network models).

3.2.4 Input to gradient models

Input data needed for contaminant gradient models are:

1. Heat output; radiation/convection output, and location and geometry of heat sources in the space.
2. Generation of pollution; location and geometry of pollution sources in the space, and how much of the generated contaminants follows the plumes generated by the heat sources.
3. Number, location and movement of occupants in the analysed space.
4. Surface temperature, size and location of cold, vertical surfaces in the space.
5. Location of, and air-flow rates in, mechanically and naturally driven air inlets and outlets in the analysed space.

Most of these data are easily available and are often used in thermal simulation programs, but some additional geometrical data are needed. However, it may be difficult to estimate how much of the contamination generated in the occupation zone follows the heat source plumes into the upper polluted zone.

3.3 Software development

Many of the models presented in the different papers, and existing models discussed in this chapter are so computational demanding that they are practically impossible to use in hand calculations. If they are to be integrated into an IAQ model the computational effort needed is even greater. Another problem is the relatively large number of inputs needed for such models. A possible solution is to implement the models into a spreadsheet. However, spreadsheets are seldom user friendly, lacks robustness, and for more complex models the calculation/simulation time can be substantial. Especially simulation over longer periods (e.g. a year) is impractical in spreadsheets.

In practise one has to resort to programming languages as C++, Delphi, Fortran and Visual Basics, for implementation of an integrated IAQ model into a software application. Due to the fact that Windows® is the dominant operative system in the end user market, most simulation programs today is developed for Windows. However, many of the simulation programs developed in the eighties and in the beginning of the nineties, was developed for the MSDOS® operative system. The EnviSim program (paper I) is developed in MS Visual

C++® for Windows. Some of the advantages with developments of software applications in modern programming languages as C++ and Delphi for Windows are :

- It is possible to design very user friendly software applications, with a graphical user interface.
- Standardization of user interface in Windows® makes it easier for users to get started with new applications, and making it easier to orientate in new programs .
- With efficient and optimised programming, the simulation time is quite modest if modern PCs are used, even for computational complex models and long term simulations (e.g. a year).
- The robustness of application written in these languages is quite good, if the programming is structured and if necessary debugging and testing has been undertaken.
- Extensive use of databases and climatic files can ease the input procedure for the user.
- Possibility for on-line help from each dialogue and result/output can also ease the input procedure and give explanations of the outputs of the model.
- The output/result possibilities in Windows application is much better than the old DOS programs. Both graphical results and numerical results are possible. It is also possible to present results in a html-file which can be read by different browsers (Netscape, Explorer, etc.)

An example of a building simulation program using the above mentioned possibilities is SCIAQ Pro[114] (developed in MS Visual C++). This is a building simulation program which calculates : temperatures, energy demand, heating and cooling load, CO_2 and RH levels, productivity loss (due to high temperatures), air flow rates due to windows airing, inter zonal air flow rates, infiltration rates and more. An example of the user interface in SCIAQ Pro is shown in figure 11. An integrated IAQ model (multizone model) can look much the same as SCIAQ Pro. In fact, it is possible that SCIAQ Pro will be the basis of an integrated IAQ model in the future.

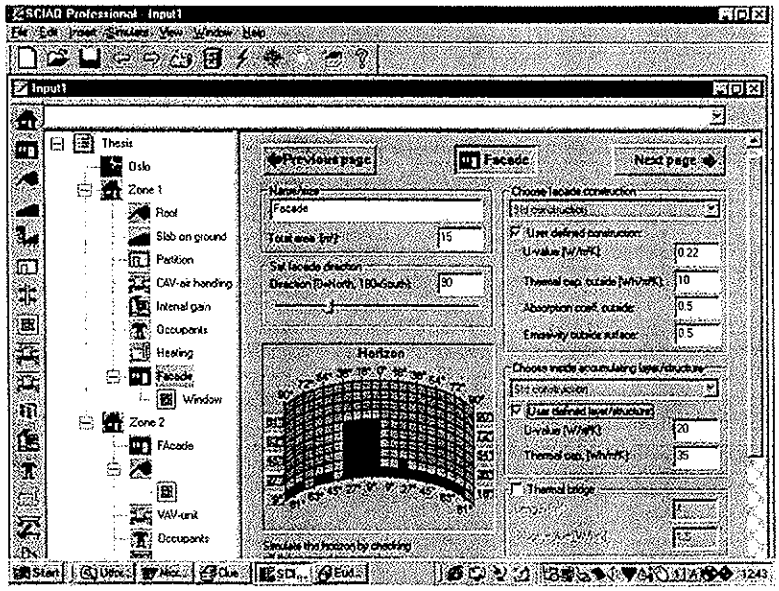

Fig. 10 Example of the user interface in SCIAQ Pro.

3.4 Practical use of models and simulation tools

If the different models proposed in this study are coupled to an air flow model, and in addition to a thermal model as SCIAQ Pro, it could be a very powerful tool for environmental analysis of buildings. Possible usage of such a tool can be :

- Evaluation and selection of indoor environmentally friendly building materials. If emission and sink rate data for building materials become easily available, such a tool can be used to select appropriate materials for different type of rooms.
- It can be used to estimate short term and long term exposure to different contaminants. Which again, can be used for a health risk evaluation for specific persons or specific buildings or rooms.
- It can be used to evaluate comfort (odour) conditions in a premise.
- It can be used for estimation of necessary air flow rate requirement to keep contaminants at a acceptable level.
- It can be used to reduce the need for high air flow rates, which makes it possible to design innovative ventilation solutions (e.g. hybrid ventilation and "modern" natural ventilation)
- It can be used to optimise between IAQ and energy use in buildings.
- It can be used for R&D purposes, e.g. to develop and evaluate new climatization concepts.

3.5 Originality

The main originality of this thesis is the attempt to synthesis models describing ventilation and air flow processes and models describing chemical source and sink effects. Other elements that can be regarded as original contributions in this thesis are :

- The interaction of sink effects with different ventilation strategies, as presented in paper III. To the authors knowledge, this has never been published before.
- The two zone contaminant and temperature gradient models derived and validated in paper V and VI, can be regarded as an original contribution. Even if other two zone contaminant and temperature gradient models has been published before, no one has been so comprehensively documented and validated as the models in this thesis.
- The documentation that strong sink and substrate effects could explain the difference between chamber and field experiments (paper VII), can also be seen as a original contribution.

3.6 Conclusions

1. A prototype of an integrated IAQ model has been developed and implemented into an user-friendly software application (EnviSim). The model simulates diurnal variation of TVOC, single VOCs and CO_2.
2. The results from controlled chamber experiments, show that the interaction between ventilation strategy (time schedules) and sorption effects influence the concentration variation and exposure in spaces with intermittent occupancy (e.g. offices). Based on

these results, it is recommended that the ventilation system is turned on a couple of hours before the occupants arrive.

3. A new sink/diffusion model describing sorption effects of organic compounds on and in materials has been developed. This model describes the sorption effects better than commonly used sink models, especially for compounds and materials with strong sink effects.
4. Models for prediction of vertical contaminant and temperature stratification in displacement ventilated rooms has been developed. The application of these models can be : prediction of contaminant distribution and ventilation efficiencies, prediction of age of air and air exchange efficiencies, prediction of temperature distribution and temperature effectiveness. The transient models can be implemented in building simulation tools for better prediction of energy use and long term exposure in displacement ventilated rooms.
5. The proposed models for vertical contaminant and temperature stratification have been validated against empirical data sets found in the literature. Both the steady state and transient temperature models predict very well for the seven cases used in the validation. The steady state and transient contaminant models predict well for most of the compared cases and variables. However, for the indices measuring the air quality in the inhalation zone, the models under-predicts the experimental results. The under-prediction is conservative if the model is to be used for determination of necessary ventilation air flow rates.
6. Results from chamber experiments show that a carpet (common sink surface) reduce the emissions from a waterbased paint significantly. The sink effect found are substantially stronger than those found in earlier sorption experiments, conducted with lower concentrations. Emission chamber experiments with spruce and aluminium as substrate for a waterbased paint, show that the emission from a porous substrate as spruce is considerably lower than for the aluminium substrate. The results from the sink- and substrate chamber experiments, together with proposed sink- and substrate models, has been used to predict the VOC concentrations in a refurbished bedroom. The concordance between predicted and measured VOC concentrations in the room are good, indicating that strong sink- and substrate effects can explain the discrepancy between chamber experiments and field experiments often found.
7. Based on the sub-models developed in this thesis, together with existing air flow models and thermal models, an integrated IAQ model could be developed. Implemented in a modern software application it could be a powerful tool for environmental analysis and design of buildings. However, the most important barrier for using IAQ models today, is that limited emission data for building materials, equipment and processes exist. Sink rate date for sink models are also limited.

4 References

1. Øie: "The role of indoor building characteristics as exposures indicators and risk factors for development of bronchial obstruction in early childhood", Ph.D. thesis, Norwegian University of Science and Technology, Dep. of Refrigeration and Air Conditioning, Trondheim, 1998.

2. Edvardsen (Editor): "Hus og helse", The Norwegian building authorities (Statens bygningsteksniske etat), 1992 (In Norwegian).

3. Fisk, Mendell, Daisey, Faulkner, Hodgson, Nematollahi and Macher: "Phase 1 of the California healthy building study : a summary", Indoor Air, Volume 3, 1993, pp. 246-254.

4. Bluyssen, Fernandes, Groes, Clausen, Fanger, Valbjørn, Bernhard and Roulet: "European audit project in 56 office buildings", Indoor Air, Volume 6, 1996, pp. 221-238.

5. Mendell: "Non-specific symptoms in office workers: A review and summary of the epidemiological literature", Indoor Air, Volume 3, 1993, pp. 227-236.

6. Kroeling: "Health and well-being disorder in air-conditioned buildings; comparative investigations of the "Building illness" syndrome", Energy & Buildings, 11, 1988, pp. 277-282.

7. World Health Organization: "Indoor Air Pollutants : Exposure and Health Effects", Copenhagen, WHO Regional Office for Europe (EURO Reports and Studies 78), 1983.

8. Sweers, Preller, Brunekreef, Boleij: "Health and indoor climate complaints of 7043 office workers in 61 buildings in the Netherlands", Indoor Air, Volume 2, 1992, pp.127-136.

9. Sverdrup, Anderson, Andersson: "A comparative study of indoor climate and human health in 74 day care centres in Malmø, Sweden" Proceedings Indoor Air '90, Volume 1, 1990, pp. 651-655.

10. Mendell: "Elevated symptom prevalence in air-conditioned office buildings: A reanalysis of epidemic studies from the united kingdom", Proceedings Indoor Air '90, Volume 1, 1990, pp. 623-629.

11. Aizlewood, Raw, Oseland: "A study of office environment in eight office buildings", Proceedings Indoor Air '96, Volume 2, 1996, pp. 895-900.

12. Cochet, Riberon, Kirchner: "Reported symptoms, ventilation performance, and building characteristics in six French office buildings", Proceedings of Healthy Buildings '95, Volume 3,1995, pp. 1359-1364.

13. Finnegan, Pickering: "Prevalence of symptoms of the sick building syndrome in buildings without expressed dissatisfaction", Proceedings Indoor Air '87, Volume 2, 1987, pp. 542-546.

14. Harrison, Pickering, Faragher, Austwick, Little, Lawton: "An investigation of the relationship between microbial and particulate indoor air pollution and the sick building syndrome", Respiratory medicine, 86, 1992, pp. 225-235.

15. Robertson: "Building sickness – are symptoms related to office lighting?", Annals of Occupational Hygiene, 33, 1989, pp.47-59.

16. Jaakkola et al.: "The Helsinki office environment study: the type of ventilation system and the sick building syndrome", Proceedings Indoor Air '93, Volume 1, 1993, pp. 285-290.

17. Skov, Valbjørn, Pedersen et al.(1990), "Influence of the of indoor climate on the sick building syndrome in an office environment", Scandinavian Journal of Work and Environmental Health", 16, pp. 1-9.

18. Jaakkola, Heinonen, Seppanen: "Mechanical ventilation in office buildings and the sick building syndrome. An experimental and epidemiological study." Indoor Air, Volume 2, 1991, pp. 111-121.

19. Godish, Spengler: "Relationship between ventilation and indoor air quality : A review", Indoor Air, Volume 6, 1996, pp.135-145.

20. Seppanen, Fisk, Mendell: "Association of ventilation rates and CO_2 concentrations with health and other responses in commercial and other buildings", Indoor Air, Volume 9, 1999, pp. 226-252.

21. Smedje, Norback, Edling: "Subjective indoor air quality in schools in relation to exposure", Indoor Air, Volume 7, 1997, pp. 143-150.

22. Sweers, Skov, Valbjørn, Mølhave: "The effect of ventilation and air pollution on perceived indoor air quality in five town halls", Energy and Buildings, 14, 1990, pp.175-181.

23. Fanger, Laurritzen, Bluyssen, Clausen: "Air pollution sources in offices and assembly halls, quantified by the olf unit" Energy & Buildings, 12, 1988, pp. 7-19.

24. Pejtersen, Øie, Skår, Clausen, Fanger: " A simple method to determine the olf load in a building", Proceedings Indoor Air '90, Volume 1, 1990, pp. 537-542.

25. Pejtersen et al.: "Air pollution sources in kindergartens", Proceedings of IAQ '91: Healthy Buildings (ASHRAE), 1991, pp. 221-224.

26. Pejtersen, Clausen, Fanger: "Olf-values of spaces previously exposed to tobacco smoking", Proceedings of Healthy Buildings '88, Volume 3, 1988, pp. 197-205.

27. Thorstensen, Hansen, Pejtersen, Clausen, Fanger: "Air pollution sources and indoor air quality in schools", Proceedings Indoor Air '90, Volume 1, 1990, pp. 531-536.

28. Fanger P.O. (1998), "Discomfort caused by odorants and irritants in the air", Indoor Air, Supplement 4/98, pp. 81-86.

29. ANSI/ASHRAE STANDARD 62-1989: "Ventilation for Acceptable Indoor Air Quality", ASHRAE 1990.

30. Fisk and Rosenfeld: "Estimates of improved productivity and health from better indoor environments", Indoor Air, Volume 7, 1997, pp. 158-172.

31. Seppanen: "Estimated costs of indoor climate in Finnish buildings", Proceedings of Indoor Air '99, Volume 4, 1999, pp. 13-18.

32. Pasanen, Teijonsala, Seppanen, Ruuskanen, Kalliokoski: "Increase of perceived odour emissions with loading of ventilation filters", Indoor Air 1994, Volume 4, 1994, pp. 106-113.

33. Pejtersen: "Sensory pollution and microbial contamination of ventilation filters", Indoor Air, Volume 6, 1996, pp.239-248.

34. Pejtersen, Bluyssen, Kondo, Clausen, Fanger: "Air pollution sources in ventilation systems", Proceedings of CLIMA 2000, Volume 3, 1989, pp. 139-144.

35. Sverdrup, Nyman: "A study of micro-organisms in the ventilation system of 12 different buildings", Proceedings Indoor Air '90, Volume 4, 1990, pp. 583-588.

36. Elixman, Linskens, Schata, Jorde: "Can airborne fungal allergens pass through an air conditioning system", Environmental International, Volume 15, 1989, pp.193-196

37. Hujanen, Seppanen, Pasanen, "Odour emissions from the used filters of air-handling units" Proceedings of IAQ '91: Healthy Buildings (ASHRAE), 1991, pp. 329-333.

38. Bluyssen, Fanger: "Addition of olfs from different pollution sources, determined from a trained panel", Indoor Air 1991, Volume 4, 1991, pp. 414-421.

39. Hanssen: Chapter four in : "Enøk i bygninger", Universitetsforlaget (In Norwegian), 1992.

40. Mattson: "On the efficiency of displacement ventilation" Ph.D. thesis, Royal Institute of Technology, Gävle, Sweden, 1999.

41. Brohus, Nielsen, " Personal exposure in displacement ventilated rooms", Indoor Air, Volume 6, 1996, pp.157-167.

42. Faulkner, Fisk, Sullivan, Wyon: "Ventilation efficiencies of desk-mounted task/ambient conditioning system", Indoor Air, Volume 9, 2000, pp. 273-281.

43. Søgnen et al.: "Bygningsnettverkets energistatistikk; Årsrapport 1999", NVEs byggoperatør, 2000 (In Norwegian).

44. Fanger: "Introduction of the olf and decipol units to quantify air pollution perceived by humans indoors and outdoors", Energy and Buildings, 12, 1988, pp.1-6.

45. CEN Report CR 1752: "Ventilation for Buildings - Design Criteria for the Indoor Environment", CEN/TC 156/WG 6, 1998.

46. Bluyssen et al. (1997), "Evaluation of VOC Emissions from Building Products – Solid Flooring Products" European Collaborative Action, Indoor Air Quality & Its Impact On Man, Report No 18, 1997. European Comission Joint Research Centre – Environmental Institute. (NOTE : Chapter 5 : Sensory evaluation, was revised in 1998)

47. Berglund et al.(1999), "Sensory Evaluation of Indoor Air Quality" European Collaborative Action, Indoor Air Quality & Its Impact On Man, Report No 20., European Comission Joint Research Centre – Environmental Institute.

48. Parine, Oreszczyn: "Occupant, trained and untrained panel responses to indoor air quality", Proceedings Indoor Air '96, Volume 1, 1996, pp. 429-434.

49. Bluyssen, Elkhuizen: "Performance of trained and untrained panels in Europe", Indoor Air '96, Volume 1, 1996, pp. 1053-1058.

50. Foreningen Dansk inneklima merkning: "Prøvningsstandard til bestemmelse af afgasning fra byggevarer", DIM, Revidert pr. 14 januar 1997. (In Danish)

51. Dansk selskap for Indeklima: "Introduktion til principperne bag inneklimamærkningen", Dansk Teknologisk Institutt, 1999. (In Danish).

52. Gustafsson, Jonnson (1993),"Trade standards for testing chemical emissions from building materials. Part 1 : Measurements of flooring materials" Proceedings Indoor Air '93, Volume 2, pp. 437-442.

53. NKB: "Nordisk seminarium om inneklimamerkningsordninger", Nordisk komiten for byggbestemmelser (NKB), Inomhusklimatutskottet., Informationbrev 1/1995. (In Swedish)

54. Dokka: "Sink- and source modelling", Working report 5/99, Dep. of Industrial Economy and Technology Management, Norwegian University of Science and Technology, 1999, (In Norwegian).

55. Sparks et.al.: " Modelling Individual Exposure from Indoor Sources" In ASTM STP 1205 : Modelling of Indoor Air Quality and Exposure, Ed. N.L. Nagda., ASTM Philadelphia, 1993.

56. Chang J.C.S., Gou Z., "Characterization of Organic Emission from a Wood Finishing Product – Wood Stain", Indoor Air, Volume 2, 1992, pp. 146–153.

57. Colombo et. al., " Chamber Testing of Organic Emission from Building and Furnishing Materials". The Science of the Total Environment, 91, 1990, pp. 237 – 249.

58. Pettenkoffer : "Uber den luftwechsel in wohngebauden", Munich, Literarich-Artistische Anstalt der J.G. Gotta'schen buchhandlung, 1858.

59. Bluyssen: " Air quality evaluated by a trained panel", Ph.D.-thesis, 1990, Technical university of Denmark

60. Brown: "Assessment of pollutant emissions from dry-process photocopiers, Indoor Air, Volume 9, 1999, pp. 259-267.

61. Malvik, Bjørseth: "Intermittent VOC emissions in buildings", Proceedings Indoor Air '99, Volume 1, 1999, pp. 476-480.

62. Vejrup: "Kemiske stoffer fra rengøringsmidler og deres betydning for inneklimaet", Ph.D. thesis, 1996, Arbeidsmiljøinstituttet & Danmarks Tekniske Universitet. (In Danish)

63. Jørgensen: "The influence of material surfaces on indoor air quality. Adsorption and desorption of volatile organic compounds", Phd-thesis, Department of Industrial Economics and Technology Management, Norwegian University of Science and Technology, 1999.

64. Jørgensen, Bjørseth: " Sorption behaviour of volatile organic compounds on material surfaces - the influence of combinations of compounds and materials compared to sorption of single compounds on single materials", Environment International, Vol. 25 (1), 1999, pp 17-27

65. Dunn, Tichenor: " Compensating for sink effects in emission test chambers by mathematical modelling", Atmospheric Environment, Volume 22, 1988, pp. 885-894.

66. Tichenor et al., "The interaction of Vapour Phase Organic Compounds with Indoor Sinks" Indoor Air, Volume 1, 1991, pp.23-35.

67. Hansson, Stymne: "Determination of material parameters for sorption of gaseous contaminants on indoor surfaces". Proceedings of Roomvent '98, Volume 1, 1998, pp. 513- 520.

68. Dunn, Chen: "Critical evaluation of the Diffusion Hypothesis in the theory of Porous Media Volatile Organic Compound (VOC) Sources and Sinks" In: ASTM STP 1205 : Modeling og Indoor Air Quality and Exposure, Ed. N.L. Nagda., ASTM Philadelphia, 1993.

69. Christenssen et al.: "Compartment Modelling of Emission, Uptake, and Reemission of Volatile Air Pollutants in a Ventilated, Furnished Room" Paper presented at the conference : Indoor Air Quality '92, Environment for People, California, 1992.

70. Axley: "Adsorption Modelling for Building Contaminant Dispersal Analysis", Indoor Air, Volume 2, 1991, pp. 147-171.

71. Van der Wal, Van Leeuwen, Hoogeveen: "A Quick Screening Method for the Sorption Behaviour of Chemicals on Indoor Materials", Proceedings of Healthy Buildings'94, Volume 1, 1994, pp. 253-258.

72. De Bortoli, Knöppel, Columbo, Kefalopoulos: (1996) "Attempting to Characterize the Sink Effect in a Small Stainless Steel Test Chamber", In: Characterizing Sources of Indoor Air Pollution and Related Sink Effects, ASTM STP 1287, 1996, pp. 307-320.

73. Kukadia, Perera: "European NatVent™ Project Completed". AIR INFILTRATION REVIEW, Volume 20, No.2, March 1999, pp.1-4 (see also : www.aivc.org/vina.html, www.aivc.org/natvent98.html)

74. IEA-ECBCS Annex 35: Hybvent, International Energy Agency (IEA).

75. Liddament: "A guide to energy efficient Ventilation", Air Infiltration and Ventilation Centre (AIVC), 1996.

76. Sherman, Modera: "Comparison of Measured and Predicted Infiltration Using the LBL Infiltration model." In: "Measured air leakage of buildings", ASTM STP 904, 1986.

77. Allard, Dorer, Feustel et al.: "Fundamentals of the multi-zone air flow model - COMIS", Technical note 29, Air Infiltration and Ventilation Centre (AIVC), 1990.

78. Walton: "CONTAM96 : a multi-zone airflow and contaminant dispersal model with a graphical user interface", Proceedings 17th AIVC Conference, Volume 1, 1996, pp. 353-355.

79. Olufsen: "Trykforhold i bygninger", Chapter 15 in : Hansen, Kjerulf-Jensen, Stampe : "Varme- og Klimateknik, Grundbog, danvak, 1992 (In Danish)

80. Tjelflaat, Sandberg: "Assessment of ventilation- and energy-efficiency in design for Large Enclosures". Proceedings ROOMVENT '96, 1996.

81. Skåret: "Ventilasjonsteknikk", Kompendium Institutt for VVS, Norge Tekniske Høgkole, Trondheim, 1986. (In Norwegian)

82. Koganei, Holbrook, Olesen, Woods: "Modelling the thermal and indoor air quality performance of vertical displacement ventilation". Proceedings Indoor Air '93, Volume 5, 1993, pp. 241-426.

83. FLOVENT, " A commersial CFD porgram for modelling indoor air flow", from Flometrics Ltd, UK. http://www.flovent.com/

84. VORTEX-2. "A commercial CFD program for modelling indooor air flow", from Flowsolve Ltd, UK. http://ourworld.compuserve.com/

85. Quingean et al. "Measurement and computation of ventilation efficiency and temperature efficiency in a ventilated room". Energy and Buildings, Volume 12, 1988.

86. Jacobsen, Nielsen: "Numerical modelling of thermal environment in a displacement ventilated room". Proceedings Indoor Air '93, Volume 5, 1993, pp.301-306.

87. Olander, Johansson, Johansson: "Tobacco smoke removal with room air cleaners", Scandinavian Journal of Working Environment Health, Volume 14, 1988, pp. 390-397.

88. Darlington, Chan, Malloch, Pilger, Dixon: "Biofiltration of indoor air: Implication for air quality", Indoor Air, Volume 10, 2000, pp. 39-46.

89. Fjeld, Levy, Bonnevie, Sandvik, Veiersted, Riise: "Foliage plants both with and without additional full-spectrum fluorescent light, may reduce indoor air health- and discomfort complaints", Proceedings Indoor Air '99, Volume 4, 1999, pp. 616-621.

90. de Gids, Phaff: "Ventilation Rates and energy consumption due to open windows - A brief overview of research in the Netherlands." Air Infiltration Review 4 (1), 1982.

91. Clausen, Laursen, Wolkoff, Rasmusen, Nielsen: "Emission of Volatile Organic Compounds from a Vinyl Floor Covering" In : ASTM STP 1205 : Modelling of Indoor Air Quality and Exposure, American Society for Testing of Materials, Philadelphia, 1993, pp. 3-13.

92. Little, Hodgson: "A Strategy for Characterizing Homogeneous, Diffusion-Controlled, Indoor Sources and Sinks" In ASTM STP 1287: Characterizing sources of indoor air pollution and related sink effects, American Society for Testing of Materials, 1996, pp. 294-304.

93. BS 5925: 1991: "Code of practise for ventialtion principles and designing for natural ventilation", British Standard Institute, 1991

94. Dorer et al.: "Calculation methods for determination of air flow rates in dwellings", CEN TC 156/WG2/AHG4/N8 (Draft), 1995.

95. Feustel: "Development of a simplified multi-zone infiltration model", Proceedings 6th Air Infiltration Centre (AIC) Conference, 1985.

96. Feustel, Sherman: "A simplified model for predicting air flow in multizone structures", Energy and Buildings, Volume 13, 1989, pp. 217-230.

97. Togari et al.: "A simplified model for predicting vertical temperature distribution in large spaces" ASHRAE Transactions, Vol.99, Part 1. pp. 84-99.

98. Inard et al., "Use of zonal model for prediction of air temperature distribution in large enclosures" Proceedings ROOMVENT '96, Yokohama, Japan, Volume 2, pp. 177-184.

99. Bluyssen et al., "Evaluation of VOC Emissions from Building Products – Solid Flooring Products" European Collaborative Action, Indoor Air Quality & Its Impact On Man, Report No 18. European Commission Joint Research Centre – Environmental Institute, 1997.

100. Andersson, Bjørseth, Clausen, Langkilde, Gabrielsson, Hult, Lindvall, Rengholt: "Klasseindelade inneklimasystem", SCANVAC, Svenska inneklimainstituttet, 1991.

101. Øie, Mørck, Børresen, Hersoug, Madsen: "Selection of building materials for good indoor air quality", Proceedings Indoor Air '93, Volume 2, 1993, pp. 629-634.

102. Swedish National Flooring Association and the Swedish National Testing and Research Institute, Trade standard : Measurement of Chemical emission from flooring materials, Stockholm, 1992.

103. Wolkoff, Nielsen: "Indoor climate labeling of building materials: The experimental approach for a prototype", In: Characterizing Sources of Indoor Air Pollution and Related Sink Effects, ASTM STP 1287, 1996, pp. 331-349.

104. Mølhave, Clausen, Berglund, de Ceaurritz, Kettrup, Lindvall, Maroni, Pickering, Risse, Rothweiler, Seifert, Younes:, "Totale volatile organic compounds (TVOC) in indoor air quality investigations", Indoor Air, Volume 7, 1997, pp. 225-240.

105. Andersson et al. (1997), "TVOC and Health in Non-industrial Indoor Environments.Report from a Nordic scientific consensus meeting at Långholmen in Stockholm, 1996", Indoor Air, Volume 7, pp. 78-91.

106. Brinke, Selvin, Hodgson, Fisk, Mendell, Koshland, Daisey, "Development of new volatile organic compound (VOC) exposure metrics and their relationship to "Sick building syndrome" symptoms", Indoor Air, Volume 8, 1998, pp. 140-152.

107. Norske byggeforskrifter av 22 januar 1997, nr. 33, Kommunal- og arbeidsdepartementet, Utgis av: Cappelen Akademiske forlag. (In Norwegian)

108. Ren Veiledning til teknisk forskrift til Plan og bygningsloven av 1997, Statens byggetekniske etat (BE), 1997. (In Norwegian)

109. Brown: "Pollutant emission properties of photocopiers and laser printers", Proceedings Indoor Air '99, Volume 5, 1999, pp. 123-128.

110. Eatough: "Assessing exposure to environmental tobacco smoke", In: Modeling of Indoor Air Quality and Exposure, ASTM STP 1205, ASTM, Philadelphia, 1993.

111. Jørgensen, Knudsen, Fanger: " The influence on indoor air quality of adsorption and desorption of organic compounds on materials", Proceedings Indoor Air '93 , Volume 2, 1993, pp. 383-388.

112. Orme, Liddament, Wilson: "An analysis and data summary of the AIVC's numerical database", Technical note 44, AIVC, 1994.

113. Ramstad (Editor), "Trehus", Håndbok 38, Norwegian Building Research Institute (NBI), 1990. (In Norwegian)

114. Dokka: "Models in SCIAQ Pro; Fundamentals of the transient simulation model SCIAQ Pro; Simulation of Climate and Indoor Air Quality, Working report no. 7/99, Departement of Industrial Economy and Technology Management, NTNU,1999.

Paper I

Dokka T.H., Bjørseth O., Hanssen S.O.

"EnviSim; A windows application for simulation of IAQ",

Proceedings Indoor Air 96' Nagoya, Volume 2, pp. 491-496.

ENVISIM; A WINDOWS APPLICATION FOR SIMULATION OF IAQ

TH Dokka[1], Dr. O.Bjørseth[1], Prof. SO Hanssen[2]

[1]Dept. Ind. Management & Work Science, Norwegian University of Science and Technology
[2]Dept. Refrigeration and Air Conditioning, Norwegian University of Science and Technology

ABSTRACT

Indoor Air Quality(IAQ) is influenced by several factors, i.e. indoor sources, sink effects, outdoor air quality, infiltration, ventilation strategy, ventilation effectiveness, use of air cleaners. It is therefore important to take into consideration all this factors when evaluating IAQ in rooms and buildings. This paper presents a general dynamic mass balance model, which incorporate the most significant factors. Based on this model a user-friendly Windows application has been developed. This program simulate concentrations of TVOC, CO_2, and single VOC-components. A database of building tightness, climatic data, data for air cleaners and active filters, etc., is implemented in the program. Examples of data for emission rates, sink rate data and outdoor air condition are also included in the database. The model and the program will be further refined and validated during the PhD study of Tor Helge Dokka.

NOMENCLATURE

A_{sink}	Total area of sink surface in the room (m^2)
C_a	Concentration of contaminants in the sink ($\mu g/m^2$)
C_i	Concentration of contaminants in the room air(in the breathing zone) ($\mu g/m^3$)
C_{ex}	Concentration of contaminant in the external air ($\mu g/m^3$)
C_e	Concentration of contaminant in the extract air ($\mu g/m^3$)
C_s	Concentration of contaminant in the supplied air ($\mu g/m^3$)
g	Total release of contaminants in the room, from building materials, persons, smoking, and appliances : ($\mu g/h$)
L_{ac}	Air capacity air cleaner (m^3/h)
L_s	Supply air through the ventilation system (m^3/h)
L_e	Extracted air through the ventilation system (m^3/h)
k_A	Mean adsorption-coefficient for the sink surfaces in the room (m/h)
k_d	Mean desorption coefficient for the sink surfaces in the room (h^{-1})
q_{ex}	Exfiltration of air from the room (m^3/h)
q_{inf}	Infiltration of external air to the room (m^3/h)
t	Time (h)
ε	Ventilation effectiveness, defined by : $\varepsilon = (C_e - C_s)/(C_i - C_s)$ (-)
η_{ac}	Air cleaner efficiency (-)
η_{ex}	Fresh air filter efficiency (-)

INTRODUCTION

Analysis of thermal environment in rooms and buildings are often done using advanced simulation programs. These programs/computer models take into consideration different heat sources, such as : radiation through windows, persons, appliances, lighting, and their variation with time. They also simulate HVAC[1]-installations, infiltration, heat transmission and heat accumulation in the building structure. With such tools the thermal environment (and

[1] HVAC = Heating, Ventilation and Air Conditioning.

energy use) can be predicted, and air conditioning can be dimensioned and optimised properly.

Design of the atmospheric environment in rooms and buildings are seldom done in the same rational way as the thermal environment. Prediction of IAQ when projecting new buildings is often neglected, or done in a superficial way. Standards and regulation often describes a minimum fresh air supply dimensioned after the number of persons in the room. Such design/dimensioning take no consideration of external air quality, filtration of air, ventilation effectiveness, emission from building materials, technical equipment and other sources, sink effects on surfaces, and more. The olf/decipol method developed by Prof. Fanger, which is central in the new European CEN-standard : Ventilation in Buildings, \1\, is a step towards a more rational way of designing atmospheric environment. But even this method neglect sink effects and variation in concentration levels, which can be important. Another disadvantage of the olf/decipol method, is that evaluation of air quality is based on subjective values that can't be measured physically.

It is therefore important to developed more objective methods for prediction of IAQ, which can be used for design of atmospheric environment in room and dimensioning of ventilation systems (natural and mechanical).

A mathematical model for prediction of concentration in rooms and single zones has been developed, and is validated and further refined in a PhD study. The present model has also been implemented in a user friendly Windows application called EnviSim.

PHYSICAL MODEL; MATHEMATICAL FORMULATION

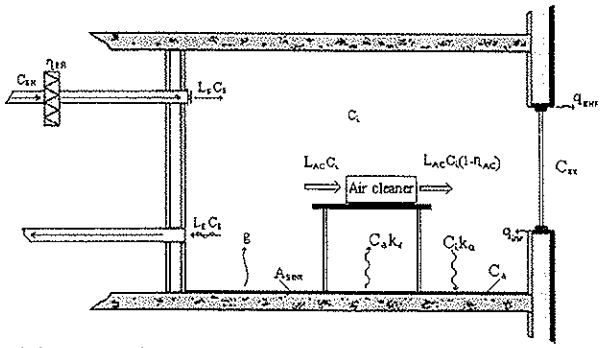

Figure 1 : Schematic contaminant model of a room

Figure 1 shows the physical model used in EnviSim. This is a single zone contaminant model, based on the following main assumptions :

- Contaminant transport between rooms/zones are negligible or balanced
- Concentration gradients in the room can be characterised by a ventilation effectiveness, and that this effectiveness don't vary significantly with time
- Adsorption and desorption of contaminants can be modelled with the dynamic Langemuir isotherm proposed by Tichenor, \2\
- All sources, ventilation, infiltration/exfiltration, external concentration, etc. are assumed to be constant in each timestep
- Exfiltrated air has the same concentration as in the breathing zone
- Infiltrated air has the same concentration as the external air

To analyse the variation of concentration with time in the room we need to formulate the contaminant mass balance in the air, and the mass balance for the contaminant in the sink (here schematically shown as a carpet, fig.1).

A dynamic mass balance for the contaminant in the room air can be stated as (see fig. 1) :

$$\overbrace{V\frac{dC_i}{dt}}^{\text{Rate of change}} = \overbrace{g + L_{sup}C_{sup} + q_{inf}C_{ex} + k_a A_{sink}C_a}^{\text{Sources / supply}} - \overbrace{\left(q_{exf}C_i + L_{ex}C_e + L_{ae}\eta_{ae}C_i + k_d A_{sink}C_i\right)}^{\text{Sinks / extract}} \tag{1}$$

where : $C_s = C_{ex}(1-\eta_{ex})$ **and** $C_e = \varepsilon C_i + (1-\varepsilon)(1-\eta_{ex})C_{ex}$

Similarly a mass balance for the sink gives :

$$\overbrace{A_{sink}\frac{dC_a}{dt}}^{Rate\ of\ change} = \overbrace{A_{sink}k_a C_i}^{Supply} - \overbrace{A_{sink}k_d C_a}^{Extract} \tag{2}$$

Mathematical solution

Equations (1) and (2) is in mathematical terms called a 2-dimensional nonhomogeneous linear system. It can more nicely be written as :

$$\begin{aligned}\frac{dC_i}{dt} &= -\alpha C_i + \beta C_a + \delta \\ \frac{dC_a}{dt} &= \varepsilon C_i - \varphi C_a\end{aligned} \tag{3}$$

Where :

$$\alpha = \frac{q_{exf} + L_{ex}\varepsilon + L_{ae}\eta_{ae} + k_d A_{sink}}{V}\ (h^{-1})\ ;\ \beta = \frac{k_a A_{sink}}{V}\ (h^{-1});$$
$$\delta = \frac{g + L_{sup}C_{ex}(1-\eta_{ex}) + q_{inf}C_{ex} - (1-\varepsilon)(1-\eta_{ex})C_{ex}L_{ex}}{V}\ \left(\frac{\mu g}{m^3 h}\right); \varepsilon = k_a\left(\frac{m}{h}\right)\ ;\ \varphi = k_d\left(h^{-1}\right) \tag{4}$$

Solution of equation (3) can be accomplished with a variety of methods, such as Laplace transform, transform to a second order differential equation, operator methods, and so on. It is here preferred to use linear algebra, with the eigenvalue/eigenvector method.

It is useful to first calculate the equilibrium(stationary) solution of (3), setting $dC_i/dt = dC_a/dt = 0$:

$$C_{i,\infty} = \frac{\delta\varphi}{\alpha\varphi - \varepsilon\beta} \quad ; \quad C_{a,\infty} = \frac{\delta\varepsilon}{\alpha\varphi - \varepsilon\beta} \tag{5}$$

To simplify the solution of equation (3) it is convenient to introduce the new variables, X_i and X_a , given by[2] :

$$X_i = C_i - C_{i,\infty} \quad ; \quad X_a = C_a - C_{a,\infty} \tag{6}$$

Substituting the new variables, X_i and X_a, into equation (3) gives raise to the new homogeneous system :

[2] These new variables transform the equilibrium point ($C_{i,\infty}$,$C_{a,\infty}$) down to origo (0,0).

$$\frac{dX_i}{dt} = -\alpha\, X_i + \beta\, X_a$$

$$\frac{dX_a}{dt} = -\varepsilon\, X_i - \varphi\, X_a \qquad (7)$$

Equation (7) can be formulated in vector-matrix form as :

$$\begin{bmatrix} \dot{X}_i \\ \dot{X}_a \end{bmatrix} = \begin{bmatrix} -\alpha & \beta \\ \varepsilon & -\varphi \end{bmatrix} \begin{bmatrix} X_i \\ X_a \end{bmatrix} \Leftrightarrow \dot{\mathbf{X}} = \mathbf{A}\mathbf{X} \;\; ; \;\; \dot{X} = \frac{dX}{dt} \qquad (8)$$

where **A** [3] is the coefficient matrix. The general solution of (8) is , \3\ :

$$\begin{bmatrix} X_i(t) \\ X_a(t) \end{bmatrix} = C_1 \mathbf{K}_+ e^{\lambda_+ t} + C_2 \mathbf{K}_- e^{\lambda_- t} \qquad (9)$$

where λ_+ and λ_- are eigenvalues of **A**, $\mathbf{K}_+$ and $\mathbf{K}_-$ are corresponding eigenvectors. C_1 and C_2 are arbitrary constants.

Eigenvalues for the coefficient matrix **A**, are given by :

$$\det(\lambda I - A) = 0 \;\Rightarrow\; \lambda_\pm = \frac{(\alpha+\varphi) \pm \sqrt{(\alpha+\varphi)^2 - 4(\alpha\varphi - \varepsilon\beta)}}{2} \qquad (10)$$

Corresponding eigenvectors for λ_+ and λ_- are :

$$\mathbf{K}_+ = \begin{bmatrix} 1 \\ \dfrac{\alpha+\lambda_+}{\beta} \end{bmatrix} = \begin{bmatrix} 1 \\ \Lambda_+ \end{bmatrix} \;\; ; \;\; \mathbf{K}_- = \begin{bmatrix} 1 \\ \Lambda_- \end{bmatrix} \;\; ; \;\; \Lambda_\pm = \frac{\alpha+\lambda_\pm}{\beta} \qquad (11)$$

The constants in (9), C_1 and C_2, can be determined by the initial values(concentrations) : $C_i(t=0) = C_{i,0}$ and $C_a(t=0) = C_{a,0}$:

$$X_i(t=0) = X_{i,0} = C_{i,0} - C_{i,\infty} \;\; ; \;\; X_i(t=0) = X_{a,0} = C_{a,0} - C_{a,\infty} \qquad (12)$$

Substituting the initial values into equation (9) gives :

$$\begin{bmatrix} X_{i,0} \\ X_{a,0} \end{bmatrix} = C_1 \mathbf{K}_+ + C_2 \mathbf{K}_- = \begin{bmatrix} 1 & 1 \\ \Lambda_+ & \Lambda_- \end{bmatrix} \begin{bmatrix} C_1 \\ C_2 \end{bmatrix} \qquad (13)$$

Using for instants Cramer's rule[4] gives C_1 and C_2 :

$$C_1 = \frac{X_{i,0}\Lambda_- - X_{a,0}}{\Lambda_- - \Lambda_+} \;\; ; \;\; C_2 = \frac{X_{a,0} - X_{i,0}\Lambda_+}{\Lambda_- - \Lambda_+} \qquad (14)$$

[3] Matrices and vectors are written with bold types

[4] Cramer's rule is a convenient method for solving small systems of linear equations. For definition and proof see \3\ page 93.

The final solution to equation (3), substituting to the original variables C_i and C_a, is then given by :

$$C_i(t) = C_1 e^{\lambda_+ t} + C_2 e^{\lambda_- t} + C_{i,\infty}$$
$$C_i(t) = C_1 \Lambda_+ e^{\lambda_+ t} + C_2 \Lambda_- e^{\lambda_- t} + C_{a,\infty} \quad (15)$$

Infiltration

Calculation of infiltration (and exfiltration) in EnviSim is done with the recognised Lawrence Berkley Infiltration Model, \5\, which is a theoretically derived infiltration model, taking account for wind-, and temperature forces and mechanical fans. Transient infiltration through large openings like windows and doors, are predicted by an semiempirical model proposed by de Gids and Phaff, \6\. This model takes account for temperature and wind driven infiltration.

Sources

EnviSim differs between four different source types : Constant emission from materials and furniture(TVOC and single component VOC), emission from persons (CO_2 and TVOC), emission from smoking (TVOC), and emission from various equipment (TVOC and single component VOC). Emission from materials and furniture are calculated by a stationary emission factor :

$$g = g'' A \quad (16)$$

where g is the emission from the material (µg/h), g" : Stationary emissionfactor (µg/m²h), A : surface area material (m²). Emission of TVOC from persons are based on Bluyssen \7\, and set to 760 µg/h. Emission of TVOC from an average smoker (timeaverage) are set to 2800 µg/h, based on \8\. Emission from equipment are set by the user, as an on-off source.

IMPLEMENTATION

The described model have been implemented in a Windows application called EnviSim, and applied for simulation of CO_2 , TVOC and single components of VOC. The simulation timestep is user selectable between 5 minutes and 1 hour. To ease input procedures the program contains a databases with building tightness, climatic data, data for air cleaners, active filters, examples of emission rates , and more.

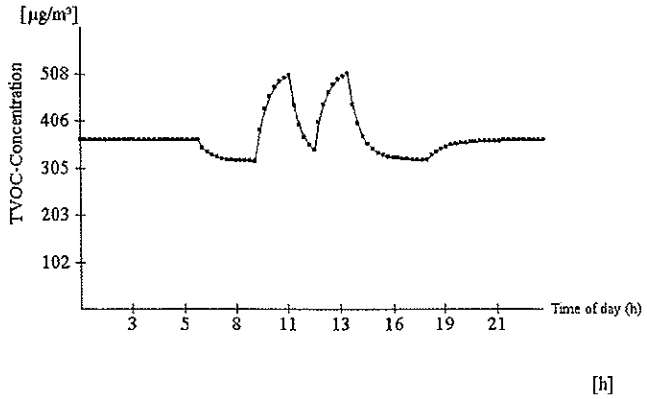

Figure 2 : Analysis of TVOC-concentration in a meeting room

Figure 2 shows an example from EnviSim, analysing TVOC-concentration in a meeting room. The meeting room, with 15 m^2 floor area, is used between 9 -11 and 12 - 14, by 7 persons, where 50 % are smokers. The emission from building materials and furniture are constant (4450 µg/h). The room is ventilated with 1.5 ACH between 06.00-18.00, and with 0.75 ACH between 18.00 and 06.00. Constant concentration in the external air are : 230 $\mu g/m^3$ (near traffic). Sinks effects on materials are moderate.

CONCLUSION

The computer model in EnviSim needs further refinement and validation, this will be done in an ongoing PhD study. The quality of the model is also dependent on good input values; the most central data are :

- Real emission data for different sources
- Characterisation of external air quality
- Sink rate data for different materials

Data will be collected in lab- and field experiments, and by literature studies, during the PhD study.

REFERENCES

\1\ *Ventilation for buildings; Design Criteria for the Indoor Environment* CEN prENV 1752, December 1994

\2\ Tichenor, BA; Guo, Z.; Dunn, ED; et al.(1991), The Interaction of Vapour face Organic Compounds with Indoor Sinks. *Indoor Air, International Journal of Air quality and Climate, 1/96*

\3\ Zill, DG *A first course in DIFFERENTIAL EQUATIONS* 5th edition, THOMSON INFORMATION/PUBLISHING GROUP

\4\ Anton, H and Rorres, C. *ELEMENTARY LINEAR ALGEBRA*, 6th edition, John Wiley & Sons

\5\ Sherman, MH and Modera, PM (1986) Comparison of Measured and Predicted Infiltration Using the LBL Infiltration model. *Measured air leakage of buildings, ASTM STP 904, ed. Trechsel and Lagus.*

\6\ de Gids, W and Phaff, H (1982) Ventilation Rates and energy consumption due to open windows - A brief overview of research in the Netherlands. *Air Infiltration Rev.* 4 (1), 4-5.

\7\ M. Bluyssen, PM. *Air quality evaluated by a trained panel* . PhD Thesis 1990, Technical university of Denmark.

\8\ Olander, L; Johansson, J; *Arbete og helsa, Luftrenarens effekt på tobakksrøk* (Swedish), Arbetsmiljøinstitutet

Paper II

Dokka T.H., Jørgensen R.B., Bjørseth O., Malvik B.

"Comparison of field experiments in a refurbished bedroom with small chamber experiments"

Proceedings Indoor Air 99' Edinburgh, Volume 5, pp. 93-98.

COMPARISON OF FIELD EXPERIMENTS IN A REFURBISHED BEDROOM WITH SMALL CHAMBER EXPERIMENTS

T.H.Dokka[1], R.B.Jørgensen[1], O.Bjørseth[1], B. Malvik[2]

[1]Department of Industrial Economy & Technology management, Norwegian University of Science and Technology
[2] SINTEF, Foundation for Scientific and Industrial Research at the Norwegian Institute of Technology

ABSTRACT

Emission testing in small test chambers has become the most commonly used method to evaluate the effect of building materials on IAQ in buildings. Emission testing in chambers is economically favourable and enables test conditions to be controlled. The question, however, is can small chamber testing be used to evaluate and predict IAQ in real indoor environments. Earlier experiments have indicated that concentrations in chambers are considerable higher than those found in field experiments.

This study compares experiments performed in a small steel chamber with a controlled field experiment in a refurbished bedroom. Mathematical models are used to predict the concentration of TVOC in the bedroom based on chamber data, and compares this with the measured concentration in the bedroom.

The predicted concentration in the bedroom is found to be up to ten times as high as the measured concentration in the bedroom. The paper provides hypothesis that can explain this discrepancy.

INTRODUCTION

In the last two decades there has been an increased awareness that the emission of volatile organic compounds (VOC) from building materials can reduce the indoor air quality (IAQ) in buildings. Standards and building codes have also begun to take pollution from building materials into consideration when designing IAQ, or establishing requirements for ventilation rates. This has led to a need for evaluation of emissions from building materials. To do this economically and efficiently, small test chambers have been used to measure the emissions from building materials. Samples of a building material are placed in a test chamber (usually made of steel or glass), in which the air exchange rate, temperature and humidity are controlled.

The question, however, is whether this small chamber testing can be used to evaluate or predict IAQ in real indoor environments (rooms or buildings). Some comparison experiments indicate that concentrations in chambers are considerably higher than those found in field experiments, [1], [2].

This paper compares calculated concentrations based on data from chamber experiments, with measured concentrations in a controlled field experiment (a refurbished bedroom).

METHODS

Chamber experiments

The chamber experiment was performed in a small steel chamber with a volume of 100 litres. An aluminium plate with a dimension of 0.3 m x 0.4 m was painted with a water-based paint and placed in the steel chamber. The water-based paint was selected from three tested water-based paints, and was chosen because of its high emission rate. The air exchange in the chamber was approximately 1.0 ACH, and the temperature and relative humidity (RH) in the chamber were respectively 21 °C (± 0.4 °C) and 53 % (± 4 %). VOC samples were collected using Tenax TA (250 mg tubes) and analysed using GC -MS. For desorption of the samples we used a Perkin Elmer ATD 400 unit. The Perkin Elmer Autosystem GC was equipped with a capillary column, CP-Wax 52-CB. The mass spectrometer was a Perkin Elmer Turbomass. For quantification purposes an external standard of toluene was used.

Air samples were taken frequently during the first week (several samples each day), followed by one samples per day for subsequent days. Air samples were taken less frequent during the last two weeks of the experiment The experiments were concluded after 30 days. This paper only includes TVOC values based on toluene as standard.

Field experiments

The field experiment was carried out in an unoccupied bedroom (sealed of from other rooms in the building). The bedroom had a volume of 20 m^3, and a floor area of 8.7 m^2. The walls in the bedroom were painted with the same water-based paint as used in the chamber experiments. The bedroom was ventilated by a small vent in the frame of the bedroom-window. The air exchange rate was measured at 0.15 ACH, which was calculated from a CO_2 decay experiment. The temperature in the bedroom was kept at 22 °C by a thermostatically controlled panel heater. The same chemical analysis and analytical conditions as in the chamber experiment were used. Air samples were taken frequently during the first week, and thereafter one sample each day. From day 10, and up to day 29 when the experiment was concluded, air samples were taken less frequently.

The walls of the bedroom consisted of hard particle board drawn with wall covering. The ceiling consisted of painted particle board, and the floor was covered by a nylon carpet.

A model for the test chamber

Since volumes, air change rate, loading (ratio of area/volume), and so on are different between the chamber and field experiments, mathematical models are needed to compare the resulting concentrations from the two experiments. To calculate concentrations in the bedroom, emission factors from the chamber experiment are required. Since emissions from painted surfaces often have exponential decaying profiles, the following expression is used to describe the time-dependent emission factor (g") of the painted surface :

$$g''(t) = g_0'' \exp(-at) \quad (1)$$

g" : time-dependent emission factor (µg/m²h), g''_0 : initial emission factor (µg/m²h), a : emission decay rate (h^{-1}) and t : time (h).

In general equation (1) cannot be used to fit concentration data from a chamber experiment, since the concentration also depends on the loading (painted area/volume) and the air change rate of the chamber. To fit concentration data, we have to make a model for the chamber, based on a mass balance. In a chamber with air change rate n, "source loading" L_{source} (painted area/chamber volume), and a decaying source as (1), the mass balance for the chamber can be written as :

$$\frac{dC}{dt} = -nC + L_{source} \cdot g_0'' \exp(-a \cdot t) \qquad (2)$$

C : concentration in the chamber ($\mu g/m^3$), n : air change per hour (h-1), L_{source} : source loading (m^2/m^3). If we assume that the initial concentration is zero : C(t = 0) = 0 , the solution to equation (2) is :

$$C(t) = \frac{L_{source} g_0''}{n - a}\left[\exp(-at) - \exp(-nt)\right] \qquad (3)$$

Given the measured concentration in the chamber as a function of time, a curve fitting routine can estimate the emission factor : g''_0 , and the rate constant : a. This model is based on the assumption of complete mixing in the chamber, and that the sink effect of the chamber walls are negligible.

A model for the bedroom

To model the bedroom we cannot ignore the sink effect. If we take as a basis the well-known sink model developed by Tichenor [3], and modify it with a exponential decaying source as described by eq. (1), the mass balance for the room air and the sink surfaces can be written as:

$$\frac{dC}{dt} = -\left(n + L_{sink} \cdot k_a\right) \cdot C + L_{sink} k_d M + L_{source} \cdot g_0'' \exp(-a \cdot t) \quad (4)$$

$$\frac{dM}{dt} = k_a C - k_d M \qquad (5)$$

M : Mass in the sink surface ($\mu g/m^2$), k_a : adsorption rate constant (m/h), k_d : desorption rate constant (h^{-1}), L_{sink} : sink surface loading (m^2/m^3) (sink area/room volume). Assuming zero initial concentration and mass in the sink, the solution to the coupled differential equations (4) and (5) is given by :

$$C(t) = C_1 \exp(\lambda_1 t) + C_2 \exp(\lambda_2 t) + a_1 \exp(-at) \qquad (6)$$

$$M(t) = C_1 K_1 \exp(\lambda_1 t) + C_2 K_2 \exp(\lambda_2 t) + b_1 \exp(at) \quad (7)$$

Where :

$$C_1 = \frac{K_2 a_1 - b_1}{K_1 - K_2} \quad ; \quad C_2 = -C_1 - a_1 \qquad (\mu g / m^3)$$

$$\lambda_{1/2} = \frac{-(n + k_a L + k_d) \pm \sqrt{(n + k_a L + k_d)^2 - 4 \cdot k_d n}}{2} \qquad (h^{-1})$$

$$K_1 = \frac{\lambda_1 + k_d}{k_a} \quad ; \quad K_2 = \frac{\lambda_2 + k_d}{k_a} \qquad (m^{-1}) \qquad (8)$$

$$a_1 = \frac{g''_0 L_{source}}{n + L_{sink} k_a \left(1 - \frac{1}{1 - a/k_d}\right) - a} \qquad (\mu g / m^3) \quad ;$$

$$b_1 = \frac{k_a}{k_d - a} a_1 \qquad (\mu g / m^2)$$

With the knowledge of source and sink data, together with the air change rate, equation (6) can be used to calculate the concentration in the bedroom.

RESULTS

Concentration of TVOC from the chamber experiments and the curve-fitted model for the chamber, equation (3), is shown in figure 1. The non-linear curve fitting was executed by the statistical software package SPSS®, and the coefficient of determination was : $R^2 = 0.95$. The estimates of the initial emission factor and the emission decay rate are shown in table 1, together with other physical data for the chamber and the bedroom.

Table 1 : Dimensions, ACH, sink rate data and source data for the calculation

	Steel chamber	Bedroom
Air change rate; n	1.00 h^{-1}	0.15 h^{-1}
Room volume, V	0.1 m^3	19.7 m^3
Sink area (carpet), A_{sink}	-	8.2 m^2
Source area (painted), A_{source}	0.09 m^2	7.1 m^2
Adsorption rate constant, k_a	-	0.286 m/h*
Desorption rate constant, k_d	-	0.172 h^{-1}*
Initial emission factor, g''_o	-	71187 $\mu g/m^2h$**
Emission decay rate, a	-	0.008 h^{-1}**

* This sink rate data is taken from an earlier sorption experiment with nylon carpet and the compound alpha-pinene, see [4].

** Found by curve fitting equation (3) to the test chamber data.

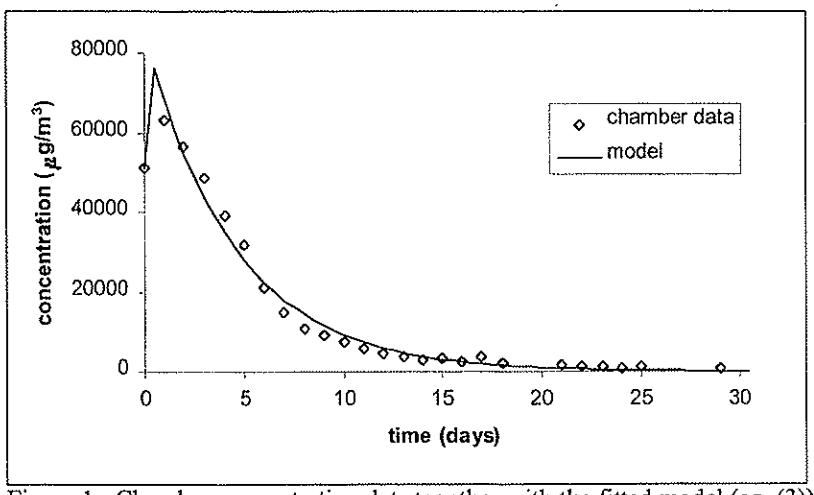

Figure 1 : Chamber concentration data together with the fitted model (eq. (3))

In figure 2 the measured concentration in the bedroom, together with the predicted concentration using equation (6) is shown. Data from table 1 is used in the calculation.

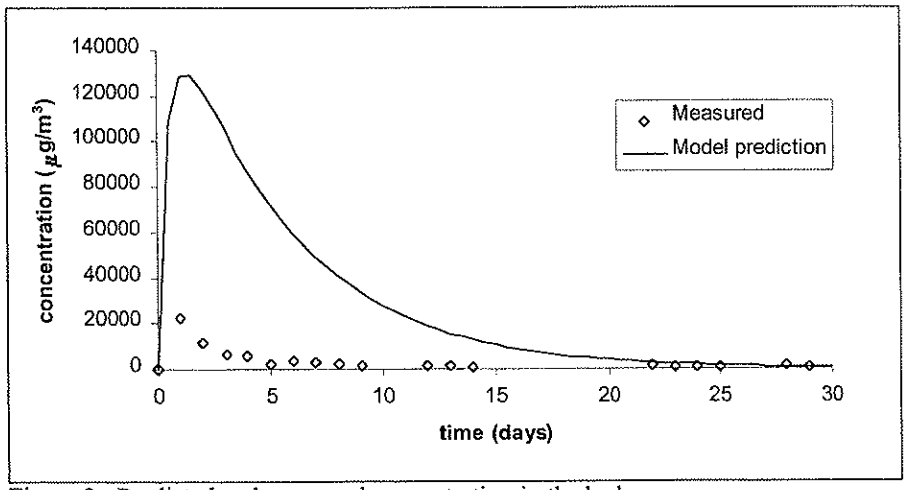

Figure 2 : Predicted and measured concentration in the bedroom

As the figure shows, the difference between prediction and measurement is rather large. Table 2 shows the predicted and measured concentrations after 1, 5, 12, 22 and 29 days.

Table 2 : Measured and predicted TVOC-concentrations in the bedroom

Days :	1	5	12	22	29
Measured (µg/m³)	22671	2510	1784	1084	655
Model prediction (µg/m³)	128400	71950	18770	2752	688

DISCUSSION

The proposed test chamber model, equation (3), seems to describe the decaying TVOC-concentration in the test chamber quite well, making it possible to estimate the initial emission factor ($g"_o$) and the emission rate constant (a).

If we look at the model prediction for the bedroom we see that it is many times higher than the measured concentration in the first 15 days, but that they approach each other after 20 days. After 29 days the predicted and measured concentration are practically the same. The large discrepancy between prediction and measurement could possibly be explained by :

1. Diffusion or "soaking" of paint or compounds in the paint into the painted wall board, with possible chemical bindings. This kind of diffusion or soaking into the painted material has also been reported in [5].
2. Strong surface adsorption with very slow desorption. Cold external walls in the bedroom can theoretically enhance the adsorption and slow the desorption of TVOC. But it is less likely that this effect alone can explain the large difference between prediction and measurement. Reversible adsorption (as modelled here with the Langmuir adsorption isotherm) cannot explain the difference.
3. Since the air exchange and scale of the chamber and the bedroom is quit different, the air velocity at the painted surface is likely higher in the chamber. This can maybe lead to higher and more rapid emission rate in the chamber compared to the bedroom.

It is recommended that further laboratory and field experiments are conducted to investigate this hypothesis.

REFERENCES

1. Tirkkonen, T. and Saarela, K. (1997) "Adsorption of VOCs on Interior Surfaces in a Full Scale Building". Proceedings of Healthy Buildings '97, Washington, Vol. 3, pp. 551-556.

2. Zellweger, C., Gehrig, R., Hill. and Hofer, P. (1995) "VOC Emissions from Building Materials: Comparison of Chamber Emission Data with Concentrations in Real Rooms", in: Maroni, M. (ed.) *Proceedings of Healthy Buildings '95, Milan, Vol. 2, pp.* 845-850.

3. Tichenor, BA; Guo, Z.; Dunn, ED; et al.(1991), The Interaction of Vapour face Organic Compounds with Indoor Sinks. *Indoor Air, International Journal of Air Quality and Climate, 1/96*

4. Jørgensen, R.B. and Bjørseth, O. (1999) " Sorption behaviour of volatile organic compounds on material surfaces - the influence of combinations of compounds and materials compared to sorption of single compounds on single materials", *Environment International,* Vol. 25 (1) pp 17-27

5. Jørgensen R., Bjørseth O., "Emission from wall paint - The influence of the wall material", Proceedings : Healthy Building Milan '95, Vol.2 pp. 977-982

Paper III

Jørgensen R.B., Dokka T.H., Bjørseth O.

"Investigations of the interaction between different ventilation strategies and the adsorption/desorption of VOCs on material surfaces "

Proceedings Indoor Air '99 Edinburgh, Volume 1, pp.402-407.

INVESTIGATION OF THE INTERACTION BETWEEN DIFFERENT VENTILATION STRATEGIES AND THE ADSORPTION/DESORPTION OF VOCs ON MATERIAL SURFACES

R.B. Jørgensen, T.H. Dokka, O. Bjørseth

Department of Industrial Economics and Technology Management, Norwegian University of Science and Technology, Norway.

ABSTRACT

The interaction between different ventilation strategies and adsorption and desorption of VOCs on material surfaces in small test chambers is investigated. Tests exposed nylon carpet to a mixture of toluene and α-pinene at two different source levels. The ventilation strategies were chosen to mimic the conditions in real buildings, i.e. with one air exchange rate during the working day (2 h^{-1}) and another during the remainder of the 24-hour period (0.67 h^{-1}). The software application "EnviSim" was used to model the concentrations in a model room based on the experimental conditions. The results show that the sorption behaviour has to be included when estimating the concentration variations in a room based on source characteristics and ventilation rates. The ventilation strategy influences the resulting concentrations and it is recommended that the ventilation system is "turned on" a couple of hours before the start of the working day and "turned down" again when the occupants have left the building.

INTRODUCTION

The adsorption and desorption of volatile organic compounds (VOC) on material surfaces is often given as the explanation when measured data fail to match expected results. In inter-comparison evaluations, sorption on chamber walls is used to explain differences between different results from different test chambers. In field studies sorption is used to explain differences between material emissions found in test chambers and material emissions found in the field.

During recent years many researchers have demonstrated the fact that material surfaces interact with VOCs. Most of this work involves relatively simple test chamber experiments where material surfaces are exposed to VOCs and the concentration in the test chamber is monitored. Based on this kind of test chamber experiment, models are set up to describe the sorption phenomenon [1]. When these sorption models are implemented as room models, the sorption appears to have a significant influence on the concentration variations of VOCs in the room [2, 3].

There are few experimental validations of the influence of sorption on the concentration of VOCs in real rooms. Sparks et al. [3] have compared data from a test house to modelled concentration predictions and Jørgensen et al. [4] have made theoretical calculations about the influence of sorption on resulting room concentrations. The results indicate that the interaction between sources, sinks, individual activity patterns and ventilation strategies has a major influence on the resulting concentrations in real rooms.

During recent years the intention of ventilation systems has changed [5]. Some countries have introduced ventilation rates based on emissions from the buildings themselves, the ventilation systems and from materials in the buildings. The influence of adsorption on and desorption from material surfaces should be taken into consideration when determining the operation of ventilation systems.

The objective of this paper is to investigate the interaction between different ventilation strategies and adsorption and desorption of VOCs on material surfaces.

METHODS

Study Design

Three different ventilation strategies were evaluated. Each ventilation strategy comprised two different ventilation rates: a low rate used during the night and a high rate used during the day. The only difference between the strategies is the change in the length of the day/night periods used. The ventilation rates and the periods used are shown in table 1.

The experiments were conducted in a 50-L glass test chamber [6] on nylon carpet (composed of 100% polyamide fibres, 100% polypropylene backing and 100% polypropylene textile texture).

Two different pollution sources were used during the experiments and both consisted of a mixture of α-pinene and toluene. The source strength during the day period (working hours) was twice the source strength during the night period, see table 1. This is based on the assumption that the occupants and their activities cause 50% of the VOC contribution, while the building and its materials cause the other 50%. The source levels are relative high due to the monitoring method used. However, this should not influence the results since these are given by the difference between night and day levels.

Table 1: Experimental conditions.

	Strategy 1	Strategy 2	Strategy 3
Day-time ventilation rate	2.07 h^{-1}	2.05 h^{-1}	2.05 h^{-1}
Day-time ventilation period	8.00 - 16.00	6.00 - 18.00	5.00 - 17.00
Night-time ventilation rate	0.66 h^{-1}	0.69 h^{-1}	0.68 h^{-1}
Night-time ventilation period	16.00 - 8.00	18.00 - 6.00	17.00 - 5.00
Source strength - working hours (8.00 - 16.00)	1.136 mg/h	1.082 mg/h	1.100 mg/h
Source strength - night period (16.00 - 8.00)	0.481 mg/h	0.448 mg/h	0.469 mg/h

The temperature was 22.02 °C (± 0.06°C) and relative humidity was 48% (± 2 %). The loading of the nylon carpet was 4.46 m^2/m^3.

In addition, one traditional sorption experiment was performed to establish the sorption constants at the actual pollution level. This experiment is not described in this paper. It was performed in the same test chamber and with the same measuring equipment as the other experiments. The equilibrium concentration before desorption was 9.83 ± 0.10 mg/m^3 (after correcting for the background concentration of 0.93 ± 0.16 mg/m^3), the air exchange rate during the desorption period was 2.04 h^{-1}. This experiment was analysed using Tichenor's one-sink model, assuming Langmuir type of sorption [1]. The sorption constants found were: adsorption rate constant k_a: 0.176 m/h, desorption rate constant, k_d: 0.177 h^{-1}. For method description see Jørgensen et al. [6]. The data analysis was performed by the non-linear curve fitting routine in the statistical software package, SPSS®.

Procedure

A sample of the nylon carpet was placed in the test chamber and conditioned with clean air for one week. The experiments were then performed with high-source dosing during

the working hours and low-source dosing during the rest of the 24-hour period. The air exchange rates were varied, as described in table 1.

Using photoacoustic spectroscopy, the concentration of the test compounds in the exhaust air from the test chamber was measured every 4 minutes. The measuring device used was an Innova 1312 (Brüel&Kjær type 1302). The instrument was calibrated for toluene.

RESULTS

An imagined office with a floor area of 10 m^2 and a volume of 25 m^3 was used to compare the experimental results to modelled concentrations based on the sorption results. The office was ventilated by a mechanical ventilation system. The IAQ program, "EnviSim" [2], is a computer program that has been developed to calculate the resulting concentration in buildings based on given input data. The sorption isotherm used of the program is the Langmuir isotherm [1]. The input data in this example comprises the experimental conditions used (loading, air exchange rates, and sorption constants). The imagined office is covered with nylon carpet and the source strengths are converted so that the resulting concentrations in the model office correspond to the experimental concentrations.

The "EnviSim" program is also used to calculate the theoretical no-sink curve of the imagined office. In this case the sorption constant is omitted, and the rest of the input data are constant. Figures 1-3 illustrate the experimental results and the modelled curves.

The experimental concentrations during the working day are shown in table 2. The values are shown for every hour (mean values from 5 measurements). With respect to comparisons between the experiments, the values are also shown as a percent of the actual equilibrium concentration (C_{eq}) for the experiment. The C_{eq}-values are calculated as mean-values during the equilibrium period.

Table 2: Experimental concentrations (mg/m^3) during the working day.

	C_{eq}	8.00	9.00	10.00	11.00	12.00	13.00	14.00	15.00	16.00
Vent. strategy 1										
Conc. (mg/m^3)	11,11	14,57	12,53	11,86	11,62	11,31	11,36	11,27	11,09	11,06
percent of C_{eq} (%)		131 %	113 %	107 %	105 %	102 %	102 %	101 %	100 %	100 %
Vent. strategy 2										
Conc. (mg/m^3)	10,71	8,06	10,38	10,55	10,78	10,80	10,74	10,76	10,71	10,72
percent of C_{eq} (%)		75 %	97 %	99 %	101 %	101 %	100 %	100 %	100 %	100 %
Vent. strategy 3										
Conc. (mg/m^3)	10.91	8,02	10,52	10,83	11,02	10,96	11,03	11.00	10,89	10,90
percent of C_{eq} (%)		74 %	96 %	99 %	101 %	100 %	101 %	101 %	100 %	100 %

DISCUSSION

In the first strategy the ventilation period is in phase with the pollution periods. This causes the air concentration to be at the maximum at the start of the working day and minimum at the end of the working day. At the end of the working day the air concentration increases since the air exchange rate decreases at that moment.

In the second strategy the air exchange rate increases from approx. 0.67 h^{-1} to approx. 2 h^{-1} two hours before the start of the working day. This means that the air concentration decreases to a low level before the start of the working day and then increases during the first

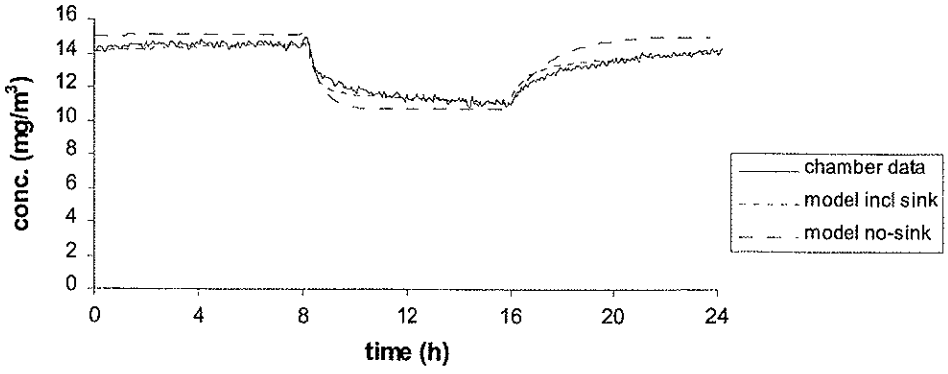

Figure 1: Ventilation strategy 1: day vent. rate 8.00-16.00, night vent. rate 16.00-8.00.

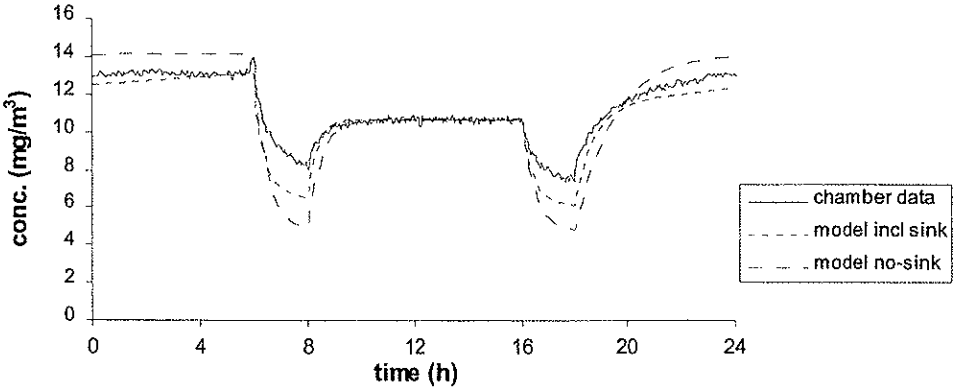

Figure 2: Ventilation strategy 2: day vent. rate 6.00-18.00, night vent. rate 18.00-6.00.

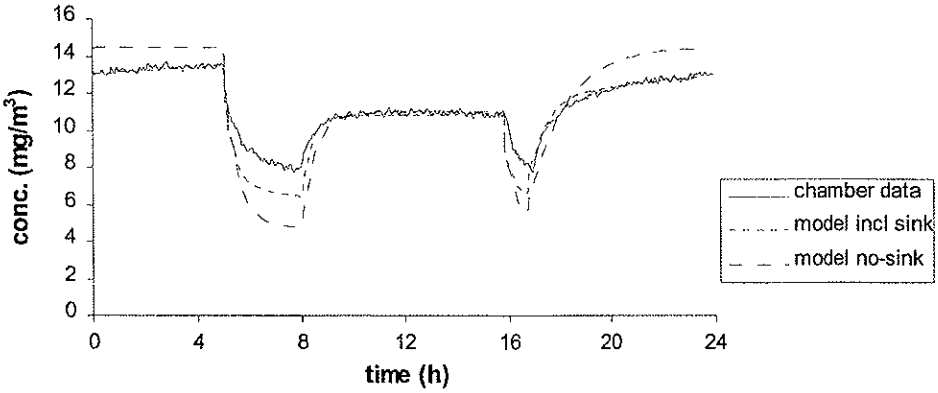

Figure 3: Ventilation strategy 3: day vent. rate: 5.00-17.00, night vent. rate: 17.00-5.00.

working hours. At the end of the working day the pollution source decreases to the "night level", while the air exchange rate remains at the high level for a further two hours. This leads to a decrease in concentration two hours before the ventilation rate is turned down to the "night level" and the air concentration increases correspondingly.

The third strategy is similar to the second strategy, but the ventilation period is moved by one hour and is now at "day level" from three hours before start of the working day to one hour after end of the working day.

The results show that the desorption of pollutants adsorbed during the night contributes to a higher concentration during the working hours when compared with the concentration levels assuming that the sink effect is negligible.

To reduce the concentration during the working hours, especially the first working hours, the ventilation strategy can be modified by elevating the air exchange rate in a period before the start of the working hours. This is done with ventilation strategies 2 and 3. The increased concentration from desorption of pollutants during working hours is reduced as the pollutants are desorbed during the morning.

As it is seen from the figures and table 2 there is a noticeable difference between the concentrations caused by ventilation strategy 1 and the strategies 2 and 3. The pollution sources are approximately equal in the three cases, the difference in ventilation strategies are the only cause to the variations in the concentrations. In strategy 1 the occupants of the building is exposed to a high level of pollution when they start working in the morning. This level decrease during the day until it reach an approximately equilibrium level after noon. The pollution level remains thereafter at this level the rest of the working day.

With ventilation strategies 2 and 3 the concentration profile are different. When the occupants arrive in the morning, the pollution level is low. The pollution level in the building then increases for two-three hours until it reaches its equilibrium level. This means that the difference between ventilation strategy 1 and 2 & 3 is that the occupants with the first strategy are exposed to a higher pollution level before noon, than in buildings ventilated after strategy 2 and 3. Since energy use for running the ventilation system is approximately proportional to the operation period, the choice of ventilation strategy is of crucial importance. Longer operation period gives higher energy use and running costs. When the purpose is to obtain good air quality, the ventilation strategies 2 and 3 are more suitable than strategy 1.

There is little difference between the resulting air concentration during the working day with the ventilation strategies 2 and 3. The concentration decrease during 2 hours (vent. strategy 2) to 8.06 mg/m^3 and during 3 hours (vent. strategy 3) to 8.02 mg/m^3. As seen from table 2, these concentrations are equivalent to 75% and 74% of the equilibrium concentrations. The difference between the concentrations during the working day for the two ventilation strategies is negligible.

Ventilation strategies 2 or 3 are normally selected because several occupants are present in the building after end of the normal working day. This demands for good air quality also in these hours. In the performed experiments the ventilation strategies are used together with an experimental design assuming presence of the occupants only in the period 8.00-16.00, this explain the unnecessarily decrease in concentration after the end of the working day.

Modelling of the results

By applying the k_a and k_d values determined in the simple desorption experiment, the night and day variations of the concentration can be calculated by the "EnviSim" program. The model predicts the concentration curves in a substantial better way when the sink effect is included than when the sink effect is ignored. This shows that the influence of sorption has to

be included when estimating the concentration variations in a room based on source characteristics and ventilation rates.

Implications

The sink effect may also have a positive effect. Occurrence of unusually high exposures causes adsorption of that pollution. The materials may slow down the increase of the concentration of pollution. By optimising the ventilation strategy the desorption of the pollution from the materials can be forced to take place at certain time periods. It is recommended that the interaction between adsorption and desorption and different ventilation strategies and the influence on the indoor air quality is evaluated further.

In these experiments only two diurnal air exchange rates are used. Another approach to minimise the resulting concentration during the working day could be further increase the air exchange rate in the morning hours before the occupants start at work. Air exchange rates could then be 3 h^{-1} from 6.00-8.00, 2 h^{-1} from 8.00-16.00 and 0.67 h^{-1} from 16.00-6.00. This would give a lower concentration in the building when the occupants start at work and with that a lower mean exposure during the working day than the strategies evaluated in this paper. It is recommended that this idea is evaluated further.

CONCLUSION

There is good agreement between the experimental results and the modelled concentrations using a model including the sink effect. Modelled concentrations using a model neglecting the sink effect do not fit the data satisfactory.

The ventilation strategy influence the resulting concentrations and it is recommended that the ventilation system is "turned on" a couple of hours before the start of the working day, and is "turned down " when the occupants has left the building.

The results show that the influence of sorption has to be included when estimating the concentration variations in a room based on source characteristics and ventilation rates.

REFERENCES

1 Tichenor, B A. et al. 1991. The interaction of vapour phase organic compounds with indoor sinks. *Indoor Air*, Vol. 1 (1), pp 23-35.

2 Dokka, T H, Bjørseth, O, Hanssen, S O. 1996. EnviSim; A windows application for simulation of IAQ. *Proceedings of Indoor Air 96*, Nagoya, Vol. 2, pp 491-496.

3 Sparks, E L, Tichenor, B A, White J B. 1993. Modeling Individual Exposure from Indoor Sources. In *Modeling of Indoor Air Quality and Exposure*, N L Nagda, Ed. ASTM STP 1205, Philadelphia, pp 245-256.

4 Jørgensen, R B, Knudsen, H N, Fanger P O. 1993. The influence on indoor air quality of adsorption and desorption of organic compounds on materials. *Proceedings of Indoor Air '93, Helsinki*, Vol. 2, pp 383-388.

5 Fanger, P O. 1995. International trends in ventilation standards. *Proceedings of Healthy Buildings, '95, Milan,* Vol. 1, pp 257-266.

6 Jørgensen, R B, Bjørseth, O, Malvik, B. 1999. Chamber testing of adsorption of VOC on material surfaces. *Indoor Air,* Vol. 9 (1) pp 2-9.

Paper IV

Jørgensen R.B., Dokka T.H., Bjørseth O.

"Introduction of a sink-diffusion model to describe the interaction between VOCs and material surfaces"

Indoor Air, Volume 10, No. 1, 2000, pp. 27-38.

Paper IV is not included in the pdf-file due to copyright

Paper V

Dokka T.H., Tjeelflaat P.O.

" Simplified models for prediction of vertical contaminant and temperature stratification in displacement ventilated rooms; Part 1 : derivation "

Submitted to Energy and Buildings.

Simplified models for prediction of vertical contaminant and temperature stratification in displacement ventilated rooms

Part 1 : Derivation

Tor Helge Dokka[1]

Per Olaf Tjelflaat[2]

[1] Department of Industrial Economics and Technology Management

[2] Department of Refrigeration and Air Conditioning,

Norwegian University of Science and Technology

Correspondence to

Tor Helge Dokka, Dep. of Industrial Economics and Technology Management, Norwegian University of Science and Technology, N-7491Trondheim, Norway.
FAX: +47 73593107
E-mail: tor.dokka@iot.ntnu.no

Computer system: Windows/ Word version 97

Abstract

Displacement ventilation is an alternative to conventional mixing ventilation in various types of rooms. Displacement ventilation is superior to mixing ventilation when it comes to removing contaminants and surplus heat in a room. In the design process of a room it is necessary to have design methods and simulation tools that can predict the vertical contaminant and temperature distribution that arise in displacement ventilated rooms. In this paper, both steady state and transient models for prediction of temperature and contaminant stratification are proposed. Sub-models for convective air flow rates, boundary layer air flow and long wave radiation exchange in the rooms are also presented. The proposed models can be used for design of displacement ventilation and for evaluation of ventilation efficiency and temperature effectiveness. The transient models can also be implemented in building simulation tools.

Keywords : Displacement ventilation, Models, Stratification, Contaminants, Ventilation efficiency, Simulation

1. Introduction

1.1 Background

The main objective of ventilation is to provide sufficiently clean air for the occupants, i.e. without any harmful or unpleasant contaminants. Secondary objectives can be the removal or supply of heat, or controlling the humidity level. With regard to air quality, this can be done by diluting contaminants and/or by supplying clean air to the inhalation or occupation zone. Conventional dilution ventilation is primarily based on the first principle (dilution/mixing) and so called displacement ventilation is mainly based on the second principle (supplying clean air and displacing polluted air).

Figure 1 : The working principles in displacement ventilation

The fact that cool air is denser than warm air, leads to a buoyancy effect of warm air raising. Above monitors, lamps, people, radiators, etc. warm air will raise towards the ceiling. Such currents of warm air are often called plumes. If there is no air supply near the ceiling, and no other "disturbing" air currents/movements, a layer of warm air will accumulate below the ceiling. The thickness of this layer is mainly dependent of the plume air flow rates and the ventilation air flow rates. This accumulation will lead to a vertical temperature gradient in the room, with low temperature at floor level and a higher temperature at ceiling level. If the pollution sources in the room are associated with the heat sources, and therefore the plumes, the pollution is also accumulated in a layer near the ceiling, causing a vertical contaminant gradient. This principle is used in displacement ventilation where clean and cool air is supplied to the lower part of the room while the polluted and warm air generated in the occupation zone is transported by the plumes to the upper zone. The height of the clean zone and the polluted zone are dependent of the magnitude of the supplied ventilation air flow and the convective air flows in the room. Displacement ventilation should ideally give much cleaner and cooler air in the inhalation and occupation zone, compared to conventional mixing ventilation. Chemical and physical measurements in laboratories and in real rooms show that the air quality in the occupation zone and the inhalation zone is substantially better than standard mixing ventilation [1-12]. In addition, laboratory and field experiments shows that people perceive the air as more pleasant in displacement ventilated rooms compared to rooms with dilution ventilation (Ørhede et.al. [13], Brohus et.al. [14]). Displacement ventilation has successfully been used in industrial premises, where large concentrated heat and pollution sources are often present at floor level. Displacement ventilation has also grown popular in comfort ventilation, especially in northern Europe.

1.2 Aims and scope of the work

In the design process of a building or room it is of interest to predict the thermal comfort, indoor air quality, the heating and cooling load and energy use during various seasons. A good simulation tool makes it possible to design optimal ventilation solutions. An optimal ventilation system should give good thermal comfort and IAQ with a minimum of energy consumption and investment in heating and cooling equipment. Most existing models and simulation tools for IAQ and energy use are based on the assumption of full mixing, and are unable to predict the advantages of displacement ventilation.

The aim of this work has been to develop both simplified hand calculation methods and more refined models for implementation in building simulation tools. Four different models for vertical temperature and contaminant stratification in displacement ventilated rooms are proposed, covering both stationary and transient conditions. All models are based on a two-zone model approach, assuming a lower clean and cool zone and a upper polluted

and warm zone. Sub-models for convective airflow from heat sources, boundary layer flow along vertical surfaces and radiation transfer models are also proposed/described.

This paper is part one of two complimentary papers. In part two, the models for temperature and contaminant stratification are validated and evaluated against empirical data sets found in existing literature. An inter-model comparison is also undertaken in part two.

2. Previous work: predictive models

Simulation tools and models based on the assumption of full mixing has for the most part been used to predict thermal conditions and IAQ in rooms with displacement ventilation, even if it has been clear that the assumption of full mixing gives inaccurate and dubious results in displacement ventilated rooms. However, various alternative methods and models have been proposed to predict the effect of displacement ventilation.

Skistad [15] has proposed a simple model ('rule of thumb') for the vertical temperature gradient, where half the difference between the extract and supply air temperature is evened out at the floor, and that the other half of the temperature difference gives rise to a linear gradient from floor to ceiling. This is claimed to be representative for offices with moderate ceiling height and normal heat loads and ventilation rates.

Mundt [1] has proposed a simplified nodal model for vertical temperature stratification, where she takes into account radiation from the ceiling to the floor, and convection from the floor surface to the supply air current along the floor. Radiation and convection is described with linearized heat transfer coefficients. Three nodal temperatures are calculated: the surface floor temperature, the air temperature in the layer near the floor, and the ceiling temperature. The extract temperature is assumed to be equal to the ceiling temperature. She also assumes a linear temperature gradient from floor to ceiling.

Mundt [1] has also developed an extended model (a four-node model), where the node temperatures are : the floor surface temperature, the air temperature in the layer near the floor, the ceiling surface temperature, and the air temperature near the ceiling. Assuming a linear temperature gradient the extract temperature can be calculated from the ceiling air temperature, if the extract opening is located below the ceiling level. This model also takes into account heat conduction through the floor and the ceiling/roof.

Based on the Mundt models, Li et.al. [16], has proposed more detailed and complex multi-node models for prediction of vertical temperature gradients. These models have more detailed radiation heat transfer analysis between the surfaces in the room, and also take into account heat conduction through walls, floor and ceiling. Because of the complexity of the model the calculations have to be implemented and executed on a computer. The models do not deal with transient (time varying) effects.

Nielsen [17] has proposed a model for the vertical temperature gradient, based on the Archimedes number. The velocity used in the Archimedes number, is the air flow rate divided by the floor area, the temperature difference is the difference between the extract and supply air temperature, and the characteristic dimension is the height of the room. The temperature gradient from the floor to the ceiling is assumed linear. Nielsen gives a design chart where the dimensionless temperature gradient in a room is given for different type of heat sources as a function of the Archimedes number. The different heat sources are: distributed heat sources, sedentary persons, ceiling light and point heat sources. The model does not deal with transient (time varying) effects. Nielsen [18] has also proposed non-linear temperature gradient models based on the same design chart as in [17].

Another type of models that can be used to predict vertical temperature and contaminant stratification is zonal models, in which a room is divided into a number of zones where full mixing is assumed in each zone. Exchange of air, contaminants and heat between the zones are often described with flow element models for boundary layer flow, plume flow above heat sources, and jet flow.

Skåret [19] has proposed a transient two-zone model to predict vertical contaminant stratification in a room. Flow element models are used to calculate the air exchange between the two zones.

Sandberg et.al. [20] has proposed a rather complex steady-state models for vertical temperature and contaminant distribution in rooms. The temperature model by Sandberg et.al. also incorporates models for long wave radiation processes in the room.

Overby [21] has proposed a two zone model for vertical temperature stratification, which he has implemented into the thermal building simulation program SUNCODE.

Togari [22] and Inard [23] has proposed more advanced multi-zone models to predict temperature gradients and stratification in rooms, also taking into account horizontal temperature gradients.

Other simplified zonal models for vertical temperature distribution have been proposed by Shilkrot & Zhivov [24] and Manzoni & Rongere [25].

Koganei et.al.[26] has proposed a two-zone model for vertical contaminant distribution, assuming piston flow in the lower clean zone. This model provides simplified expressions for the air exchange efficiency and the contaminant removal efficiency.

The most advanced models for prediction of vertical contaminant and temperature stratification is CFD models (CFD : Computational Fluid Dynamics). CFD models are based on the governing equations for fluid

flow and heat transfer, i.e. conservation of mass, energy and momentum, and different rate laws (e.g. Fourier's law and Fick's law), together with turbulence models. CFD models (or codes) can be divided into general CFD codes and special purpose codes. Use of a general purpose CFD code, such as Phoenix, in building application is shown by Quingean [27]. Examples of special purpose CFD models for building applications are Flovent [28] and Vortex-2 [29]. However, the modelling of thermal plumes and boundary layer flow, which is important in displacement ventilated rooms, is difficult in CFD models, as shown by Jacobsen & Nielsen [30].

It is also possible to use physical scale models to predict and study displacement ventilation in real rooms. Often water is used as the medium in such scale models. Scale models to study displacement ventilation have been used by Sandberg & Lindstrøm [31, 32], Hunt & Linden [33], Cooper & Linden [34] and Cooper et.al. [35].

Table 1 : Capabilities of the different theoretical models

Model (first author)	Type of model	Vertical temperature gradients	Vertical contaminant gradients	Transient calculation	Heat conduction	Mathematical solution	Horizontal gradients
Skistad	Nodal	x			(x)[2]	Analytical	
Mundt, simplified	Nodal	x				Analytical	
Mundt, extended	Nodal	x			x	Analytical	
Li et.al.	Nodal	x			x	Numerical	
Nielsen	Nodal	x			(x)[2]	Analytical	
Skåret	Zonal		x	x		Analytical	
Overby	Zonal	x		x	x	Numerical	
Togari	Multi-Zone	x		x	x	Numerical	(x)[4]
Inard	Multi-Zone	x		x	x	Numerical	x
Koganei	Zonal		x	x		Analytical	
Shilkrot	Zonal	x				Analytical	
Manzoni	Zonal	x		x	x	Numerical	
Sandberg et.al.	Zonal	x	x		x	Numerical[3]	
CFD-codes	CFD	x	x	(x)[1]	(x)[1]	Numerical	x

[1] Both transient cases and heat conduction can in principle be calculated in CFD-codes, but due to complexity of the modelling and interpretation of the results, this is rarely done.
[2] Heat conduction is not explicitly treated in these models, but the models assume knowledge about the extract temperature, which is partly a function of the transmission loss.
[3] The thermal model has to be solved numerically due to the non-linear radiation expressions. The contaminant model can supposedly be solved analytically if not coupled to the thermal model.
[4] This model has vertical zones along the walls for treatment of the boundary layer flow (down draught) along vertical walls and windows, but has no general model for treatment of horizontal temperature gradients.

3. Ventilation efficiency indices

Different indices are used to describe how effective a ventilation system is to remove contaminants and heat from a room, and/or to supply fresh air to the occupants. A rather large number of indices has been proposed to describe the effectiveness of the ventilation system of a room. The most common indices are the air exchange efficiency and the contaminant removal efficiency. These two indices can be evaluated in several ways: for a point in the room, in the inhalation zone, in the occupation zone or in the complete room. In comfort ventilation the occupation zone and inhalation zone evaluation is likely to be the most representative and practical, but mean room values are also often used. The inhalation zone in this context is assumed to be the zone with the same concentration as the occupants are inhaling (exposed to), and is taken to be in the height to the nose (approximately 10 cm below top of head). The horizontal extension of the inhalation zone is often less than the thickness of the human boundary layer, which has implications for the quality of the inhaled air. This is more discussed in more depth in section 7.

3.1 Contaminant indices

The contaminant removal efficiencies (also called ventilation efficiencies) are defined as, see Tjelflaat & Sandberg [36]:

$$\varepsilon^c = \frac{C_e - C_s}{<C> - C_s} \quad \text{complete room}$$

$$\varepsilon^c_{occ} = \frac{C_e - C_s}{C_{occ} - C_s} \quad \text{occupation zone} \qquad (1)$$

$$\varepsilon^c_{exp} = \frac{C_e - C_s}{C_{exp} - C_s} \quad \text{inhalation zone (exposure)}$$

where C_s and C_e are the concentrations in the supply and extract air, <C> is the mean concentration in the room, C_{occ} the mean concentration in the occupied zone and C_{exp} the concentration in the inhalation zone (concentration of exposure). The contaminant removal efficiency expresses how much better the air quality is compared to perfect mixing ventilation (perfect mixing: $\varepsilon^c = 1.0$). The height of the occupation zone is determined in each case, but a height of 1.2 m is used where there is mainly seated activity, while 1.8 m is used in rooms with standing/walking activities.

Brohus & Nielsen [3] has introduced another efficiency for the exposure of inhaled contaminants, particularly relevant for displacement ventilated rooms, called the effectiveness of entrainment in the human boundary layer, defined as:

$$\eta_e = \frac{C_p - C_{\exp}}{C_p - C_{fl}} \tag{2}$$

where C_p is the concentration outside the human boundary layer at the same height as the inhalation zone, C_{exp} is the concentration in the inhalation zone, and C_{fl} is the concentration at floor level (assumed representative for the lower clean zone). (2) expresses the ability to entrain clean air from floor level to the inhalation zone (height of exposure). If all the air in the inhalation zone comes from the clean air at floor level the efficiency is 1.0.

3.2 Air exchange efficiency indices

In comfort ventilation the pollution sources are often diffuse and consist of many different components, making it difficult to estimate the contaminant removal efficiency. An alternative way to evaluate ventilation efficiency, is the concept of 'age of air' and the air exchange efficiency, assuming that the contaminant concentration is rising from the supply to the extract. Extracted "old" air is therefore assumed more contaminated than supplied 'fresh' air. The air exchange efficiency in the complete room, in the occupation zone and the inhalation zone are defined as [36]:

$$\begin{aligned}
\varepsilon^a &= \frac{\tau_n}{2 \cdot <\bar{\tau}>} && \text{complete room} \\
\varepsilon^a_{occ} &= \frac{\tau_n}{\bar{\tau}_{occ}} && \text{occupation zone} \\
\varepsilon^a_{\exp} &= \frac{\tau_n}{\bar{\tau}_{\exp}} && \text{inhalation zone (exposure)}
\end{aligned} \tag{3}$$

where τ_n is the nominal time constant for the ventilation air flow, defined as:

$$\tau_n = \frac{V}{\dot{V}_v} \tag{4}$$

where V is the air volume and $\dot{V}_v$ is the ventilation air flow. The air exchange efficiency in the occupation zone and the inhalation zone are also often called local air exchange indices.

The mean age of air in the complete room can be assessed by measuring the concentration in the extract during a tracer gas decay experiment, where the age of air is calculated as [2]:

$$<\bar{\tau}>= \frac{\int_0^\infty C_e(t) \cdot t \cdot dt}{\int_0^\infty C_e(t) \cdot dt} \tag{5}$$

The age of air at a point in the room can be measured based on a tracer gas decay experiment, where the age of air is calculated as [2]:

$$\tau_p = \frac{1}{C(0)} \int_0^\infty C_p(t)dt \qquad (6)$$

where $C(0)$ is the initial concentration in the room (full mixing required), and $C_p(t)$ is the concentration at the point as a function of time(t) in the decay phase., A representative point is measured for the inhalation zone, and for the occupation zone several points are measured, and a mean value is calculated. In a room with complete mixing it can easily be shown that: $\tau_p = \tau_n$ and $\varepsilon^a = \varepsilon^a_{occ} = \varepsilon^a_{\exp} = 1.0$.

3.3 Temperature indices

In cases with heat surplus the temperature can be viewed as a contaminant. Similar to the contaminant removal efficiency, the temperature effectiveness in the complete room can be defined as [37]:

$$\eta = \frac{T_e - T_s}{<T> - T_s} \qquad (7)$$

where $<T>$ is the mean room air temperature, and T_e and T_s respectively the extract and supply air temperatures.

A better indicator of the thermal comfort of occupants is perhaps the temperature effectiveness for the occupation zone, defined as [38]:

$$\eta_{occ} = \frac{T_e - T_s}{T_{occ} - T_s} \qquad (8)$$

where T_{occ} is the mean temperature in the occupied zone.

The normalised floor temperature (κ) , often reported in the literature on displacement ventilation [1, 16-18], is an alternative way to describe the temperature efficiency in displacement ventilated rooms:

$$\kappa = \frac{T_{fl} - T_s}{T_e - T_s} \qquad (9)$$

where T_{fl} is the air temperature near the floor, usually measured approximately 10 cm above the floor surface.

4. Models for calculation of convective air flow around and above heat sources

To predict the distribution of contaminants and air temperature in a room, we need models that can predict the buoyancy driven convective air flows (plumes) created by heat sources in a room. Quite a lot of work has been done to quantify these air flows, both experimental and theoretical [1, 15, 19, 21, 39-48]. Some of this work is reviewed here, and suitable models for application in the two-zone models are proposed.

4.1 Convective air flow models, uniform temperature

For the sake of mathematical simplicity, different types of heat sources are often modelled as point sources and line sources. The sources modelled as point sources are: occupants, computers, desk lamps, printers, etc. Fluorescent lamps and long convective panel heaters are often modelled as line sources.

Figure 2 : Idealised plume above a point source, with an assumed Gaussian temperature and velocity distribution.

Based on conservation of momentum and energy, and the assumption of Gaussian distribution of temperature and velocity, the following simple expression for the convective air flow above a point source is theoretical derived (see for example [1]):

$$\dot{V}_{point} = k_v \cdot P_{point}^{1/3} \left(z + z_p\right)^{5/3} \qquad (10)$$

The convective heat output from the source (P_{point}) is given in W. The value of k_v ranges in the literature from 4.0 to 8.0, see Popiolek et.al. [46]. Popiolek et.al. recommends the value of 6.0, which they state will predict the air flow within ± 20 %. Equation (10) is valid in a still environment (without air movements), and without any vertical temperature gradients.

Figure 3 : Idealised plume above a line source, with an assumed Gaussian temperature and velocity distribution.

For a line source with length L, with the same assumptions as the point source, the air flow can be expressed as, (see for example [39]) :

$$\dot{V}'_{linc} = 14 \cdot P_{linc}^{1/3}\left(z + z_p\right) \cdot L \tag{11}$$

The convective heat from the source (P_{line}) is given in W/m. For extended sources ($l_k \neq 0$) the distance to the virtual origin point (z_p) must be estimated. The literature includes several methods for estimating z_p [1, 15, 41, 46]. In most cases z_p is given as a linear function of the cross sectional dimension (l_k) of the source :

$$z_p = a \cdot l_k \tag{12}$$

The a value range in the literature from 0.7 to ~3.0 [1, 15, 41, 45, 46]. A theoretical value of a can be found if we assume that there is no contraction of the plume above the source, and the spread angle is 12° (see Fig. 2 and 3). The distance to the virtual point can then be estimated by the following expression:

$$z_{p,upper} = \frac{l_k}{\tan 12^\circ} \approx 2.5 \cdot l_k \tag{13}$$

This value: $a = 2.5$ can be taken to be the upper limit for the distance to the virtual origin [15]. As proposed by Skistad [15], a lower limit for a can be estimated if we assume that the plume narrows to 80 % of the characteristic dimension at $l_k/3$ above the source :

$$z_{p,lower} = \frac{0.8 \cdot l_k}{2 \cdot \tan 12^\circ} - l_k / 3 \approx 1.7 \cdot l_k \tag{14}$$

The cross sectional dimension of the source can be taken as the diameter for circular sources, and for line sources it can be taken as the width of the source. For rectangular or other shaped sources, approximated as point sources, it can be taken as the square root of the source area, [41] : $l_k \approx \sqrt{A_{source}}$.

Convective air flow above a wall mounted radiator or electric panel heater is often encountered in practice. The line source model can be an approximation, but the distance to the virtual origin is difficult to assess. Based on measured data, Overby [21] has modified the line source model to predict the air flow above a wall mounted radiator (electric or water based):

$$\dot{V}_{rad} = 8 \cdot \left(\frac{P_{c,rad}}{L_{rad}}\right)^{1/3} \left(z - h_{rad} + 1.61\right) \cdot L_{rad} \tag{15}$$

where $P_{c,rad}$ is the convective heat output of the radiator (W), h_{rad} the height from the floor to the top of the radiator, and L_{rad} the length of the radiator. z is the height from the floor.

4.2 Convective air flow models, stratified surrounding

In a displacement ventilated room there will normally be a temperature gradient ($dT/dz \neq 0$), and the model derived for uniform temperature will therefore not be generally valid. Mundt [1] has proposed models for convective air flow rates in rooms with temperature gradients. These models are theoretically derived and based on the work by Morton [49]. For point sources the proposed model is given by the following equations :

$$\dot{V}_{point} = 2.38 \cdot P_{point}^{3/4} \left(\frac{dT}{dz}\right)^{-5/8} m_1 \quad (16a)$$

$$m_1 = 0.004 + 0.039 \cdot z_1 + 0.38 \cdot z_1^2 - 0.062 \cdot z_1^3 \quad (16b)$$

$$z_1 = 2.86 \cdot (z + z_p) \left(\frac{dT}{dz}\right)^{3/8} P_c^{-0.25} \quad (16c)$$

$$z_p = 2.09 \cdot l_k \quad (16d)$$

Mundt [1] also gives the maximum rise of the plume (point source):

$$z_{max} = 0.98 \cdot P_{point}^{0.25} \left(\frac{dT}{dz}\right)^{-3/8} \quad (16e)$$

where dT/dz is the temperature gradient in the room (assumed linear). Likewise, for a line source the equations are:

$$\dot{V}'_{line} = 4.82 \cdot (P_{line})^{2/3} \left(\frac{dT}{dz}\right)^{-0.5} \sqrt{a} \quad (17a)$$

$$\sqrt{a} = 0.004 + 0.477 \cdot z_1 + 0.029 \cdot z_1^2 - 0.018 \cdot z_1^3 \quad (17b)$$

$$z_1 = 5.76 \cdot (z + z_p) \left(\frac{dT}{dz}\right)^{0.5} P_c^{-1/3} \quad (17c)$$

$$z_p = 1.9 \cdot l_k \quad (17d)$$

The maximum rise of the plume for a line source is given by:

$$z_{max} = 0.51 \cdot P_{line}^{0.33} \left(\frac{dT}{dz}\right)^{-0.5} \quad (17e)$$

Mundt also proposes taking into account the boundary layer thickness for vertically extended sources when estimating the distance to the virtual point (z_p), in equation (16d) and (17d). But this requires knowledge about the temperature difference between the source and the room air, which often can be difficult to assess. The influence of the boundary layer thickness is often minor, and has been omitted here.

4.3 Wall plumes and plumes adjacent to each other

When convective sources is located near walls, corners or adjacent to each other the air flow is reduced significantly. Based on symmetry arguments, Koefoed [39] has derived the following reduction factors for the different cases:

1. When a point or line source is located near a wall the air flow is reduced to 63 % of that of a free plume.
2. When a point source is located in a corner the air flow is reduced to 40 % of that of a free plume.
3. When two equal sources are so close to each other that they create one plume, the air flow for each source is reduced to 63 % of that of a single free plume.

The 63 % reduction factor for wall plumes has been experimentally verified by Kofoed [3].

4.4 A proposed model for convection air flows induced by a person

Convective air flows around and above people are of special interest, since occupants are often the major heat source in many displacement ventilated rooms (for example schools, meeting rooms, theatres). Theoretical models have been developed based on idealised shapes imitating the human body (often cylinders), and experiments have been done to quantify convective air flows induced by people.

A model for convective air flow around and above a person has been developed by the authors based on the following assumptions:

- A person can be modelled as a cylinder (with height h_{per} and diameter d_{per}). The diameter of the person is derived from the given surface area and the height of the person.
- When the height of the lower clean zone is below the height of the person, the convective air flow is mainly governed by the boundary layer air flow around the person. The boundary layer flow can then be calculated with the lower expression given in equation (18), which is theoretically derived in appendix A.
- When the height of the lower clean zone (zone 1) is above the height of the person, the convective air flow is mainly governed by plume air flow. The expression for a point source with uniform temperature surroundings (see equation (10)) can be used to estimate this air flow.
- The transition region between boundary layer flow and plume flow around the top of the person is taken as the larger of the two calculated air flows.

Based on these assumptions the convective air flow above and/or around a person can be calculated as:

$$\dot{V}_{per} = max\begin{cases} 6.0 \cdot \left(P_{per}\right)^{1/3}\left(z - h_{per} + a \cdot d_{per}\right)^{5/3} \\ 8.61 \cdot d_{per}\left(\frac{P_{per}}{A_{per}}\right)^{0.3} z^{1.2} \end{cases} \qquad (18)$$

$$d_{per} = 2 \cdot \left(-h_{per} + \sqrt{h_{per}^2 + A_{per}/\pi}\right) \qquad (19)$$

The surface area of an average adult person (A_{per}) can be set at $1.8\ m^2$ [50]. The height of an average adult seated and standing can respectively be set at: $h_{p,sit}$ = 1.2 m, and $h_{p,stan}$ = 1.75 m. The distance z in equation (18) is the distance from the floor level. At normal room temperature conditions and with normal indoor clothing and activity the convective part of the sensible heat output of a person can be estimated at 50 % (50 % radiation). Under other circumstances the convective heat output from a person can be estimated by the heat balance algorithms of Fanger [50].

4.5 Comparison of measurements and model prediction

The convective air flows above a vertical circular cylinder, used as a simulator for a person, has been investigated (see fig. 4). Experiments are reported by Mundt [1] and Kofoed [39]. The human simulator used is 1 meter high and has a diameter of 0.4 meters, which gives a surface area of 1.38 m².

Figure 4: Dimension of the cylinder used in the experiments by Mundt [1] and Kofoed [39].

Table 2: Comparison between model prediction and measurements, with temperature gradient of 0-0.1 K/m.

Height above floor	**1.25 m**	**1.5 m**	**1.75 m**	**2.0 m**	**2.25 m**
Experiments					
Kofoed [39], Air flow : 0 l/s	17 l/s	32 l/s	39 l/s	52 l/s	56 l/s
Kofoed [39], Air flow : 4.2 l/s	26 l/s	34 l/s	43 l/s	66 l/s	64 l/s
Model prediction					
Gradient model, Mundt [1]	20 l/s	29 l/s	39 l/s	50 l/s	62 l/s
Expression (18), lower limit : a = 1.7	20 l/s	29 l/s	40 l/s	52 l/s	66 l/s
Expression (18), upper limit : a = 2.5	32 l/s	43 l/s	56 l/s	70 l/s	85 l/s

Table 3 : Comparison between model prediction and measurements, with temperature gradient of 0.3 K/m.

Height above floor	1.25 m	1.5 m	1.75 m	2.0 m	2.25 m
Experiments					
Kofoed [39], Air flow : 4.2 l/s	23	29	33	43	52
Model prediction					
Gradient model, Mundt [1]	20 l/s	29 l/s	39 l/s	50 l/s	62 l/s
Expression (18), lower limit: a = 1.7	20 l/s	29 l/s	40 l/s	52 l/s	66 l/s
Expression (18), upper limit: a = 2.5	32 l/s	43 l/s	56 l/s	70 l/s	85 l/s

Table 4 : Comparison between model prediction and measurements, with temperature gradient of 0.6 K/m.

Height above floor	1.1 m	1.4 m	1.8 m	2.2 m
Experiments				
Mundt [1] , 20.8 l/s, Lab 1	23 l/s	32 l/s	35 l/s	46 l/s
Mundt [1], 41.6 l/s, Lab 1	24 l/s	35 l/s	43 l/s	60 l/s
Mundt [1], 20.8 l/s, Lab 2	30 l/s	40 l/s	52 l/s	66 l/s
Mundt [1], 41.6 l/s, Lab 2	35 l/s	49 l/s	62 l/s	76 l/s
Mundt [1], 20.8 l/s, Lab 3	24 l/s	30 l/s	40 l/s	48 l/s
Mundt [1], 41.6 l/s, Lab 3	29 l/s	40 l/s	*	68 l/s
Mundt [1], 20.8 l/s, Lab 4	32 l/s	44 l/s	47 l/s	*
Model prediction				
Gradient model, Mundt [1]	16 l/s	26 l/s	41 l/s	59 l/s
Expression (18), lower limit: a = 1.7	15 l/s	25 l/s	42 l/s	63 l/s
Expression (18), upper limit: a = 2.5	26 l/s	39 l/s	59 l/s	82 l/s

* Not measured or not a reliable measurement.

In table 2-5, calculated air flows with the models of Mundt, expression (16), and the proposed human model expression (18) and (19), are compared to the experimental results of Mundt and Kofoed. Air flows for different heights above the floor and different temperature gradients are compared. The heat output for the human simulators is 100 W, where 50 W is estimated to be convection [1]. In equation (18) both the upper and lower limit values of a, respectively *2.5* and *1.7*, are calculated.

Table 5 : Comparison between model prediction and measurements, with temperature gradient of 1.2-1.5 K/m.

Height above floor	1.1 m	1.4 m	1.8 m	2.2 m
Experiments				
Mundt [1] , 41.6 l/s, Lab 1	21 l/s	27 l/s	31 l/s	*
Mundt [1], 41.6 l/s, Lab 2	29 l/s	37 l/s	43 l/s	*
Mundt [1], 41.6 l/s, Lab 3	26 l/s	37 l/s	46 l/s	*
Mundt [1], 70 l/s, Lab 5	26 l/s	37 l/s	52 l/s	77 l/s
Model prediction				
Gradient model; Mundt [1]	16 l/s	26 l/s	41 l/s	59 l/s
Expression (18), lower limit: a = 1.7	15 l/s	25 l/s	42 l/s	63 l/s
Expression (18), upper limit: a = 2.5	26 l/s	39 l/s	59 l/s	82 l/s

* Not measured or not a reliable measurement.

4.6 Discussion and recommendation of convective air flow models

The gradient model of Mundt and the proposed human model, expression (18), with the lower limit value (a = 1.7) predict very similar air flow rates. The human model with the upper limit value (a = 2.5) predicts considerably higher air flows. For the experiments with small temperature gradients (table 2 and 3), the gradient model or the 'lower limit' model predicts best. For the experiments with higher temperature gradient (table 4 and 5) the human model with the upper limit value predicts best up to 1.4 m, but for 1.8 and 2.2 m above the floor it over-predicts the air flows.

In comfort ventilation with normal ventilation rates (1 - 4 ACH) the front between the clean and polluted zone is approximately in the range 0.8 – 1.4 meters above the floor. In this height range there is small difference between the two models, and the simplest can be used (the human model based on uniform room temperature). A compromise for the value of a in equation (18) seems to be: $a \approx 1.9$.

Mierzwinski & Popiolek [48] have measured air flow rates 0.75 meter above a seated person, and reports the air flows to be between 28 l/s and 56 l/s. Assuming the height of the seated person to be 1.2 m and the convective heat output to be 40 W, the prediction of the model is: 40 l/s and 55 l/s, for the lower (a = 1.7) and upper (a = 2.5) limits respectively, i.e. the proposed model seems to give a reasonable prediction also for real persons.

Mundt [1] also reports the measurement of plume air flow rates above a desk lamp, a heated box simulating a computer and a fluorescent light. Appendix B gives a comparison of model prediction and measurements for these heat sources. Both the uniform temperature model and the gradient model of Mundt predicts the air flow satisfactorily, but the spread in the measured data is considerable. The large influence of the temperature gradient on the air flow, found in earlier studies [42, 43], is not found in the study of Mundt. The lower limit value (a = 1.7) of the uniform temperature model predicts in most cases better than the upper limit value (a = 2.5). Based on these results a value of : $a \approx 1.8$ in equation (12) is recommended, if additional information is not available.

5. Boundary layer flow along vertical surfaces

Down draught along vertical cold surfaces, like poorly insulated walls or external windows, can in a displacement ventilated room result in transport of contaminated air from the upper polluted zone to the lower clean occupation zone. It is therefore of importance to estimate these air flows as accurate as possible. Based on a theoretical derivation, using conservation of momentum and energy, and assuming turbulent flow, Skåret [19] has derived the following expression:

$$\dot{V}_{dr} = k_1 \cdot w \cdot \Delta T^{0.4} z^{1.2} \qquad (20)$$

where ΔT is the difference between the room air temperature (T_a) and the surface temperature (T_f) of the cold surface, and w and z the height and width of the cold surface respectively. The value of k_1 in the literature is reported to be between 2.1 and 2.9, [2, 19, 21]. However, if the flow is laminar, the following expression is proposed [2, 21]:

$$\dot{V}_{dr} = k_2 \cdot w \cdot \Delta T^{0.25} z^{0.75} \qquad (21)$$

Mattson [2] gives the value: k_2 = 2.4 , while Overby [21] reports: k_2 =2.75 . If the flow is laminar or turbulent can be determined by the Grashof number [2]:

$$Gr = \frac{\beta \cdot g \cdot \Delta T \cdot z^3}{\nu^2} < 1 \cdot 10^9 \Rightarrow \text{Laminar flow} \qquad (22)$$

With the volume expansion coefficient (β) and the kinematic viscosity (ν) evaluated at normal room temperature (~20 °C), equation (22) can be reduced to:

$$\Delta T \cdot z^3 < 6.7 \Rightarrow \text{Laminar flow} \qquad (23)$$

Thus, if the product of the temperature difference and height of the cold surface to the third power is less than 6.7, the flow can be regarded as laminar and equation (21) can be applied. Otherwise, if $\Delta T z^3 > 6.7$, the flow can be regarded as turbulent, and equation (20) can be applied. Equation (20) and (21) can also be used to calculate the rising air flow along a warm vertical surface, e.g. a solar heated wall or window.

Figure 5 : Down draught along a cold vertical surface

Figure 6 : Air flow rate per meter width along a vertical cold or warm surface, as a function of the temperature difference between the surface and the surrounding air and the height of the surface. A value of k_1 = 2.5 in equation (20) and a value of k_2 = 2.57 in equation (21) has been used.

6. Proposed models for radiation exchange and radiation distribution in the room

In a room with a vertical temperature gradient the temperature in the upper polluted zone will be higher than in the lower clean zone. The temperature difference causes a radiation exchange between the two zones, which

strongly influences the temperature gradient in displacement ventilated rooms. This has been verified experimentally by Li et.al.[16, 52]. A simplified model for this radiation exchange is proposed below.

The distribution of radiation from different heat sources on the surfaces in the room can also be of importance for the vertical temperature gradient in the room, and some simplified distribution factors are proposed in sub-section 6.2.

6.1 Long wave radiation exchange between zones

Figure 7 : Two-zone long wave radiation transfer model.

The radiation exchange between the upper zone (zone 2) and the lower zone (zone 1) can be modelled with a few assumptions:

- The room is assumed to be a cuboid (see Fig. 7), divided into a lower zone (zone 1) with uniform surface temperature (T_1) and an upper zone (zone 2) with uniform surface temperature (T_2). This is consistent with the assumption in the two-zone model, see section 9.
- The two zones are assumed to be grey surfaces with emissivity ε_1 and ε_2.

The radiation transfer between any two grey opaque surfaces that form an enclosure is calculated as [51]:

$$q_{r21} = \frac{\sigma\left(T_2^4 - T_1^4\right)}{R_{tot}} \tag{24}$$

The temperatures T_1 and T_2 have to be given in absolute temperature (K). The total resistance to radiation transfer (R_{tot}) is given as the sum of two surface resistances (R_{S1} and R_{S2}) and one space/view resistance (R_{view}):

$$R_{tot} = R_{S1} + R_{view} + R_{S2} = \frac{1-\varepsilon_1}{A_1\varepsilon_1} + R_{view} + \frac{1-\varepsilon_2}{A_2\varepsilon_2} \tag{25}$$

The view resistance between zone 2 and zone 1 is given as:

$$R_{view} = \left(A_f F_{c\to 1} + 2\cdot A_{sw}F_{sw\to 1} + 2\cdot A_{lw}F_{lw\to 1}\right)^{-1} \tag{26}$$

F_{c-1} is the view factor between the ceiling and the horizontal plane dividing zones 1 and 2, which can be calculated by this rather bulky equation [51]:

$$F_{C\to 1} = \frac{2}{\pi XY}\left\{\begin{array}{l} \ln\left[\dfrac{\left(1+X^2\right)\left(1+Y^2\right)}{1+Y^2+X^2}\right]^{1/2} \\ -X\arctan X - Y\arctan Y \\ +X\left(1+Y^2\right)^{1/2}\arctan\left(\dfrac{X}{\left(1+Y^2\right)^{1/2}}\right) \\ +Y\left(1+X^2\right)^{1/2}\arctan\left(\dfrac{Y}{\left(1+X^2\right)^{1/2}}\right) \end{array}\right\} \tag{27}$$

where:

$$X = \frac{l}{h_2} \qquad ; \qquad Y = \frac{w}{h_2} \tag{28}$$

The view factor between the walls in zone 2 and the plane dividing the two zones is given by:

$$F_{W\to 1} = \frac{1}{\pi\cdot W}\left(\begin{array}{l} W\cdot\arctan\dfrac{1}{W} + H\cdot\arctan\dfrac{1}{H} + U^{0.5}\arctan\dfrac{1}{U^{0.5}} \\ +0.25\cdot\ln\left\{\dfrac{\left(1+W^2\right)\left(1+H^2\right)}{1+U^2}\cdot\left[\dfrac{W^2\left(1+U^2\right)}{\left(1+W^2\right)\cdot U^2}\right]^{W^2}\cdot\left[\dfrac{H^2\left(1+U^2\right)}{\left(1+H^2\right)\cdot U^2}\right]^{H^2}\right\} \end{array}\right) \tag{29}$$

where H, W and U for the short wall (width: w) are given as:

$$H = \frac{h_2}{w} \quad ; \quad W = \frac{l}{w} \quad U = H^2 + W^2 \tag{30}$$

while for the long wall (length: l) they are given as :

$$H = \frac{h_2}{l} \quad ; \quad W = \frac{w}{l} \quad U = H^2 + W^2 \tag{31}$$

The floor area (A_{fl}) and the wall areas in zone 2 are simply calculated as:

$$A_{fl} = l \cdot w \; ; \quad A_{sw} = w \cdot h_2 \; ; \quad A_{lw} = l \cdot h_2 \tag{32}$$

For interpretation it is convenient to define a by floor area normalised radiation heat transfer coefficient:

$$\alpha_r = \frac{q_{r21}}{A_{fl}(T_2 - T_1)} \tag{33}$$

Figure 8 : Normalised radiation heat transfer coefficient (α_r) as a function of emissivity (ε), the ratio of the width and length of the room (w/l) and the ceiling height (h_{ceil}). The temperatures in the zone has been held constant at $T_1 = 21$ ° C and $T_2 = 25$ °C, and the height of zone 1 is set at 1.2 m.

As can be seen from figure 7, the by floor area normalised radiation heat transfer coefficient (α_r), does not vary too much in rooms with a normal height (2.4 – 3.2 m), normal width and length ratio (1.0 – 0.5), and for normal emissivity of the room surfaces (0.85 – 0.98). The influence on the radiation coefficient (α_r) by the temperatures (T_1 and T_2) is of minor importance in the normal temperature range (18 – 30 °C). The radiation coefficient has been calculated for rooms with floor area in the range 16 – 22.5 m². The influence of the size of the room is minor for small and medium large rooms (~10–70 m²), but can be important for larger rooms. A rough approximation for the radiation heat transfer coefficient for room with normal size, shape and surfaces can be:

$$\alpha_{r,norm} \approx 4 \tag{34}$$

This is somewhat lower than : $\alpha_r = 5$ W/m²K proposed by Mundt [1].

6.2 Distribution of radiation heat gain from heat sources

Figure 9 : Distribution of radiation heat output from heat sources in the two zones.

Another issue of importance for the vertical temperature distribution is how the radiation from the heat sources is distributed between the lower and upper zones. A rough estimation can be made by weighting the radiation output by the surface area in the two zones, according to the following:

$$q_{rad11} = q_1(1 - \varphi_{con1}) \cdot \alpha_1 \tag{35.a.}$$

$$q_{rad21} = q_1(1 - \varphi_{con1}) \cdot (1 - \alpha_1) \tag{35.b.}$$

$$q_{rad21} = q_2(1 - \varphi_{con2}) \cdot \alpha_2 \tag{35.c.}$$

$$q_{rad22} = q_2(1 - \varphi_{con2})(1 - \alpha_2) \tag{35.d.}$$

where α_1 and α_2 is the surface area ratios :

$$\alpha_1 = \frac{A_1}{A_1 + A_{fl}} \tag{36.a.}$$

$$\alpha_2 = \frac{A_2}{A_2 + A_{fl}} \tag{36.b.}$$

where A_1 and A_2 are the surface areas of zones 1 and zone 2. q_1 and q_2 are the total sensible heat outputs of a heat source in zones 1 and 2, respectively. φ_{con1} and φ_{con2} are the convective component for the heat sources in zones 1 and zone 2, respectively.

7. A steady state two-zone model for vertical contaminant stratification

A steady state model for vertical contaminant stratification has been developed. The model is based on a two-zone model approach as illustrated in figure 10, with a lower clean zone (zone 1) and a upper polluted zone (zone 2). Air exchange between the two zones is calculated with sub-models for plumes and the boundary layer flow presented in preceding sections. In the next section the model is extended to treat transient conditions. The steady state contaminant model is based on the following assumptions:

- The concentration within the two zones are uniform.
- A constant part (φ_{con}) of the contaminants generated by hot sources in zone 1 is following the convective air flow (the plume) up into zone 2. This is called the convective factor.
- The height of the clean zone is determined from an air mass balance which states that the supplied ventilation air plus the down draught air flow, equals the convective air flow from hot sources in zone 1.
- The supplied air flow equals the extract air flow.
- Diffusive and turbulent transport of contaminants between the two zones is assumed negligible compared to the convective transport.
- The supply air unit is located well within zone 1, and the extract air unit is located in zone 2.
- Exfiltration and infiltration from the external environment and other adjacent rooms are assumed negligible compared to the ventilation air flow.
- Sink effects (adsorption) on material surfaces in the room are assumed negligible.

Figure 10: Principles and variables in the contaminant two-zone model

7.1 Air mass balance, and the height of zone 1(clean zone)

If we assume that the density of air is constant, an air mass balance of zone 1 (clean zone) can be written as (see figure 10):

$$\overbrace{\dot{V}_v + \dot{V}_{dr}(h_1)}^{\text{Air flow to zone 1}} = \overbrace{\dot{V}_{con}(h_1)}^{\text{Air flow from zone 1}} \tag{37}$$

The air mass balance for zone 2 gives the same result. In practice, only the ventilation air flow ($\dot{V}_v$) is known, and the down draft air flow ($\dot{V}_{dr}$) and the convective air flow ($\dot{V}_{con}$) are dependent on the height of the clean zone (h_1), i.e. the height of zone 1 has to be iterated until equation (37) is satisfied. Expressions for calculation of the convective air flows (plumes) and down draft air flow (boundary layer air flow) are given in section 4 and 5, respectively.

7.2 Mass balance of contaminants

Referring to figure 10 and the above mentioned assumptions, a steady state contaminant mass balance for zone 1 and zone 2 are given as:

$$g_1 + (1-\varphi_{con})g_{con} + \dot{V}_v C_s + \dot{V}_{dr} C_2 - \dot{V}_{con} C_1 = 0 \tag{38.a.}$$

$$g_2 + \varphi_{con} g_{con} + \dot{V}_{con} C_1 - \dot{V}_{dr} C_2 - \dot{V}_v C_2 = 0 \tag{38.b.}$$

The solution to these two equations can be written as:

$$C_{1\infty} = \overbrace{C_s}^{\text{Concentr. in supply air}} + \frac{\overbrace{g_1 + g_{con}(1-\varphi_{con})}^{\text{Contaminant generation in zone 1}}}{\dot{V}_v} + \frac{\overbrace{\omega \cdot (g_2 + g_{con}\varphi_{con})}^{\text{Contaminant transfer from zone 2}}}{\dot{V}_v} \tag{39.a.}$$

$$C_{2\infty} = \overbrace{C_s}^{\text{Conc. in supply air}} \quad \frac{\overbrace{g_1 + g_{con} + g_2}^{\text{Total contaminant generation in both zones}}}{\dot{V}_v} \tag{39.b.}$$

where the contaminant transfer factor (ω) is given by:

$$\omega = \frac{\dot{V}_{dr}}{\dot{V}_{con}} \tag{40}$$

The units most often used for concentration in indoor environments are µg/m³ , mg/m³ or ppm (parts per million).

7.3 Calculation of contaminant efficiency indices

From the derived expressions in the preceding section, the mean concentration in the complete room and in the occupation zone can be calculated as:

$$< C >= C_{1\infty} h_1 + C_{2\infty}(h_{ceil} - h_1) \tag{41.a.}$$

$$C_{occ} = \begin{cases} C_{1\infty} & ;\text{if } h_1 \geq h_{occ} \\ \dfrac{C_{1\infty} h_1 + C_{2\infty}(h_{occ} - h_1)}{h_{occ}} & ;\text{if } h_{occ} > h_1 \end{cases} \tag{41.b.}$$

where h_{occ} is the height of the occupation zone. The contaminant removal efficiency in the complete room and in the occupation zone can now be calculated (see definitions in section 3):

$$\varepsilon^C = \frac{C_{2\infty} - C_s}{< C > - C_s} \tag{42.a.}$$

$$\varepsilon^C_{occ} = \frac{C_{2\infty} - C_s}{C_{occ} - C_s} \tag{42.b.}$$

If we assume that air in the human boundary layer (see section 3) is entrained evenly from floor level to the height of the inhalation zone (h_{exp}), the mean concentration entrained in the human boundary layer is given by the expression:

$$C_{exp} = \begin{cases} C_{1\infty} & ;\text{if } h_1 \geq h_{exp} \\ \dfrac{C_{1\infty} h_1 + C_{2\infty}(h_{exp} - h_1)}{h_{exp}} & ;\text{if } h_{exp} > h_1 \end{cases} \tag{43}$$

where we have assumed that the entrained concentration is the same as the concentration in the inhalation zone (discussed below). h_{exp} is the height to the inhalation zone (exposure). The contaminant removal efficiency in the inhalation zone can now be calculated as:

$$\varepsilon^C_{exp} = \frac{C_{2\infty} - C_s}{C_{exp} - C_s} \tag{44}$$

If the height of zone 1 is below the height to the inhalation zone ($h_1 < h_{exp}$), the effectiveness of entrainment in the human boundary layer (η_e), (defined in section 3), can be estimated as:

$$\eta_e = \frac{C_{2\infty} - C_{\exp}}{C_{2\infty} - C_{1\infty}} \tag{45}$$

In cases where the lower clean zone is higher than the inhalation zone ($h_1 > h_{exp}$), expression (45) is undetermined ($\eta_e = 0/0$). This only means that the inhaled concentration is the same as the concentration in the clean zone ($C_{exp} = C_{1\infty}$). If equation (43) is introduced into (45), and assuming $h_1 < h_{exp}$, the following relationship is revealed:

$$C_{\exp} = C_p - \eta_e\left(C_p - C_f\right) \approx C_{2\infty} - \frac{h_1}{h_{\exp}}\left(C_{2\infty} - C_{1\infty}\right) \Rightarrow \eta_e \approx \frac{h_1}{h_{\exp}} \tag{46}$$

The fact that η_e can be estimated by the height of the clean zone divided by the height to the inhalation zone, was first proposed by Brohus & Nielsen [3]. Brohus & Nielsen has also derived expression (46) empirically, based on their own experiments and other experiments found in the literature.

7.4 Results and discussion

From expression (39.a.) it can be seen that the steady state concentration in zone 1 consists of three terms:

- The concentration in the supply air (C_s)
- The contaminant production in the occupation zone, divided by the ventilation air flow. This is the concentration we get when the supply air is clean, and there is no transfer of air down from zone 2.
- The last term can be interpreted as the contaminant transfer from zone 2. If there is no return air to zone 1 ($\dot{V}_{dr} = 0$), the transfer factor becomes zero ($\omega = 0$), and no contaminant from the zone 2 is transferred to zone 1.

Obvious measures to keep the air in the occupation zone as clean as possible are therefore to supply clean ventilation air, reduce 'cold' pollution sources in zone 1 (e.g. using low polluting building materials), and preventing down draught of air from zone 1.

The steady state concentration in zone 2 (39.b.) is given as the supply air concentration plus the total contaminant generation in both zones divided by the ventilation air flow. This is the same concentration as we get with full mixing ventilation. This is an interesting result, since intuition would say that the concentration in the upper polluted zone using displacement ventilation would be higher than the mean concentration in a fully mixed room.

It is of interest to study a limiting case:

- there is no 'cold' pollution sources in zone 1 ($g_1 = 0$)
- and no pollution generation in zone 2 ($g_2 = 0$)
- and most of the contaminant generation from the hot sources in zone 1 is following the convective air current ($\varphi_{con} = 0.9$).
- The down draft air flow is assumed small (~1 l/s).

This can be regarded as a rough model for a well insulated room where the dominating pollution source is bioeffluents from people. Three outputs from the model has been calculated: the contaminant removal efficiency in the occupation zone (ε^c_{occ}), the height of zone 1 (h_1) and the effectiveness of entrainment in the human boundary layer (η_e). This outputs have been calculated as a function of the specific ventilation air flow rate, for different heat source levels.

Figure 11: Contaminant removal efficiency in the occupation zone (ε^c_{occ}) as a function of the different heat source levels and specific ventilation air flow rate ($\dot{V}''_v$) in a 10 m² office room. The height of the occupation zone is 1.2 m (seated activity).

Figure 12: The height of the clean zone (zone 1) as a function of the different heat source levels and specific ventilation air flow rate in a 10 m² office room.

Figure 13: The effectiveness of entrainment in the human boundary layer (η_e) as a function of the different heat source levels and specific ventilation air flow rate in a 10 m² office room. The height of the inhalation zone (h_{exp}) is set at 1.1 m (seated activity).

In figure 11 we see that even for small air flow rates the ventilation efficiency in the occupation zone is high (not below 1.9), the influence of the heat sources are strong, and the ventilation efficiency is reduced considerable for higher heat loads. A maximum contaminant removal efficiency of approximately 8.7 is the limit for all four heat source levels. Comparing the contaminant removal efficiency in figure 11 with the height of zone 1 in figure 12, reveals that when the height of zone 1 is above the height of the occupation zone, the contaminant removal efficiency limit of 8.7 is approached.

Superior air quality in the occupation zone can therefore be achieved by supplying sufficient ventilation air flows which match the convective air flows at the height of the occupation zone. Raising of the clean zone can be achieved by either supplying higher air flow rates, or reducing the heat output (especially the convective part) from sources in the occupation zone, hence reducing the need for feed air to the convective plumes. If possible, the last option (reducing the heat sources) is clearly the most cost and energy efficient, since it reduces the need for ventilation and it also reduces the energy demand for appliances and lighting.

Figure 12 and 13 show that the effectiveness of entrainment in the human boundary layer (η_e) approaches 1.0 when the height of the clean zone (h_1) approaches the height to the inhalation zone(h_{exp}). Figure 13 also shows that even if the polluted zone is drawn below the inhalation zone ($h_1 < h_{exp}$), most of the inhaled air is entrained from the clean zone. This fact has implication for the design of displacement ventilation.

The 'old' design rule for displacement ventilation (see e.g. Mathisen [53]) can be stated as: "**Supply air flow rates has to be dimensioned so the height of the clean zone is equal to or larger than the height of the occupation zone**". This design rule results in supply air flow rates equal to or higher than those used in conventional mixing ventilation. And the cost and energy reduction potential of displacement ventilation systems are poorly utilised.

The 'new' design rule, using the theory of entrainment in the human boundary layer, could be stated: "**The supply air flow rate can be dimensioned so the height of the clean zone is below the height to the inhalation zone ("height of the nose"). The air quality will still be substantially better than with mixing ventilation**". With this design rule the air flow rate could be lower than those used in conventional mixing ventilation, and significant reduction in costs and energy use could be achieved.

The fact that the air quality in the human boundary layer is substantially better than outside the boundary (at same height) has been experimentally verified in several studies: Mundt [1], Mattson [2], Brohus & Nielsen [3], Holmberg et.al. [5], Nickel [7], Hatton & Awbi [9] and Kruhne & Fitzner [54]. However, as Brohus&Nielsen pointed out, the human boundary layer is disturbed by human movement, giving possible poorer inhaled air quality. In such cases (for example sports halls and shopping malls) the concentration outside the human boundary layer at inhalation zone height is a more conservative estimate of the concentration to which the occupants are exposed.

8. A transient two-zone model for vertical contaminant stratification

In cases with varying ventilation air flows and/or very transient pollution sources (e.g. people in a classrooms) the concentrations will be transient until a new steady state conditions are reached . To analyse such situation a transient (time dependent) model is required. The steady state model in section 7 is easily extended to a transient model by adding terms for mass accumulation in the mass balance for the two zones.

8.1 Transient mass balances of contaminants

Referring to Fig.10, the transient rate mass balances for the two zones become:

$$g_1 + (1-\varphi_{con})g_{con} + \dot{V}_v C_s + \dot{V}_{dr} C_2 - \dot{V}_{con} C_1 = V_1 \frac{dC_1}{dt} \tag{47.a.}$$

$$g_2 + \varphi_{con} g_{con} + \dot{V}_{con} C_1 - \dot{V}_{dr} C_2 - \dot{V}_e C_2 = V_2 \frac{dC_2}{dt} \tag{47.b.}$$

where V_1 and V_2 are the air volumes of zones 1 and 2 respectively, and t is time. All other variables are the same as in the steady state model. Equations (46.a.) and (46.b.) are two coupled ordinary linear differential equations, which in matrix notation can be written:

$$\frac{d}{dt}\overbrace{\begin{bmatrix} C_1 \\ C_2 \end{bmatrix}}^{\vec{C}} = \overbrace{\begin{bmatrix} a_{11} & a_{12} \\ a_{21} & a_{22} \end{bmatrix}}^{\vec{A}} \overbrace{\begin{bmatrix} C_1 \\ C_2 \end{bmatrix}}^{\vec{C}} + \overbrace{\begin{bmatrix} b_1 \\ b_2 \end{bmatrix}}^{\vec{B}} \tag{48}$$

Where the arrow denotes a vector or a matrix. $\vec{A}$ is the coefficient matrix, also called the transport matrix, and $\vec{B}$ is the source vector. The new coefficients are:

$$a_{11} = -\frac{\dot{V}_{con}}{V_1} \quad ; \quad a_{12} = \frac{\dot{V}_{dr}}{V_1}$$
$$a_{21} = \frac{\dot{V}_{con}}{V_2} \quad ; \quad a_{22} = -\frac{\dot{V}_{dr} + \dot{V}_v}{V_2} \tag{49}$$

$$b_1 = \frac{g_1 + g_{con}(1-\varphi_{con}) + \dot{V}_v C_s}{V_1} \; ; \; b_2 = \frac{g_2 + g_{con}\varphi_{con}}{V_2} \tag{50}$$

The system (48) can, for example, be solved by the eigenvalue/eigenvector method. As shown in Dokka et.al.[55] the general solution to a system on the mathematical form of (48) is given as:

$$C_1(t) = d_1 \exp(\lambda_1 t) + d_2 \exp(\lambda_2 t) + C_{1\infty} \tag{51.a.}$$

$$C_2(t) = d_1 k_1 \exp(\lambda_1 t) + d_2 k_2 \exp(\lambda_2 t) + C_{2\infty} \tag{51.b.}$$

where d_1 and d_2 are arbitrary integrating constants which can be determined from the initial values (concentrations). The steady state concentrations $C_{1\infty}$ and $C_{2\infty}$ is the same as those derived in the section 7. The eigenvalues (λ) and the entries in the eigenvectors (k) are given as:

$$\lambda_{1/2} = \frac{(a_{11} + a_{22}) \pm \sqrt{(a_{11} + a_{22})^2 - 4 \cdot (a_{11}a_{22} - a_{12}a_{21})}}{2} \tag{52}$$

$$k_1 = \frac{\lambda_1 - a_{11}}{a_{12}} \quad ; \quad k_2 = \frac{\lambda_2 - a_{11}}{a_{12}} \tag{53}$$

By introducing the initial values (concentrations) $C_1(0)$ and $C_2(0)$ into (51), the constants d_1 and d_2 can be determined:

$$d_1 = \frac{[C_1(0) - C_{1\infty}]k_2 - C_2(0) + C_{2\infty}}{k_2 - k_1} \tag{54.a.}$$

$$d_2 = \frac{C_2(0) - C_{2\infty} - [C_1(0) - C_{1\infty}]k_1}{k_2 - k_1} \tag{54.b.}$$

For the sake of interpretation it is often convenient to introduce the time constants, defined as the reciprocal of the eigenvalues with opposite sign:

$$\theta_1 = -\frac{1}{\lambda_1} \quad ; \quad \theta_2 = -\frac{1}{\lambda_2} \tag{55}$$

8.2 Derivation of age of air expressions

From the definition in section 3, the room mean age of air can be derived by integrating expression (51.b.):

$$< \bar{\tau} >= \frac{\int_0^\infty C_2(t) \cdot t \cdot dt}{\int_0^\infty C_2(t) \cdot dt} = \frac{\theta_1^2 [k_2 - 1] k_1 + \theta_2^2 [1 - k_1] k_2}{\theta_1 [k_2 - 1] k_1 + \theta_2 [1 - k_1] k_2} \tag{56}$$

Referring to the definition in section 3, the age of air in zone 1 can be calculated as:

$$\bar{\tau}_1 = \frac{1}{C(0)} \int_0^\infty C_1(t) dt = \frac{\theta_1 [k_2 - 1] + \theta_2 [1 - k_1]}{k_2 - k_1} \tag{57}$$

where we have set $C_1(0) = C_2(0) = C(0)$ (full mixing before start of decay), and since there is no source in the transient part of a tracer gas experiment : $C_{1\infty} = C_{2\infty} = 0$. Similar integration of the concentration in zone 2, gives the age of air in zone 2:

$$\bar{\tau}_2 = \frac{\theta_1 k_1 [k_2 - 1] + \theta_2 k_2 [1 - k_1]}{k_2 - k_1} \tag{58}$$

It can be shown that the age of air in zone 2 is equal to the nominal time constant, defined in section 3: $\bar{\tau}_2 = \tau_n = V / \dot{V}_v$. The mean age of air in the occupation zone is then easily calculated:

$$\bar{\tau}_{occ} = \begin{cases} \bar{\tau}_1 & ; \text{if } h_1 \geq h_{occ} \\ \dfrac{\bar{\tau}_1 h_1 + \bar{\tau}_2 (h_{occ} - h_1)}{h_{occ}} & ; \text{if } h_{occ} > h_1 \end{cases} \tag{59}$$

Similarly the mean age of air in the inhalation zone (exposure) is given by the expression:

$$\bar{\tau}_{exp} = \begin{cases} \bar{\tau}_1 & ; \text{if } h_1 \geq h_{exp} \\ \dfrac{\bar{\tau}_1 h_1 + \bar{\tau}_2 (h_{exp} - h_1)}{h_{exp}} & ; \text{if } h_{exp} > h_1 \end{cases} \tag{60}$$

From the definition in section 3, and the expressions for the 'age of air' presented here, the air exchange efficiencies for the mean room air, the occupation and inhalation zone can be calculated.

We can also define an apparent air flow rate for the occupation and inhalation zone in a displacement ventilated room. This is the air flow rate required in a perfectly mixed ventilation system, which gives the same age of air in the occupation or inhalation zone as the displacement system. The apparent air flow rates for the occupation and inhalation zone can therefore be calculated as:

$$\dot{V}_{app,occ} = \frac{V}{\bar{\tau}_{occ}} = \varepsilon^a_{occ} \dot{V}_v \quad ; \quad \dot{V}_{app,exp} = \frac{V}{\bar{\tau}_{exp}} = \varepsilon^a_{exp} \dot{V}_v \tag{61}$$

8.3 Results and discussion

The following facts can be drawn from the presented transient model:

- It can be shown that the eigenvalues are always negative, which implicates that the exponential expressions in the model approach zero when t becomes large. This again implies that the concentrations in the two zones approach the steady state concentrations ($C_{1\infty}$, $C_{2\infty}$).
- How fast the steady state concentrations are approached is determined by the time constants, expression (55). Large time constants means that steady state conditions are approached slowly. Large time constants are typically associated with low ventilation and large air volumes (high ceilings), typical in old buildings. Typical modern buildings with high ventilation and small room volumes leads to small time constants, and fast transients (steady state conditions are approached fast) .

- The time constants (55) are functions of the ventilation air flow rate, the convective air flow, the down draft air flow, the height of the two zones and therefore the ceiling height.
- The height of the clean zone (h_l) is derived the same way as in the steady state model, by expression (37)

To illustrate the effect of the different variables on the air exchange efficiencies and the apparent air flow rate the same cases as in section 7 have been calculated (different air flow rates and different heat source levels). The results is shown in figure 14 and 15.

Figure 14: The air exchange efficiency in the inhalation zone as a function of specific air flow rate, and with different heat source strength levels in the occupation zone. The room is 10 m², with a ceiling height of 2.5 meters, and the down draught air flow is assumed small (~1 l/s). The height of the inhalation zone is set at 1.1 meters (seated activity).

Figure 15: The apparent air flow rate in the inhalation zone as a function of specific air flow rate, and with differing heat source strength levels in the occupation zone. Other data as in figure 14.

As seen from figure 14, the air exchange efficiency in the inhalation zone rises to a given point, dependent on the heat source level, and from there decreases with increasing ventilation air flow rate. Comparing figure 14 with figure 12 reveals that this maximum point occurs when the height of the clean zone (h_l) is equal to the height of the inhalation zone (h_{exp}). For ventilation rates above this point/value, the nominal time constant is decreasing faster than the age of air in the inhalation zone, leading to an decrease in the air exchange efficiency. This fact has also been experimentally proven by Mierzwinski et.al. [56], who found that the air exchange efficiency (complete room) reduced significantly (2- 20 %) when the air flow was doubled from 5 to 10 air changes per hour. The heat load was varied between 15 W/m² and 62 W/m², in these experiments.

In figure 15 the apparent air flow rate in the inhalation zone is shown. If the ventilation air flow is adjusted to the convective air flow from heat sources so the height of zone one is near the height of the inhalation zone, the apparent air flow is approximately twofold of the real ventilation air flow. If the models presented here and the age of air concept are accepted, this means that only half the air flow is necessary compared to conventional mixing ventilation, if the same air quality shall be achieved in the inhalation zone. A 50 % reduction in air flow rate will lead to a significant reduction in energy use and ventilation plant costs.

Another variable that influences the air exchange efficiency, is the height of the ceiling. High ceilings were often used in old buildings to keep the air in the occupation zone acceptable. In figure 16 the air exchange efficiency in the inhalation zone is calculated for different ceiling heights, and for the four different heat source levels. The ventilation air flow rate is kept constant at 2 l/sm² (20 l/s).

Figure 16: The air exchange efficiency in the inhalation zone as a function of ceiling height, and with different heat source levels in the occupation zone. The room is 10 m², with a specific air flow rate of 2 l/sm², and the down draught air flow is assumed small (~1 l/s). The height to the inhalation zone is set to 1.1 meters (seated activity).

As seen from figure 16 the height of the ceiling has a strong influence on the air exchange efficiency in the inhalation zone. For example, in the case with 1 person and 1 PC in the occupation zone (normal heat load in offices), the efficiency is rising approximately 62 % per meter raised ceiling height. By raising the ceiling from 2.4 m to 3.2 m, which is in the 'normal' ceiling height range, the air exchange efficiency in the inhalation zone is increased from 2.05 to 2.58. This is equal to say that the apparent air flow rate in the inhalation zone is increased from 4.1 l/sm² to 5.2 l/sm² (the specific ventilation air flow rate is 2 l/sm²).

9. Models for vertical temperature stratification

In this section a simplified two-zone heat balance model is proposed. To simplify the model , complete mixing is assumed within the upper and lower zones. However, this is only true outside the thermal plume. In the thermal plume the temperature will be higher. When expressions for the mean temperature in the lower and upper zone are derived, it is shown how these can be used to predict more realistic linear and non-linear temperature distribution occurring in displacement ventilated rooms. Both a steady state model and a transient model are presented.

Figure 17: Principles and variables in the two-zone heat balance model.

9.1 Heat balances

The thermal two-zone model is based on the following assumptions:

- The temperature within the two zones is assumed to be uniform
- The effective internal heat capacity of a construction is concentrated at one point in the construction, or more correct in the middle of the accumulating layer of the construction. This heat accumulating layer (also

called the building structure) can be estimated from an analytical solution of the general one dimensional heat diffusion equation, see for example [57].

- The room air temperature, the surface temperature and the temperature in the heat accumulating layer are assumed to be equal in each zone.
- All the convective output from heat sources in zone 1 is assumed transported by the plume into zone 2.
- The supply air flow rate is assumed equal to the extract air flow rate.
- The supply air device are located well within zone 1, and the extract air device is located in zone 2.
- Exfiltration and infiltration from the outside and other adjacent rooms are assumed negligible compared to the ventilation air flow.
- The height of zone 1 is determined the same way as in section 7.1, with expression (37).

Referring to figure 17 and the above stated assumptions, a heat balance for zone 1 and zone 2 can be written:

$$\overbrace{q_{rad11}+q_{rad21}}^{\text{Radiation gain}}+\overbrace{C_{air}\dot{V}T_s}^{\text{Supply air flux}}-\overbrace{C_{air}\dot{V}_{con}T_1}^{\text{Convective flow flux}}$$
$$+\overbrace{\alpha_r A_{fl}\left(T_2-T_1\right)}^{\text{Radiation heat transfer}}+\overbrace{C_{air}\dot{V}_{dr}T_2}^{\text{Down draft flux}}-\overbrace{H_{tr1}\left(T_1-T_{a1}^*\right)}^{\text{Transmission loss}}=\overbrace{C_{a1}\frac{dT_1}{dt}}^{\text{Heat accumulation}} \tag{62.a.}$$

$$\overbrace{q_{con1}+q_{con2}}^{\text{Convection heat gain}}+\overbrace{q_{rad12}+q_{rad22}}^{\text{Radiation heat gain}}+\overbrace{C_{air}\dot{V}_{con}T_1}^{\text{Convective flow flux}}-\overbrace{\alpha_r A_{fl}\left(T_2-T_1\right)}^{\text{Radaition heat transfer}}$$
$$-\overbrace{C_{air}\dot{V}_{dr}T_2}^{\text{Down draft flux}}-\overbrace{H_{tr2}\left(T_2-T_{a2}^*\right)}^{\text{Transmission loss}}-\overbrace{C_{air}\dot{V}T_2}^{\text{Extract air flux}}=\overbrace{C_{a2}\frac{dT_2}{dt}}^{\text{Heat accumulation}} \tag{62.b.}$$

where C_{a1} and C_{a2} are the total effective heat capacities of zones 1 and 2 respectively, t is time, C_{air} is the volumetric heat capacity of air. H_{tr1} and H_{tr2} are the specific transmission losses from zones 1 and 2 respectively:

$$H_{tr1}=\sum U_1\cdot A_1 \tag{63.a.}$$

$$H_{tr2}=\sum U_2\cdot A_2 \tag{63.b}$$

where U is the U-value and A is the area for the different constructions in each zone. T_a is the temperature on the other side of the construction (adjacent room or the external environment). If the constructions in each zone are facing rooms or the external environment, with different temperatures, a weighted mean temperature must be calculated:

$$T_a^*=\frac{\sum U_i A_i T_{ai}}{\sum U_i A_i} \tag{64}$$

Equation (62.a.) and (62.b.) are mathematically similar to the transient contaminant model (section 8), and in matrix notation can be written:

$$\frac{d}{dt}\overbrace{\begin{bmatrix}T_1\\T_2\end{bmatrix}}^{\vec{T}}=\overbrace{\begin{bmatrix}a_{11}&a_{12}\\a_{21}&a_{22}\end{bmatrix}}^{\vec{A}}\overbrace{\begin{bmatrix}T_1\\T_2\end{bmatrix}}^{\vec{T}}+\overbrace{\begin{bmatrix}b_1\\b_2\end{bmatrix}}^{\vec{B}} \tag{65}$$

here the entries in the transport matrix ($\vec{A}$) and the source vector ($\vec{B}$) are:

$$a_{11} = -\frac{C_{air}\dot{V}_{con} + \alpha_{rad} A_{fl} + H_{tr1}}{C_{a1}} \quad ; \quad a_{12} = \frac{C_{air}\dot{V}_{dr} + \alpha_{rad} A_{fl}}{C_{a1}}$$
$$a_{21} = \frac{C_{air}\dot{V}_{con} + \alpha_{rad} A_{fl}}{C_{a2}} \quad ; \quad a_{22} = -\frac{C_{air}\left(\dot{V}_{dr} + \dot{V}_{v}\right) + \alpha_{rad} A_{fl} + H_{tr2}}{C_{a2}} \tag{66}$$

$$b_1 = \frac{C_{air}\dot{V}_{v}T_s + q_{net1} + H_{tr1}T^{*}_{a1}}{C_{a1}} \; ; \; b_2 = \frac{q_{net2} + H_{tr2}T^{*}_{a2}}{C_{a2}} \tag{67}$$

where q_{net1} and q_{net2} are the net heat gain in zones 1 and 2:

$$q_{net1} = q_{rad11} + q_{rad21} - q_{tr1} \tag{68.a}$$

$$q_{net2} = q_{con1} + q_{con2} + q_{rad12} + q_{rad22} - q_{tr2} \tag{68.b.}$$

9.2 Steady state model

A steady state model can be derived by setting $dT_1/dt = dT_2/dt = 0$ in (65), and solving for the unknown temperatures (T_1 and T_2). Solving for the unknown temperatures can, for example, be done by Cramer's rule, which gives:

$$T_{1\infty} = \frac{\det A_1}{\det A} = \frac{a_{12}b_2 - a_{22}b_1}{a_{11}a_{22} - a_{12}a_{21}} \tag{69.a.}$$

$$T_{2\infty} = \frac{\det A_2}{\det A} = \frac{a_{21}b_1 - a_{11}b_2}{a_{11}a_{22} - a_{12}a_{21}} \tag{69.b.}$$

It can easily be shown that the effective heat capacities (C_{a1}, C_{a2}), cancel out from expression (69), i.e. the steady state temperature is not a function of the heat capacity in the room.

9.3 Transient model

The thermal model (65) is mathematically equivalent to the transient contaminant model (section 8), and the general transient solution is given as:

$$T_1(t) = d_1 \exp(\lambda_1 t) + d_2 \exp(\lambda_2 t) + T_{1\infty} \tag{70.a.}$$

$$T_2(t) = d_1 k_1 \exp(\lambda_1 t) + d_2 k_2 \exp(\lambda_2 t) + T_{2\infty} \tag{70.b.}$$

The eigenvalues (λ) and the entries in the eigenvectors (k) are given as:

$$\lambda_{1/2} = \frac{trA \pm \sqrt{trA^2 - 4 \cdot \det A}}{2} \tag{71}$$

$$k_1 = \frac{\lambda_1 - a_{11}}{a_{12}} \quad ; \quad k_2 = \frac{\lambda_2 - a_{11}}{a_{12}} \tag{72}$$

where the determinant of the transport matrix ($detA$) is defined in expression (69),and trA is the trace of the transport matrix, given as :

$$trA = a_{11} + a_{22} \tag{73}$$

By introducing the initial values (temperatures) $T_1(0)$ and $T_2(0)$ into (70), the integrating constants d_1 and d_2 can be determined:

$$d_1 = \frac{[T_1(0) - T_{1\infty}]k_2 - T_2(0) + T_{2\infty}}{k_2 - k_1} \tag{74.a.}$$

$$d_2 = \frac{T_2(0) - T_{2\infty} - [T_1(0) - T_{1\infty}]k_1}{k_2 - k_1} \tag{74.b.}$$

The time constants are defined as:

$$\theta_1 = -\frac{1}{\lambda_1} \quad ; \quad \theta_2 = -\frac{1}{\lambda_2} \tag{75}$$

9.4 Models for the vertical temperature distribution

If there were no radiation processes occurring in the room the vertical temperature distribution would be similar to the contaminant distribution in the room, with a rather clear boundary between the lower cool zone and the upper warm zone. In practice, radiation heat gain distribution and long wave radiation between room surfaces will smooth out the stratification, giving more linear temperature profiles. The model presented in the preceding section calculates the bulk temperature in zones 1 and 2. As mentioned earlier, the temperature in each zone is never uniform, and a more realistic temperature distribution is required. In offices and similar rooms, with fewer and weaker heat sources, and relatively high air flow rates (2-6 ach), the temperature gradient is often approximately linear [1,15,17], see figure 18. In such cases the temperature gradient (dT/dz) can be calculated as linear from floor to ceiling, intercepting the bulk temperatures in the middle of zone 1 and zone 2. The linear temperature gradient can then be calculated as:

$$\frac{dT}{dz} = \frac{2 \cdot (T_2 - T_1)}{h_{ceil}} \tag{76}$$

The temperature in the room as a function of height from the floor (z) can be calculated as:

$$T_{lin}(z) = T_1 + \left(z - \frac{h_1}{2}\right)\frac{dT}{dz} \tag{76}$$

Figure 18: Typical and idealised vertical temperature distribution in office-like rooms, with fewer and weaker heat sources and relatively high air flow rates.

However, in rooms with many heat sources and moderate ventilation (relative to the heat sources), the temperature will be more non-linear as illustrated in Fig. 19. Recirculation gives a nearly uniform temperature in zone two, while a rather steep temperature gradient arises in zone 1. Such temperature gradients are common in classrooms, meeting rooms, theatres, and similar rooms, where the occupant density is high, see [2, 15]. A non-linear model for such temperature distributions can be made, assuming uniform temperature in zone 2, and the entire gradient taken in zone 1 (see Fig. 19). This gives the following expressions for the gradient in zone 1:

$$\frac{dT_{nlin}}{dz_1} = \frac{2 \cdot (T_2 - T_1)}{h_1} \tag{77}$$

The temperature as a function of the height from the floor for this non-linear model is given as:

$$T_{nlin}(z) = \begin{cases} T_1 + \left(z - \frac{h_1}{2}\right)\frac{dT_{nlin}}{dz_1} & ; \ if \ h_1 < z \\ T_2 & ; \ if \ h_1 \geq z \end{cases} \tag{78}$$

Figure 19: Typical and idealised vertical temperature distribution in rooms with many heat sources, and relatively moderate air flow rates.

9.5 Calculation of temperature indices

From the expressions derived in the preceding sections the mean temperature (<T>) and the temperature effectiveness (η) for the complete room can be calculated as:

$$< T >= \frac{T_1 h_1 + T_2 h_2}{h_{ceil}} \tag{79}$$

$$\eta = \frac{T_2 - T_s}{< T > - T_s} \tag{80}$$

The mean temperature (T_{occ}) and the temperature effectiveness in the occupation zone (η_{occ}) can be calculated:

$$T_{occ} = \begin{cases} \dfrac{T_1 h_1 + (h_{occ} - h_1) T_2}{h_{occ}} & ; \; if \; h_1 < h_{occ} \\ T_1 \; ; \; if \; h_1 \geq h_{occ} \end{cases} \tag{81}$$

$$\eta_{occ} = \frac{T_2 - T_s}{T_{occ} - T_s} \tag{82}$$

The floor temperature (T_{fl}) is usually measured 10 cm above the floor when assessing the normalised floor temperature (κ). Depending on the temperature distribution used, the floor temperature and normalised floor temperature can be calculated as:

$$T_{fl} = \begin{cases} T_1 + \left(0.1 - \dfrac{h_1}{2}\right) \dfrac{dT}{dz_1} \; ; \text{ with linear distribution} \\ T_1 + \left(0.1 - \dfrac{h_1}{2}\right) \dfrac{dT_{nlin}}{dz_1} ; \text{ with non - linear distribution} \end{cases} \tag{83}$$

$$\kappa = \frac{T_{fl} - T_s}{T_2 - T_s} \tag{84}$$

9.6 Results and discussion

In figure 20 and 21 the temperature effectiveness (η_{occ}) and the normalised floor temperature (κ) has been calculated with the steady state model (sub-section 9.2), for the same cases as in sub-sections 7.4 and 8.3 (10 m^2 office room). Additional data for the thermal calculation (e.g. heat transmission data) is given in the figure text. It is seen from Fig. 20 that the temperature effectiveness in the occupation zone is increasing steadily with increasing ventilation air flow, starting from around 1.1-1.2 and increasing to 1.6-1.7. Compared to the contaminant removal efficiency presented in Fig. 11, the temperature effectiveness is much smaller. This is mainly due to radiation heat gain from heat sources, long wave radiation heat transfer from the zone 2 to zone 1, and heat conduction through walls, floor and ceiling. In contrast to the contaminant removal efficiency, the heat source level, and hence the convective air flow rate, does not influence the temperature effectiveness to a great extent.

The normalised floor temperature, shown in Fig. 21, is decreasing steadily with increasing ventilation air flow rate. This means that the air temperature 10 cm above the floor is approaching the supply temperature, when the ventilation air flow is increasing. Figure 21 also shows that the heat source level, and therefore the convective air flow rate has almost no influence on the normalised floor temperature.

As Mattson [2] points out, steady state conditions rarely occur in real displacement ventilated rooms. This is due to heat accumulation in the building structure, giving rise to thermal time constants much larger than the nominal time constant for the ventilation (τ_n). In the transient thermal model time constant 1 is in all practical cases much larger than time constant 2: $\theta_1 >> \theta_2$. This implies that in step down or step up experiments, time constant 1 determines how fast steady state is reached. θ_1 can therefore be called the dominating time constant. In figure 22 the dominating time constant has been calculated for rooms with different constructions (light to

very heavy constructions), and with different ventilation air flow rates. Other data are equal to those used in Fig. 20 and 21. Even with light constructions and high ventilation (6 l/sm²) the dominating time constant has a value of approximately 2.0 (see Fig. 22), which is about 15 times higher than the nominal time constant of the ventilation air flow ($\tau_n \approx 7$ minutes). After three time constants approximately 95 % of the total temperature change has elapsed, which can be a practical way to define steady state conditions. I.e. that the steady state temperatures are reached after approximately 6 hours. In real rooms (offices, classrooms, meeting rooms, etc.) the occupants seldom stay in the room for such a long period, and steady state conditions are therefore unlikely to happen, even in rooms with small thermal time constants.

Figure 20: The temperature effectiveness in the occupation zone as a function of specific air flow rate, and with different heat source levels in the occupation zone. The room is 10 m², with a ceiling height of 2.5 meters, and the down draught air flow is assumed small (~1 l/s). The height of the occupation zone is set at 1.2 meters (seated activity). U-values for the walls, floor and ceiling are respectively 0.35W/m²K, 0.2 W/m²K and 0.2 W/m²K. The temperature in the air surrounding the simulated room is set at 20°C, and the supply air temperature is 16°C. The by floor area normalised radiation heat transfer coefficient is 4.0 W/m²K.

Figure 21: The normalised floor temperature as a function of specific air flow rate, and with different heat source levels in the occupation zone. The data for the simulated room is the same as in Fig. 20.

Figure 22 : The dominating time constant as a function of specific air flow rate, and with different weight of the constructions in the room. The light room consist of composite walls, floor and ceiling. The medium heavy room consist of composite walls, floor with carpet and acoustic ceiling below the concrete floor. The heavy room consist of lightweight concrete walls, concrete floor with thin floor covering and acoustic ceiling below the concrete floor. The very heavy room consist of masonry walls and massive concrete floor and ceiling. Otherwise the same data as used in Fig. 20 apply.

10. Conclusion

Models for prediction of vertical contaminant and temperature stratification in displacement ventilated rooms have been developed. Both steady state and transient models have been proposed. These models can be used to:

- predict contaminant removal efficiency in the inhalation zone, the occupation zone and in the complete room.
- predict age of air and air exchange efficiency in the inhalation zone, occupation zone, and in the complete room.
- predict temperature distribution and temperature effectiveness under both steady state and transient conditions.
- the transient models proposed can be implemented in building simulation tools for better prediction of, for example, energy use and long-term exposure in displacement ventilated rooms.
- design optimal ventilation solutions, giving prescribed air quality with low energy use and ventilation plant costs.

The developed contaminant models indicate that the polluted zone can be drawn below the nose level (inhalation zone) without deteriorating the inhaled air quality significantly. This is verified by experiments described in the literature. This opens for design of displacement ventilation with substantially reduced air flows compared to conventional mixing ventilation, with significant reduction in energy use and ventilation plant costs. This apply for rooms with moderate human movements (offices, classrooms, theatres, etc.).

By use of the developed transient thermal model, it is shown that steady state conditions are unlikely to occur in real rooms. This has also been verified in experimental studies.

In an accompanying paper (part 2), the prediction from the proposed models is compared to experimental data found in the literature. The steady state thermal model is also compared to other simplified models.

11. Nomenclature

A	Area (m²)
$\vec{A}$	Transport matrix
a	Entries in the transport matrix (h or s), or a constant
$\vec{B}$	Source vector
b	Entries in the source vector
C	Concentration (mg/m³, µg/m³ or ppm) or heat capacity (Wh/K or J/K))
d	Integrating constants or diameter (m)
F	View factor (-)
Gr	Grashof's number (-)
g	Contaminant generation rate (mass/time) or acceleration of gravity (m/s²)

H	Specific transmission loss (W/K)
h	Height (m)
k	Entries in the eigenvector (-) or a constant
L	Length (m)
l	Cross sectional dimension (m)
P	Convective heat output (W)
q	Heat flow (W)
t	Time (h or s)
T	Temperature (°C or K)
U	U-value (W/m²K)
V	Air volume (m³)
$\dot{V}$	Air flow rate (l/s)
w	Width (m)
z	Vertical space co-ordinate (m)

Greek letters

α	Radiation heat transfer coefficient (W/m²K) or area ratio (-)
β	Volume expansion coefficient (1/K)
ε	Efficiency (-)
φ	Convective part (-)
η	Effectiveness (-)
λ	Eigenvalues (h or s)
κ	Normalised floor temperature (-)
θ	Time constant (h or s)
τ	Age of air or time constant (h or s)
π	3.1415
ν	Kinematic viscosity (m²/s)
ω	Contaminant transfer factor (-)

Subscript

1	Zone 1 or number 1
2	Zone 2 or number 2
a	Ambient or accumulating layer
air	Air (heat capacity)
app	Apparent
c	Convective
ceil	Ceiling
con	Convective
dr	Down draught
e	Extract or entrainment
exp	Exposure or inhalation zone
f	Surface (temperature)
fl	Floor
k	Characteristic
lin	Linear
line	Line source
n	Nominal
net	Net gain
nlin	Non-linear
max	Maximum
occ	Occupation zone
p	Point or pole point
per	Person
point	Point source
r	Radiation
rad	Radiator or radiation
s	Supply
tr	Transmission
v	Ventilation

∞ Steady state (infinity)

Super script

a Air exchange
c Contaminant removal
T Temperature

Acknowledgement

This work has been financially supported by the Norwegian Research Council, Project no. 111372\330.

References

[1] Elisabeth Mundt 1996, "The performance of displacement ventilation systems; Experimental and Theoretical studies", Ph.D. thesis, Royal Institute of Technology, Stockholm 1996.

[2] Mattson M.; "On the efficiency of displacement ventilation" Ph.D. thesis, Royal Institute of Technology, Gavle, Sverige 1999.

[3] Brohus H., Nielsen P.V., " Personal Exposure in Displacement Ventilated Rooms", Indoor Air 6/96, pp.157-167. Munksgaard 1996.

[4] Heiselberg P., Sandberg M., "Convection from a slender cylinder in a ventilated room", Proceedings Roomvent '90, Oslo Norway. 1990.

[5] Holmberg.R.B. et. al., "Inhalation-zone air quality provided by displacement ventilation". Proceedings Roomvent '90, Oslo Norway. 1990.

[6] Cox C.W.J. et. al., " Displacement ventilation systems in office rooms : A field study". Proceedings Roomvent '90, Oslo Norway. 1990.

[7] Nickel J., "Air quality in a conference room with tobacco smoking ventilated with mixed or displacement ventilation" . Proceedings Roomvent '90, Oslo Norway. 1990.

[8] Palonen J. et. al., "Displacement ventilation in a lecture hall, a case study". Proceedings Roomvent '90, Oslo Norway. 1990.

[9] Hatton A., Awbi H.B., " A study of the air quality in the breathing zone" Proceedings ROOMVENT '98 Stockhom, Sweden, Vol.2, pp. 159 – 166.

[10] Tanabe S.I., et.al., "Field study on the ventilation effectiveness and thermal comfort in a concert hall with displacement ventilation system" Proceedings ROOMVENT '98 Stockhom, Sweden, Vol.2, pp. 181 – 188.

[11] Tanabe S.I., Kimura K.I., "Comparison of ventilation performance and thermal comfort among displacement, underfloor and, ceiling based air distribution systems by experiments in a real sized office chamber". " Proceedings ROOMVENT '96 Yokohama, Japan, Vol.3, pp. 299 - 306.

[12] Mierzwinski S., Popiolek Z., Trzeciakiewicz Z, "Experiments on two–zone air flow forming in displacement ventilation". Proceedings ROOMVENT '96 Yokohama, Japan, Vol.3, pp. 339 – 346.

[13] Ørhede E., Breum N.O., Skov T., " Percieved and Measured Indoor Climate with Dilution versus Displacement Ventialtion : an Intervention Study in a Sewing plant", Indoor Air 6/96, pp. 151-156. Munksgaard 1996.

[14] Brohus H. et.al., "Perceived air quality in a displacement ventilated room", Proc. Indoor Air '96 Nagoya, Japan, Vol.1, pp. 811-816. 1996

[15] Skistad H., "Displacement ventilation", Research Studies Press Ltd, John Wiley & Sons inc., 1994.

[16] Li Y., Sandberg M., Fuchs L., "Vertical temperature profiles in Rooms Ventilated by Displacement: Full-Scale Measurement and Nodal Modelling. Indoor Air, 2, 225 – 243 (1992)

[17] Nielsen P.V., "Temperature distribution in a displacement ventilated room" Proc. ROOMVENT '96, Yokohama, Japan, 1996.

[18] Nielsen P.V., "Vertical temperature distribution in a room with displacement ventilation". IEA Annex 26: Energy efficient ventilation of large enclosures, Rome, 1995. PAPER No. 48. INDOOR ENVIRONMENTAL TECHNOLOGY. University in Aalborg.

[19] Skåret E., "Ventilasjonsteknikk", Kompendium Institutt for VVS, Norges Tekniske Høgkole, Trondheim 1986. (In Norwegian).

[20] Sandberg E., Koskela H., Hautalamoi T., "Convective flows and vertical temperature gradient with the active displacement air distribution" Proceedings ROOMVENT '98 Stockhom, Sweden, Vol.1, pp. 61 – 68.

[21] Overby H., "Vertikale temperatur gradienter i rum med konvektive strømninger", Ph.D. thesis, The University of Aalborg, Dep. of Building Technology and Structural Engineering. 1993. (In DFanish).

[22] Togari et al. "A simplified model for predicting vertical temperature distribution in large spaces" ASHRAE Transactions, Vol. 99, Part 1. pp. 84-99.

[23] Inard C., Meslem A., Depecker P., "Use of zonal model for prediction of air temperature distribution in large enclosures" ROOMVENT '96, Yokohama, Japan, Vol. 2, pp. 177-184. 1996

[24] Shilkrot E.O., Zhivov A.M., "Zonal model for displacement ventilation design". Proceedings ROOMVENT '96 Yokohama, Japan, Vol. 2, pp. 449 – 458.

[25] Manzoni D., Rongere F.X., "Simplified models of displacement ventilation systems" Proceedings ROOMVENT '96 Yokohama, Japan, Vol. 2, pp. 449 – 458.

[26] Koganei M., Holbrook G.T., Olesen B., Woods J., "Modelling the thermal and indoor air quality performance of vertical displacement ventilation". Proceedings of Indoor Air '93, Helsinki, Vol. 5, pp. 241-426.

[27] Quingean C.,et.al. "Measurement and computation of ventilation efficiency and temperature efficiency in a ventilated room" Energy and Buildings, no. 12, 1988.

[28] FLOVENT, "A commercial CFD program for modelling indoor air flow" from Flometrics Ltd, UK. http://www.flovent.com/

[29] VORTEX-2. A commercial CFD program for modelling indoor air flow, from Flowsolve Ltd, UK. http://ourworld.compuserve.com/

[30] Jacobsen T:V:& Nielsen P.V., "Numerical modelling of thermal environment in a displacement ventilated room". Proceedings Indoor Air '93 Helsinki Finland.

[31] Sandberg M., Lindstrøm S., "Stratified flows in ventilated rooms – A model study", Proceedings Roomvent '90, Oslo Norway. 1990.

[32] Sandberg M., Lindstrøm S., "A model for ventilation by displacement". Proceedings Roomvent '87, Stockholm, Sweden. 1987.

[33] Hunt G.R, Linden P.F., "The fluid mechanics of natural ventilation – displacement ventilation by buoyancy-driven flows assisted by wind". BUILDING AND ENVIRONMENT, Vol.34, No. 6, 1999, pp. 707-720.

[34] Cooper P., Linden P.F., "Natural ventilation of enclosures with multiple point sources or a vertically distributed source of buoyancy" " Proceedings ROOMVENT '96 Yokohama, Japan, Vol. 3, pp. 203 – 210.

[35] Cooper P., Mayo G.A., Sørensen P., "Natural displacement ventilation of an enclosure with a distributed buoyancy source applied to one vertical wall". Proceedings ROOMVENT '98 Stockhom, Sweden, Vol. 1, pp. 45 – 51

[36] P.O. Tjelflaat, M. Sandberg, "Assessment of Ventilation- and Energy-Efficiency in Design for Large Enclosures". ROOMVENT '96, Yokohama, Japan 1996.

[37] Farex; "Dimensjonering av tilluft" Farex klima as 1989. (In Norwegian).

[38] Sørensen H.H., "Ventilation principer " Chapter 1 in : " Ventilation ståbi", Editor: H.H. Sørup, Teknisk Forlag AS, 1988. (In Danish).

[39] Kofoed P., "Thermal plumes in ventilated rooms." Ph.D. thesis, University of Aalborg, 1991

[40] Elisabeth Mundt 1991, "Temperaturgradienter och konvektionsfløden vid deplacerende ventilation" Licensiat avhandling, KTH 1991. (In Swedish).

[41] Tjelflaat P.O. "Forelesningsnotater i fag 67163 Strømning i ventilerte rom", Inst. for Klima- og kuldeteknikk, NTH,Trondheim 1995. (In Norwegian).

[42] Danielson P.O., "Convective flow and temperature in rooms with displacement system." Proc. ROOMVENT '87 Stockholm 1987.

[43] Fitzner K.; "Förderprofil einer Wärmerquelle bei verschiden Temperaturgradienten und der Einfluß auf die Raumströmung bei Quellüftung." Ki Klima-Kälte Heizung, No 10, 1989. (In German).

[44] Koefoed P., Nielsen P.V., "Thermal plumes in ventilated rooms – Measurement in stratified surroundings and analysis by use of an extrapolation method". Proceedings Roomvent '90, Oslo Norway. 1990.

[45] Hautalampi T., Sandberg E., Koskela H., "Behaviour of convective plumes with active displacement air flow patterns", Proceedings ROOMVENT '98 Stockhom, Sweden, Vol.1, pp. 415 – 421.

[46] Popiolek Z., Treciakiewicz S., Mierzwinski S., "Improvement of a plume volume flux calculation method", Proceedings ROOMVENT '98 Stockhom, Sweden, Vol. 1, pp. 423 – 430.

[47] Hyldegaard C.A., "Thermal plumes above a person", Proceedings ROOMVENT '98 Stockhom, Sweden, Vol. 1, pp. 407 – 413.

[48] Mierzwinski S.& Popiolek Z. ; " The convective plume above the human body as a factor of the ventilation process ". Technical University, Gliwice, Poland.

[49] Morton B.R., Taylor G., Turner J.S., "Turbulent gravitational from maintained and instantaneous sources. Proc. Royal Soc. Vol. 234 A p. 1. 1956.

[50] Fanger P.O; "Indeklima" Chapter 2 in : "Varme- og klimateknikk". Editors: Stampe and Kjerulf Jensen, 1992. (In Danish).

[51] Cengel Y.A, "Heat transfer. A practical approach". McGraw Hill 1998

[52] Li Y., Sandberg M., Fuchs L., "Effects of thermal radiation on airflow with displacement ventilation : an experimental investigation". Energy and Buildings, 19 (1993) pp. 263 – 274. 1993.

[53] Mathisen H.M., "Displacement Ventilation . the Influence of the Characteristics of the Supply Air Terminal Device on the Airflow Pattern", Indoor Air, 1, 47-64 (1991).

[54] Kruhne H, Fitzner K., "Air quality in the breathing zone with displacement flow", Proceedings ROOMVENT '94 Krakow, Poland, Vol. 2, pp. 93 – 101.

[55] Dokka, T.H., Bjørseth, O. and Hanssen, S.O. (1996) "Envisim; a windows application for simulation of IAQ ", in: Yoshizawa, S., Kimura, K., Ikeda, K., Tanabe, S. and Iwata, T. (eds.) Proceedings of Indoor Air '96, Nagoya, Vol. 2, pp. 491-496.

[56] Mierzwinski S., Nawrocki W. and Trzeciakiewisz Z., "Air exchange efficiency under displacement ventilation conditions" , Proceedings ROOMVENT '94 Krakow, Poland, Vol. 2, pp. 103 – 112.

[57] CEN EN 832 Thermal performance of buildings - Calculation of Energy Use for Heating -Residential Buildings

Appendix A : Theoretical derivation of boundary layer air flow around a person

Skåret [19] has theoretically derived the following expression for the rising air flow along a vertical heated surface:

$$\dot{V} = 2.9 \cdot w \cdot \Delta T^{0.4} z^{1.2} \tag{A.1}$$

ΔT is the difference between the room air temperature (T_a) and the surface temperature (T_f) of the hot surface, w and z is the height and width of the cold surface respectively. Expression (A.1) is derived using conservation of momentum and energy, and assuming turbulent flow.

The surface temperature of the person is most often unknown, but the convective heat output of the person (P_{per}) can often be estimated. The convective heat transfer coefficient gives a relationship between the temperature difference (ΔT) and the convective heat output (P_{per}). The convective heat transfer coefficient for a vertical plate can be calculated by the following expression, [51]:

$$Nu = 0.1 \cdot R_a^{1/3} \tag{A.2}$$

Inserting physical data for air at 20 °C into (A.2), gives the following expression for the convective coefficient:

$$\alpha_c = 1.21 \cdot \Delta T^{1/3} \tag{A.3}$$

Here, we have assumed turbulent flow and that the cylinder can be regarded as a vertical plate. The convective heat output form the person can know be calculated as:

$$P_{per} = A_{per} \alpha_c \Delta T \tag{A.4}$$

Inserting (A.4) and (A.3) into (A.1) gives the following expressions for the boundary air flow rate along a person:

$$\dot{V}_{per} = 8.61 \cdot \left(\frac{P_{per}}{A_{per}} \right)^{0.3} z^{1.2} d_{per} \tag{A.5}$$

which is the expression for the boundary layer flow along a person given in section 4.4.

Appendix B : Comparison of plume model prediction and measurements

A.1 Desk lamp

Plume flow rates above a desk lamp placed 1.2 meters above the floor (top of the lamp) has been measured [1]. The diameter of the desk lamp was 5 cm, and the heat output where 60 W, where 1/3 was assumed to be convective heat. For more details about the experiments see Mundt [1]. Table 1 and 2 show results from the experiments compared to model predictions.

Table A1: Comparison between model prediction and measurements for a desk lamp, gradient 0.8 K/m

Height above floor	**1.6 m**	**1.8 m**	**2.0 m**	**2.25 m**
Experiments				
Mundt [1], Air flow : 20.8 l/s	6 l/s	11 l/s	12 l/s	13 l/s
Mundt [1], Air flow : 41.6 l/s	5 l/s	9 l/s	11 l/s	12 l/s
Model prediction				
Gradient model (Mundt), expression (16)	4 l/s	7 l/s	11 l/s	16 l/s
Expression (10), lower limit: a = 1.7	5 l/s	9 l/s	13 l/s	19 l/s
Expression (10), upper limit: a = 2.5	6 l/s	10 l/s	14 l/s	20 l/s

Table 2: Comparison between model prediction and measurements for a desk lamp, gradient 2.4 K/m

Height above floor	1.6 m	1.8 m	2.0 m	2.25 m
Experiments				
Mundt [1], Air flow : 21 l/s	6 l/s	10 l/s	13 l/s	*
Mundt [1], Air flow : 42 l/s	5 l/s	10 l/s	13 l/s	12 l/s
Model prediction				
Gradient model (Mundt), expression (16)	4 l/s	8 l/s	11 l/s	15 l/s
Expression (10), lower limit: a = 1.7	5 l/s	9 l/s	13 l/s	19 l/s
Expression (10), upper limit: a = 2.5	6 l/s	10 l/s	14 l/s	20 l/s

A.2 Computer simulator

Plume flow rates above a computer simulator with the top 1.05 meters above the floor have been measured [1]. The 'computer' was cubic with all sides equal to 30 cm. The heat output was 75 W, where 2/3 was assumed to be convective heat. For more details about the experiments see Mundt [1]. Table 3 and 4 show results from the experiments compared to model predictions.

Table A3: Comparison between model prediction and measurements for a computer simulator, temperature gradient 0.6-0.7 K/m

Height above floor	1.45 m	1.85 m	2.25 m
Experiments			
Mundt [1], Air flow : 42 l/s	16 l/s	30 l/s	54 l/s
Mundt [1], Air flow : 70 l/s	20 l/s	31 l/s	40 l/s
Model prediction			
Gradient model (Mundt)	**19 l/s**	**33l/s**	**49 l/s**
Expression (10), lower limit: $a = 1.7$	19 l/s	35 l/s	54 l/s
Expression (10), upper limit: $a = 2.5$	28 l/s	46 l/s	67 l/s

Table A4: Comparison between model prediction and measurements for a computer simulator, temperature gradient 2.0 K/m

Height above floor	1.45 m	1.85 m	2.25 m
Experiments			
Mundt [1], Air flow: 42 l/s	20 l/s	31 l/s	40 l/s
Model prediction			
Gradient model (Mundt)	19 l/s	31 l/s	43 l/s
Expression (10), lower limit: $a = 1.7$	19 l/s	35 l/s	54 l/s
Expression (10), upper limit: $a = 2.5$	28 l/s	46 l/s	67 l/s

A.3 Fluorescent light

Plume flow rates above a fluorescent light 1.2 meters above the floor have been measured [1]. The light was 1.25 meters long. The diameter was small, so the distance to the pole-point could be ignored. The heat output was 36 W, where 1/3 was assumed to be convective heat. For more details about the experiments see Mundt [1]. Table 5 and 6 show results from the experiments compared to model predictions.

Table A5: Comparison between model prediction and measurements, with temperature gradient 0.3–0.5K/m.

Height above floor	1.3 m	1.6 m	1.8 m	2.0 m
Experiments				
Mundt [1] , 42 l/s, 0.3 K/m	*	11 l/s	*	22 l/s
Mundt [1] , 42 l/s, 0.4 K/m	*	11 l/s	25 l/s	*
Mundt [1] , 21 l/s, 0.5 K/m	*	16	23 l/s	25 l/s
Model prediction				
Gradient model (Mundt)	3 l/s	12 l/s	19 l/s	25 l/s
Expression (11), lower limit: $a = 1.7$	3 l/s	14 l/s	20 l/s	27 l/s
Expression (11), upper limit: $a = 2.5$	3 l/s	14 l/s	20 l/s	27 l/s

Table A6: Comparison between model prediction and measurements, with temperature gradient 2.0–2.1K/m.

Height above floor	**1.3 m**	**1.6 m**	**1.8 m**	**2.0 m**
Experiments				
Mundt [1], 42 l/s, 2.0 K/m	7 l/s	16 l/s	*	*
Mundt [1], 42 l/s, 2.1 K/m	*	15 l/s	21 l/s	*
Mundt [1], 21 l/s, 2.1 K/m	*	15 l/s	21 l/s	*
Model prediction				
Gradient model (Mundt)	3 l/s	12 l/s	18 l/s	22 l/s
Expression (11), lower limit: $a = 1.7$	3 l/s	14 l/s	20 l/s	27 l/s
Expression (11), upper limit: $a = 2.5$	3 l/s	14 l/s	20 l/s	27 l/s

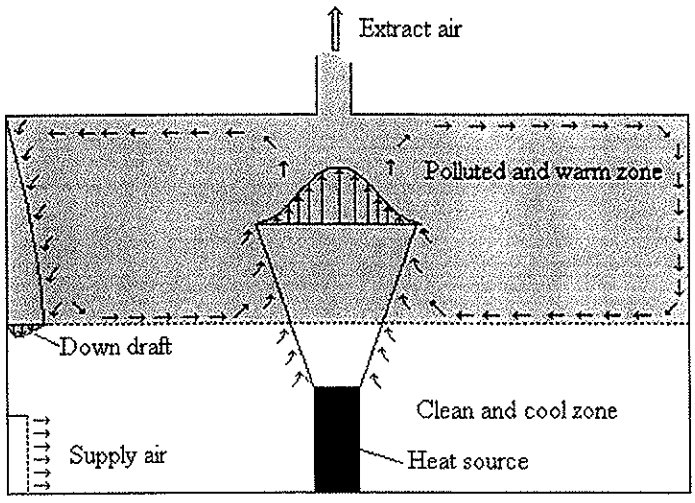

Figure 1 : The working principles in displacement ventilation

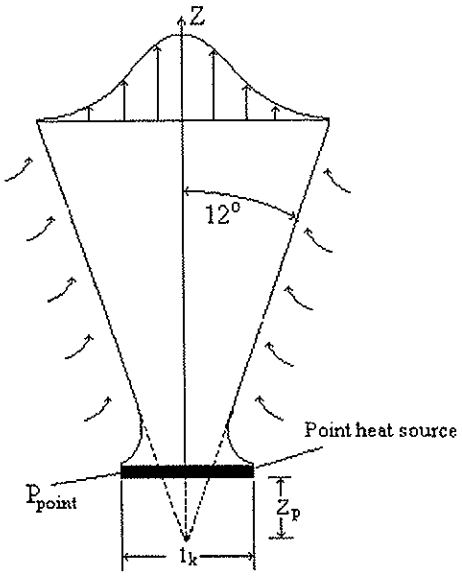

Figure 2 : Idealised plume above a point source, with an assumed Gaussian temperature and velocity distribution.

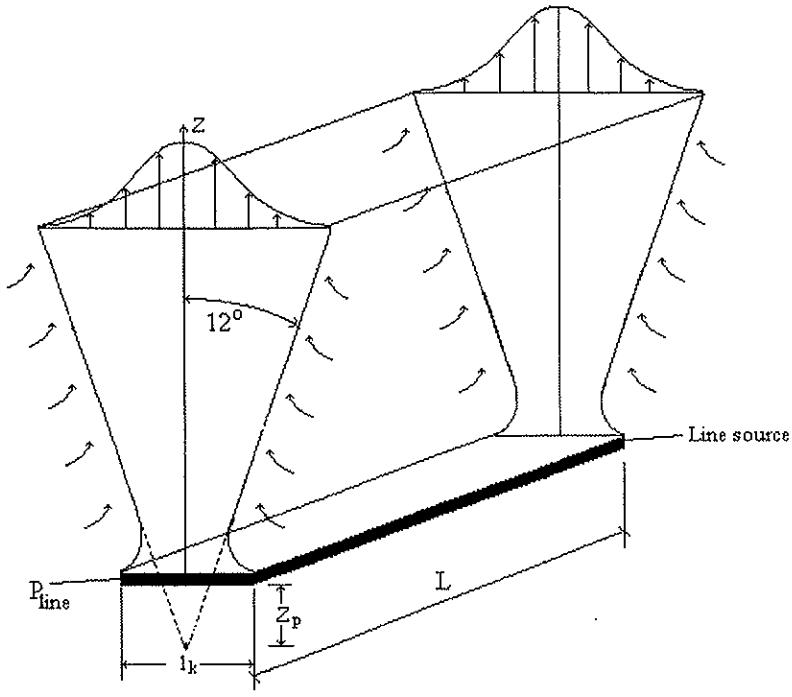

Figure 3 : Idealised plume above a line source, with an assumed Gaussian temperature and velocity distribution.

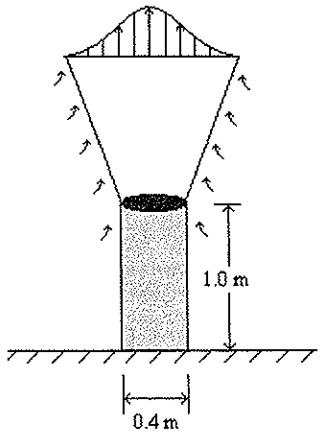

Figure 4: Dimension of the cylinder used in the experiments by Mundt [1] and Kofoed [39].

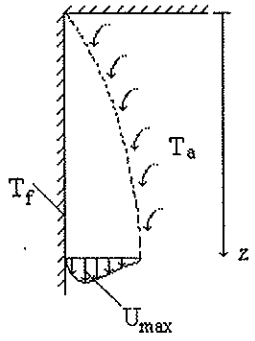

Figure 5 : Down draught along a cold vertical surface

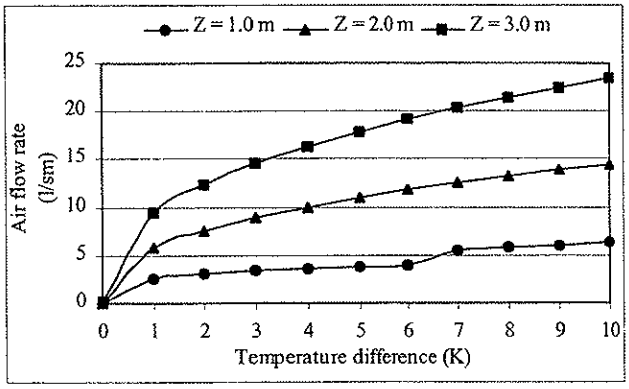

Figure 6 : Air flow rate per meter width along a vertical cold or warm surface, as a function of the temperature difference between the surface and the surrounding air and the height of the surface. A value of $k_1 = 2.5$ in equation (20) and a value of $k_2 = 2.57$ in equation (21) has been used.

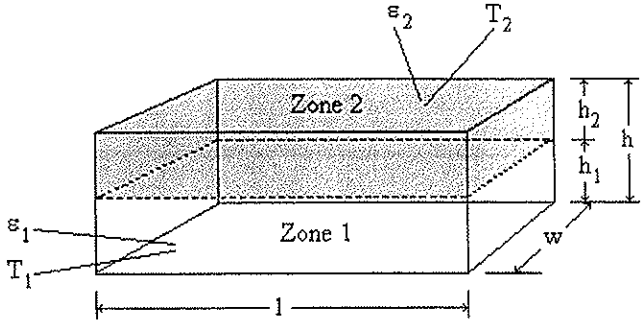

Figure 7 : Two-zone long wave radiation transfer model

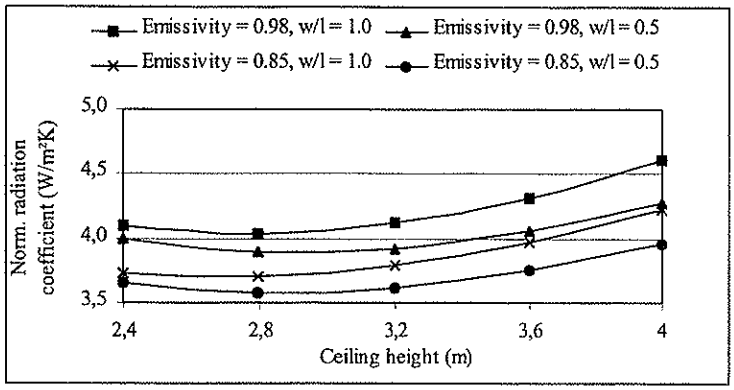

Figure 8 : Normalised radiation heat transfer coefficient (α_r) as a function of emissivity (ε), the ratio of the width and length of the room (w/l) and the ceiling height (h_{ceil}). The temperatures in the zone has been held constant at T_1 = 21 ° C and T_2 = 25 °C, and the height of zone 1 is set at 1.2 m.

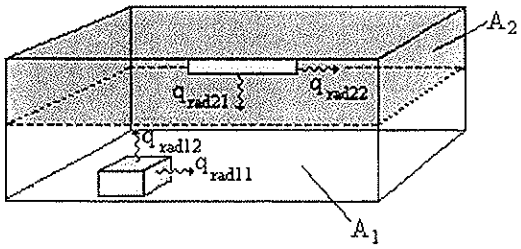

Figure 9 : Distribution of radiation heat output from heat sources in the two zones.

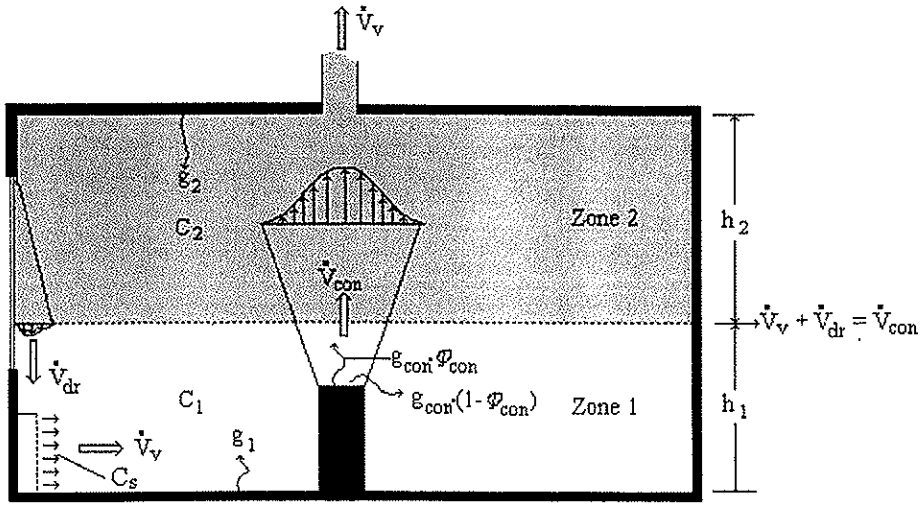

Figure 10: Principles and variables in the contaminant two-zone model

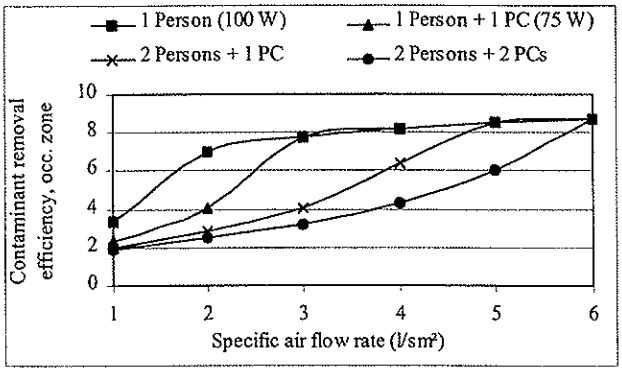

Figure 11: Contaminant removal efficiency in the occupation zone (ε^{c}_{occ}) as a function of the different heat source levels and specific ventilation air flow rate ($\dot{V}''_v$) in a 10 m² office room. The height of the occupation zone is 1.2 m (seated activity).

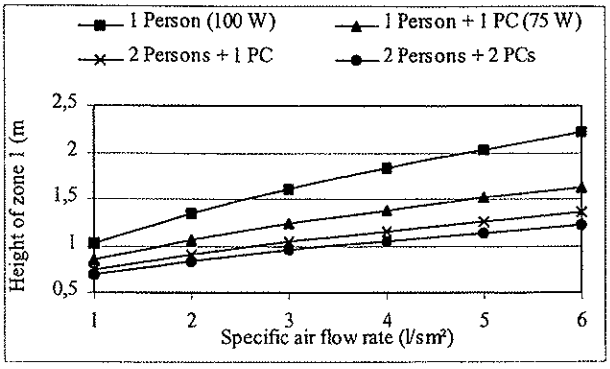

Figure 12: The height of the clean zone (zone 1) as a function of the different heat source levels and specific ventilation air flow rate in a 10 m² office room.

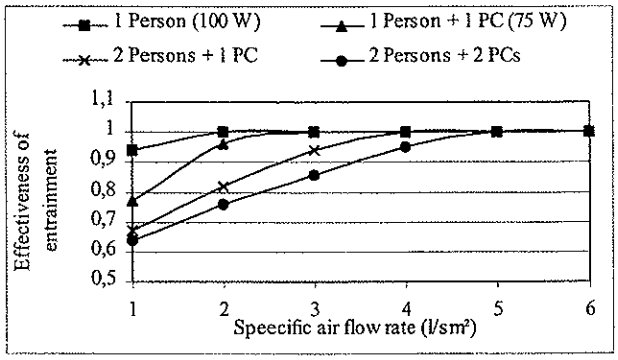

Figure 13: The effectiveness of entrainment in the human boundary layer (η_e) as a function of the different heat source levels and specific ventilation air flow rate in a 10 m² office room. The height of the inhalation zone (h_{eq}) is set at 1.1 m (seated activity).

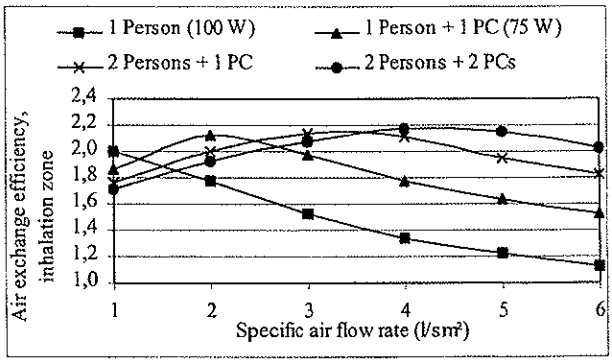

Figure 14: The air exchange efficiency in the inhalation zone as a function of specific air flow rate, and with different heat source strength levels in the occupation zone. The room is 10 m², with a ceiling height of 2.5 meters, and the down draught air flow is assumed small (~1 l/s). The height of the inhalation zone is set at 1.1 meters (seated activity).

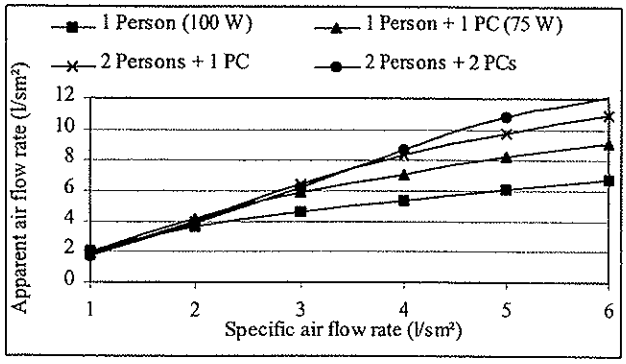

Figure 15: The apparent air flow rate in the inhalation zone as a function of specific air flow rate, and with differing heat source strength levels in the occupation zone. Other data as in figure 14.

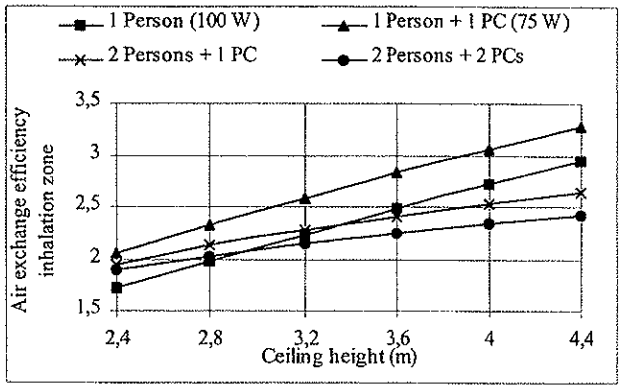

Figure 16: The air exchange efficiency in the inhalation zone as a function of ceiling height, and with different heat source levels in the occupation zone. The room is 10 m², with a specific air flow rate of 2 l/sm², and the down draught air flow is assumed small (~1 l/s). The height to the inhalation zone is set to 1.1 meters (seated activity).

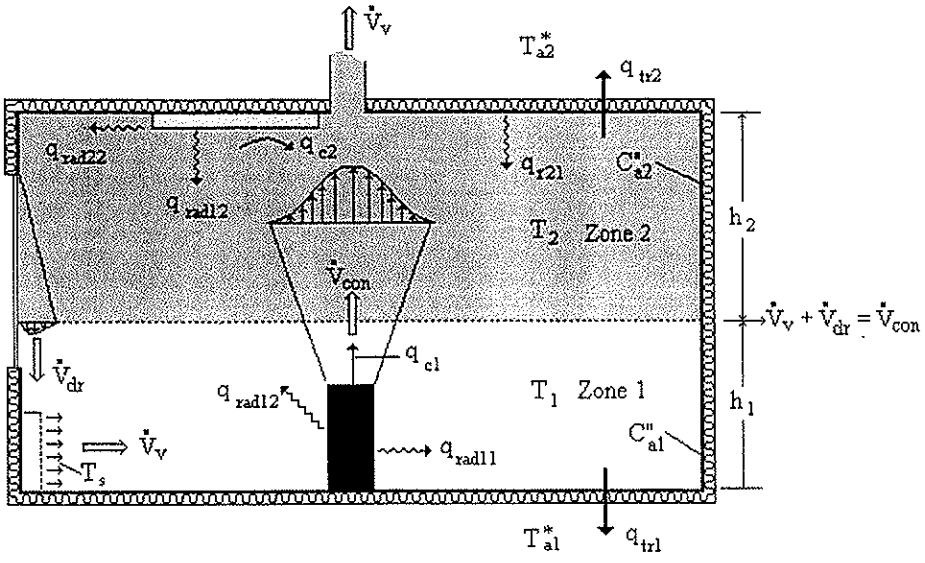

Figure 17: Principles and variables in the two-zone heat balance model.

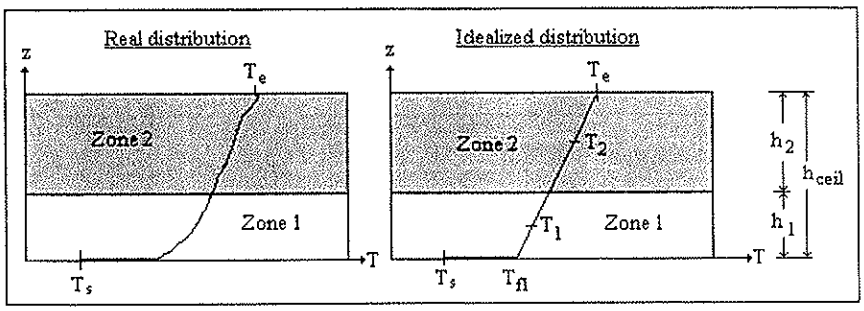

Figure 18: Typical and idealised vertical temperature distribution in office-like rooms, with fewer and weaker heat sources and relatively high air flow rates.

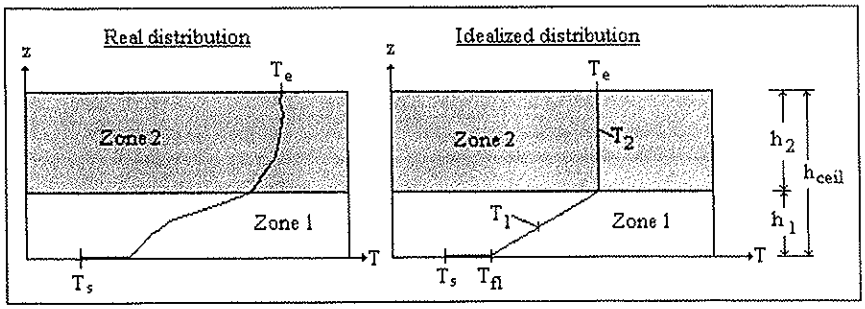

Figure 19: Typical and idealised vertical temperature distribution in rooms with many heat sources, and relatively moderate air flow rates.

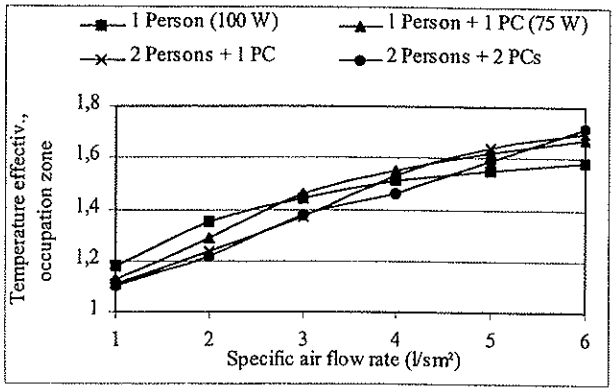

Figure 20: The temperature effectiveness occupation zone as a function of specific air flow rate, and with different heat source levels in the occupation zone. The room is 10 m², with a ceiling height of 2.5 meters, and the down draught air flow is assumed small (~1 l/s). The height of the occupation zone is set at 1.2 meters (seated activity). U-values for the walls, floor and ceiling are respectively 0.35W/m²K, 0.2 W/m²K and 0.2 W/m²K. The temperature in the air surrounding the simulated room is set at 20°C, and the supply air temperature is 16°C. The by floor area normalised radiation heat transfer coefficient is 4.0 W/m²K.

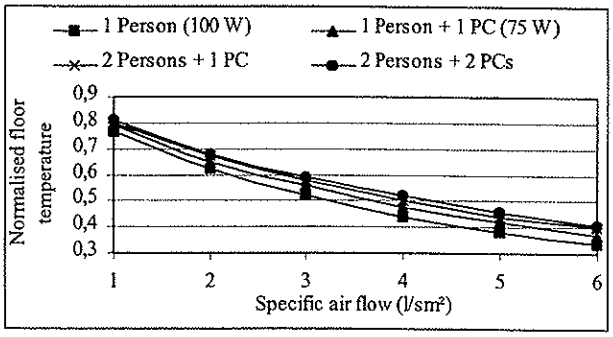

Figure 21: The normalised floor temperature as a function of specific air flow rate, and with different heat source levels in the occupation zone. The data for the simulated room is the same as in figure 20.

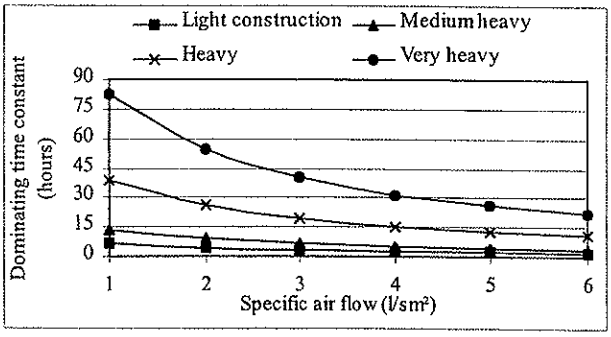

Figure 22 : The dominating time constant as a function of specific air flow rate, and with different weight of the constructions in the room. The light room consist of composite walls, floor and ceiling. The medium heavy room consist of composite walls, floor with carpet and acoustic ceiling below the concrete floor. The heavy room consist of lightweight concrete walls, concrete floor with thin floor covering and acoustic ceiling below the concrete floor. The very heavy room consist of masonry walls and massive concrete floor and ceiling. Otherwise the same data as used in figure 20 apply.

Paper VI

Dokka TH, Tjeelflaat P.O.

" Simplified models for prediction of vertical contaminant and temperature stratification in displacement ventilated rooms; part 2 : validation",

Submitted to Energy and Buildings.

Paper VII

Dokka TH, Jørgensen R., Bjørseth O., Malvik B.

" The influence of substrate- and sink effects on VOC emissions from water-based paints - implication to model prediction in real rooms"

Submitted to Indoor Air

The influence of substrate- and sink effects on VOC emissions from water-based paints - implication to model prediction in real rooms

T.H.Dokka[1]

R.B.Jørgensen[1]

O.Bjørseth[1]

B. Malvik[2]

[1]Department of Industrial Economy & Technology management, Norwegian University of Science and Technology
[2] SINTEF, Foundation for Scientific and Industrial Research at the Norwegian Institute of Technology

Correspondence to

Tor Helge Dokka, Dep. of Industrial Economics and Technology Management, Norwegian University of Science and Technology, N-7491 Trondheim, Norway.
FAX: +47 73593107
e-mail: tor.dokka@iot.ntnu.no

Computer system: Windows 98/Word version 97

Abstract

Emission testing in small test chambers has become the most commonly used method to evaluate the effect of building materials on VOC concentrations in indoor air. Several studies have shown that the concentration of VOCs found in field experiments are substantially lower than those measured in small test chambers, especially for wet sources like water-based paints. Hypotheses put forward to explain this discrepancy have included strong sink effects or strong substrate effects. This study involves controlled chamber experiments to test these hypotheses.

The experiments show a strong sink effect by a carpet on emissions from a water-based paint. This sink effect is much stronger than those found in earlier sorption experiments, and cannot be explained by first order reversible adsorption kinetics only.

Substrate experiments with water-based paint applied on both wood and aluminium substrates show that the emission from the wood substrate is substantially lower than the emission from the aluminium substrate, indicating a strong substrate effect of the wood panel.

Data from the sink and substrate chamber experiments, together with mathematical models, is used to predict the concentration of VOCs in a bedroom. The prediction is compared to VOC measurements in the bedroom under controlled conditions. The predicted concentrations are in good agreement with the measured concentrations, and these findings can explain the often reported discrepancy between field and chamber experiments. Models to predict VOC concentrations in real rooms, based on emission, sink and substrate data are proposed.

Keywords : Sink effects, substrate effects, water-based paint, mathematical models, chamber experiments, field experiments.

Introduction

There has been growing concern the last decades about the influence of indoor air quality (IAQ) on people's health and well-being. The emission of volatile organic compounds (VOCs) from building materials is suspected as being a possible cause of degraded IAQ in buildings. This has led to a requirement for testing and labelling of building materials, and a few countries have introduced voluntary labelling of building materials (Wolkoff and Nielsen, 1993; Gustafsson and Johnsen, 1993).

Due to economical and space saving reasons, small chamber testing has become the most used method for the evaluation of VOC emissions from buildings materials. However, several studies show that the concentrations found in small chamber tests are substantially higher than those found in real buildings (Zellweger et al., 1995; Dokka et al., 1999). Fig. 1, from the study of the authors (Dokka et al., 1999), shows that the modelled TVOC concentrations, based on data from small chamber experiments, are substantially higher than those measured in the field. Suggested hypotheses to explain the difference in this study included: strong sink effects of materials in the room, strong substrate effects of material painted on the wall, and scaling/boundary layer effects due to the magnitude difference between the chamber and the real room (field experiment).

Strong sink effects have been reported by Chang (Chang, 1997 a.), when studying the sink effect of carpet on emissions from a latex paint (water-based). The calculated equilibrium constant, a measure of the strength of the sink, was up to 20 times higher than earlier reported values from sorption experiments (Tichenor et al., 1991; Chang and Guo, 1993; Jørgensen and Bjørseth, 1999).

Strong substrate effects when studying emissions from a latex paint has been reported by Chang (Chang et al., 1997 b.). Chang found that the amount of VOCs emitted from a painted

stainless steel plate were up to ten times higher than those emitted from a painted gypsum board. Similar results has been reported by Jørgensen (Jørgensen and Bjørseth, 1995)

The aim of this study has been to investigate if strong sink effects and/or strong substrate effects can explain why concentrations found in field experiments are often much lower than concentrations found in comparable test chamber experiments. To investigate this, two test chamber experiments and one field experiment have been conducted. Different models to describe the source, sink and substrate behaviour are also proposed.

Experimental design and methods

This study is based on three different experiments, which consist of five different experiment series (see below). The three experiments are :

1. A chamber experiment with a water-based paint (hereafter called paint A), which provided emission and sink data for model prediction and comparison to the field experiment.
2. A field experiment in a bedroom sealed off from rest of the building, where walls were painted with paint A.
3. A follow up chamber study with another water-based paint (hereafter called paint B), to investigate the influence of substrate effects on emissions from paint B.

The three experiments consisted of five experiment series :

1.a. : Paint A applied to an aluminium plate in an otherwise empty chamber.

1.b. : Paint A applied to an aluminium plate in a chamber with wool carpet as the sink.

2.a. : Paint A painted on walls in a sealed bedroom (field experiment).

3.a. : Paint B applied to an aluminium plate in an otherwise empty chamber.

3.b. : Paint B applied on wood panel (spruce) in an otherwise empty chamber.

Air change rate, dimensions and other physical data for the different experiments are shown in Table 1.

Table 1 Air exchange, dimensions, and sink- and source loading for the different experiments.

Experiment series :	1.a	1.b.	2.a	3.a.	3.b.
Air exchange	0.53 h^{-1}	0.50 h^{-1}	0.15 h^{-1}	0.53 h^{-1}	0.5 h^{-1}
Air volume chamber/room	0.1 m^3	0.1 m^3	19.7 m^3	0.1 m^3	0.1 m^3
Source area paint	0.101 m^2	0.101 m^2	7.1 m^2	0.104 m^2	0.102 m^2
Sink area	-	0.115 m^2	8.2 m^2	-	-
Source loading	1.01 m^2/m^3	1.01 m^2/m^3	0.36 m^2/m^3	1.04 m^2/m^3	1.02 m^2/m^3
Sink loading	-	1.15 m^2/m^3	0.42 m^2/m^3	-	-

Chamber experiments with paint A

This experiment was performed in a small polished steel chamber with a volume of 100 litres. An aluminium plate with a dimension of 0.3 m x 0.4 m was painted with paint A and placed in the chamber. Paint A was selected from three tested water-based paints and was chosen because of its high emission rate. The air exchange rate (Table 1) in the chamber was measured with a flow meter. The temperature and relative humidity (RH) in the chamber were respectively 21°C (± 0.4°C) and 53% (± 4%). VOC samples were collected using Tenax TA (250 mg tubes) and analysed using GC-MS. A Perkin Elmer ATD 400 unit was used for thermal desorption of the samples. The Perkin Elmer Autosystem GC was equipped with a capillary column, CP-Wax 52-CB. The mass spectrometer was a Perkin Elmer Turbomass. For quantification purposes an external standard of toluene was used.

Air samples were taken frequently during the first week (several samples each day), followed by one sample per day for subsequent days. Air samples were taken less frequently during the last two weeks of the experiment. The experiments were terminated after 30 days.

Field experiments

The field experiment was carried out in an unoccupied bedroom (sealed off from other rooms in the building). The walls were painted with paint A. The bedroom was ventilated by a

small passive vent in the frame of the bedroom window. The air exchange rate was measured at 0.15 ach, which was calculated from a CO_2 decay experiment. The temperature in the bedroom was maintained at 22°C by a thermostatically controlled panel heater. The same chemical analysis and analytical conditions as in the chamber experiment were used. Air samples were taken frequently during the first week, and thereafter one sample each day. From day 10, and up to day 29 when the experiment was terminated, air samples were taken less frequently.

The walls of the bedroom consisted of hard particle board drawn with wall covering. The ceiling consisted of painted particle board, and the floor was covered by a nylon carpet.

Chamber experiments with paint B

This chamber experiment was performed in the same type of chambers as the experiments with paint A. An aluminium plate with a dimension of 0.3 m x 0.4 m was painted with paint B, and placed in the chamber. The paint is a commonly used water-based paint, from one of the larger manufacturers of paint on the Norwegian market. The air exchange rate (Table 1) in the chamber was measured with a flow meter. The temperature and relative humidity (RH) in the chamber were respectively 22.8°C (± 0.5°C) and 41% (± 3%). Sampling and chemical analysis were the same as for paint A. Air samples were taken twice a day the first week, followed by one sample per weekday for subsequent weeks. Air samples were taken less frequent after one month, and the experiment was ended after 1917 hours (80 days).

Modelling

Source model

Since volumes, air change rate, loading (ratio of area/volume), and so forth are different between chamber and field experiments, mathematical models are needed to compare

(translate) the resulting concentrations. Emissions from painted surfaces often have exponential decaying profiles, but often ends at a quasi stationary level. The following expression can be used to describe the time-dependent emission factor (g'') of the painted surface:

$$g''(t) = g''_0 \exp(-at) + g''_\infty \qquad (1)$$

g'' : time dependent emission factor (μg/m²h), g''_o : initial emission factor (μg/m²h), g''_∞ : steady state level emission factor (μg/m²h) a : emission rate constant (h^{-1}) and t : time (h).

In general, equation (1) cannot be used to fit concentration data from a chamber experiment since the concentration also depends on the loading (painted area/volume) and the air change rate of the chamber. To fit concentration data we have to make a model for the chamber based on a mass balance. In a chamber with air change rate n, source loading L_{source} (painted area/chamber volume), and a decaying source as (1), the mass balance for the chamber can be written as:

$$\frac{dC}{dt} = -nC + L_{source} \cdot \left(g''_0 \exp(-a \cdot t) + g''_\infty\right) \quad (2)$$

C : concentration in the chamber (μg/m³), n : air change per hour (h-1), L_{source} : source loading (m²/m³). If we assume that the initial concentration is zero : $C(t = 0) = 0$, the solution to equation (2) is:

$$C(t) = \frac{L_{source} g''_0}{n - a}\left[\exp(-at) - \exp(-nt)\right] + \frac{L_{source} g''_\infty}{n}\left[1 - \exp(-nt)\right] \qquad (3)$$

Given the measured concentration in the chamber as a function of time, a curve fitting routine can estimate the emission factor : g''_o, and the rate constant : a. This model is based on the assumption of complete mixing in the chamber, and that the sink effect of the chamber walls is negligible.

Sink model 1: Tichenor's sink model

In real rooms or chamber experiments with sink materials (e.g. carpet), the sink effect cannot be ignored. If we take as a basis the commonly used sink model developed by Tichenor (Tichenor et al.,1991) and modify it with a exponential decaying source as described by eq. (1), the mass balance for the room air and the sink surfaces can be written as:

$$\frac{dC}{dt} = -\left(n + L_{\text{sink}} \cdot k_a\right) \cdot C + L_{\text{sink}} k_d M + L_{source} \cdot \left(g''_0 \exp(-a \cdot t) + g''_\infty\right) \quad (4)$$

$$\frac{dM}{dt} = k_a C - k_d M \qquad (5)$$

M : Mass in the sink surface (mg/m²), k_a : adsorption rate constant (m/h), k_d : desorption rate constant (h^{-1}), L_{sink} : sink surface loading (m^2/m^3) (sink area/room volume). Assuming zero initial concentration and mass in the sink, the solution to the coupled differential equations (4) and (5) is given by:

$$C(t) = C_1 \exp(\lambda_1 t) + C_2 \exp(\lambda_2 t) + a_1 \exp(-at) + b_1 \quad (6)$$

$$M(t) = C_1 K_1 \exp(\lambda_1 t) + C_2 K_2 \exp(\lambda_2 t) + a_2 \exp(-at) + b_2 \quad (7)$$

where :

$$
\begin{aligned}
C_1 &= \frac{K_2(a_1+b_1)-a_2-b_2}{K_1-K_2} \quad ; \quad C_2 = -C_1-a_1-b_1 \qquad (\mu g/m^3) \\
\lambda_{1/2} &= \frac{-(n+k_a L+k_d) \pm \sqrt{(n+k_a L+k_d)^2-4\cdot k_d n}}{2} \qquad (h^{-1}) \\
K_1 &= \frac{k_a}{\lambda_1+k_d} \quad ; \quad K_2 = \frac{k_a}{\lambda_2+k_d} \qquad (m) \\
a_1 &= \frac{g_0'' L_{source}}{n-a+L_{sink}k_a\left(1-\frac{1}{1-a/k_d}\right)} \quad (\mu g/m^3) \quad ; \; a_2 = \frac{k_a}{k_d-a}a_1 \quad (\mu g/m^2) \\
b_1 &= \frac{g_\infty'' L_{source}}{n} \; (\mu g/m^3) \quad ; \qquad b_2 = \frac{k_a}{k_d}\frac{g_\infty'' L_{source}}{n} \qquad (\mu g/m^2)
\end{aligned}
\tag{8}
$$

Sink model 2: Empirical sink model

The chamber experiment with and without the carpet as a sink, and with paint A as the source, indicate that the carpet has the following influence on the concentration:

1. The initial emission is lower with the carpet present, indicating a lower net initial emission factor.
2. A faster decay in the first phase of the emission process with the carpet present, indicating a higher net value of the emission rate constant (a).
3. Generally a higher steady state concentration in the chamber after a long time (500 – 700 h), indicating a slow steady desorption from the carpet.
4. The emission process has the same exponential decaying nature, both with and without the carpet.

These observations can be described by modifying the source model (1) with some sink-related factors: an adsorption factor which reduces the net initial emission, an emission rate factor that scale (increase) the emission rate constant, and a desorption rate constant raising

the steady state concentration level. The net emission to the chamber air, including source and sink effects, is proposed described by the following expression :

$$G_{net}(t) = \left(A_{\text{source}} g''_{\infty} - A_{\text{sink}} K_a\right)\exp(-f \cdot a \cdot t) + \left(A_{\text{source}} g''_{\infty} + A_{\text{sink}} K_{\text{d}}\right) \quad (9)$$

G_{net} : net emission rate (mg/h), K_a : adsorption rate factor (mg/m²h), K_d : steady state desorption rate (mg/m²h), f : emission rate factor, A_{sink} : sink area (m²) and t : time (h). Introducing this net emission source into a mass balance similar to (2), gives the following mass balance:

$$\frac{dC}{dt} = -nC + \left(L_{source} g''_0 L_{\text{sink}} - K_a L_{\text{sink}}\right)\exp(-f \cdot a \cdot t) + \left(L_{source} g''_{\infty} + L_{\text{sink}} K_d\right) \quad (10)$$

L_{sink} : sink loading (m²/m³). Assuming the initial concentration to be zero : $C(t = 0) = 0$, the solution to equation (10) is:

$$C(t) = \frac{L_{source} g''_0 - L_{\text{sink}} K_a}{n - f \cdot a}\left[\exp(-f \cdot a \cdot t) - \exp(-nt)\right] + C_{\infty}\left[1 - \exp(-nt)\right] \quad (11)$$

where C_∞ is the steady state concentration:

$$C_{\infty} = \frac{L_{source} g''_{\infty} + L_{\text{sink}} K_d}{n} \quad (12)$$

Given the measured concentration (in the sink experiment) in the chamber as a function of time, and assuming a, g''_0 and g''_∞ as known from emission experiments, a non-linear curve fitting routine can estimate the sink related parameters f, K_a and K_d.

Introducing a substrate factor

From earlier experiments and the experiments conducted in this study, it seems that the VOC emission from a porous/permeable substrate is reduced in the first part of the experiment, but the "steady state" emission level is almost equal for both the permeable substrate and the non-permeable substrate (e.g. steel or aluminium). A simple model to take this into account could be to introduce a substrate factor that scale down the initial emission factor in eq. (1):

$$g''_{perm}(t) = F_{sub} g''_0 \exp(-at) + g''_\infty \quad (13)$$

g''_{perm} : emission factor for the permeable substrate (mg/m²h), F_{sub} : substrate factor (-). g''_0, a and g''_∞ is the initial emission factor, the emission rate constant and the steady state emission factor for the non-permeable substrate (defined before). Inserting (13) into a mass balance similar to eq. (2) and solving with the same initial conditions ($C(0) = 0$) gives the following expression for the concentration in the chamber:

$$C(t) = \frac{F_{sub} L_{source} g''_0}{n-a}\left[\exp(-at) - \exp(-nt)\right] + \frac{L_{source} g''_\infty}{n}\left[1 - \exp(-nt)\right] \quad (14)$$

Parameter estimation

When fitting experimental data from the chamber experiments to the different source-, sink- and substrate models (eq. (3), (6), (11) and (14)), a non-linear regression curve fitting routine in the statistical software package SPSS® was used.

When fitting the experimental data from experiment 1.a. and 3.a. to the source model (eq. (3)), it was assumed that the steady state concentration level was reached. The steady state

concentration was taken to be the mean of the three last measured concentrations, and the steady state emission were calculated as : $g''_{\infty} = n*C_{\infty}/L_{source}$. With the steady state emission level known, the unknown parameters found by the curve fitting routine were the emission rate constant (a) and the initial emission factor (g''_0).

Fitting the experimental data from experiment 1.b. to Tichenor's sink model (eq. (6)), the values for a, g''_0 and g''_{∞} were assumed known (parameters estimated from experiment 1.a.). With these parameters known, the unknown parameters found by the curve fitting routine were the adsorption rate constant (k_a) and the desorption rate constant (k_d).

Fitting the experimental data from experiment 1.b. to the empirical sink model (eq. (11)), the same values for a, g''_0 and g''_{∞} as for Tichenor's model were used. It was also assumed that a steady state concentration level had been reached (taken as the mean of the last three measured concentrations), making it possible to calculate a steady state desorption rate (K_d) as : $K_d = (C_{\infty}* n - L_{source}*g''_{\infty})/L_{sink}$. The unknown parameters (K_a and f) were then found by the curve fitting routine.

When fitting the experimental data from experiment 3.b. to the substrate model (eq. (14)), the values for a, g''_0 and g''_{∞} was assumed known (parameters estimated from experiment 3.a.). The substrate factor (F_{sub}) was found by the curve fitting routine.

Results and discussion

Sink models

Figure 2 shows the sink experiment with the carpet and emission of TVOC from paint A, together with the curve-fit of the two sink models. It is clear that the empirical sink model describe the experimental data better than Tichenor's model. The best fit for Tichenor's model (Table 2) is found with a very small value of the desorption rate constant, indicating a extremely slow desorption from the carpet (k_d). In fact, the 95 % asymptotic confidence

interval for this parameter (k_d) contains zero, which in a parameter estimation setting means that this parameter is redundant in the model. Physically, this indicates that the adsorbed mass is not re-emitted from the carpet, i.e. that the carpet acts as an irreversible sink, or the desorption is very slow. Similar results have been reported by Chang (Chang et al., 1997 b.). In all cases, it seems that Tichenor's theoretical sink model, based on linear and reversible sorption kinetics, fails to describe the influence of the sink effect from the carpet on the emission of TVOC from paint A. The same holds true for propylene glycol (dominant VOC) emitted from paint A, the desorption term in the sink model seems redundant. The parameter estimation of the empirical sink model (Table 4) indicate, however, a slow steady state desorption from the carpet. Due to the better description of the experimental data, the proposed empirical sink model is used to describe the sink effect in the remaining of the paper.

Table 2 Curve fitted parameters for Tichenor's sink model (eq.(6)), from the sink experiment with carpet and the emission of propylene glycol and TVOC from paint A.

Compund	TVOC	Propylene glycol
k_a (m/h)	0.484	0.458
(95 % conf.inter.)	(±0.0008-0.0012)	(±0.0008-0.0012)
k_d (h^{-1})	0.0002	0.0002
(95 % conf.inter.)	(±0.0007-0.011)	(±0.0008-0.012)
K_e (m)	2420	2292
R^2	0.907	0.923

Emission and sink experiments in chambers

The six major VOCs emitted from paint A were: acetic acid, 1-acetoxy-2-propanol (acetoxy propanol), propylene glycol, 2-oxo-propanoic acid (propanoic acid), 2-2(buthoxy-etoxy)-ethanol (BEE) and 2-2(buthoxy-etoxy)-ethanol acetate (BEEA). The four compounds: propylene glycol, propanoic acid, BEE and BEEA, in that order, are the most dominant VOCs emitted from paint A (amounts to 96 % of the emitted mass). However, all six compounds are counted when calculating TVOC (TVOC = sum of the 6 compounds).

Fig. 4-8 show the emission of TVOC and the four dominating compounds from paint A, with and without the carpet present in the chamber. As expected, the carpet dampens the initial emission from the paint. The strength of the sink effect from the carpet is different for the different compounds. Propanoic acid has the strongest sink effect, while the sink effect for BEEA is rather weak. Another effect of the carpet seems to be that maximum emission comes earlier with the carpet present in the chamber. Intuitively one would expect the opposite to occur, i.e. that the maximum emission would be later when the carpet was present. This emission/sink behaviour is therefore difficult to explain. The emission from the paint also seems to decay faster with the carpet present in the chamber. This behaviour cannot be explained with linear and reversible sorption kinetics (e.g. Tichenor's model) as shown in the previous sub-section (Sink models). Lastly, the steady state emissions are somewhat higher with the carpet present, indicating a slow and seemingly steady desorption (re-emission) from the carpet.

The source model (eq. (3)) describing the emission from paint A fits the experimentally data acceptably. The parameter estimated values and the regression coefficients for TVOC and the different compounds are shown in Table 3.

The proposed empirical sink model (eq. (11)) also fits the experimental data (experiment 1.b.) for TVOC and the different compounds well. The regression coefficients and the parameter estimated values for the empirical sink model are shown in Table 4. The decay factor (f) varies very much for the different compounds. Propanoic acid has a decay factor of nearly 7, which means that the emission decay rate is much faster when the carpet is present. Acetoxy propanol and BEE have only slightly higher decay rates with the carpet present. The steady state concentration level for TVOC is approximately twice as high with the carpet present, indicating substantial desorption from the carpet. As the value of the steady state

desorption rate (K_d) in Table 4 shows, the variation between compounds are large, with propylene glycol (dominant VOC) as the compound with the highest desorption rate.

Table 3 Curve fitted parameters for the source model (eq.(3)), with data from the experiment without carpet (experiment 1.a.).

	a (h^{-1})	g''_0 (mg/m^2h)	g''_∞ (mg/m^2h)	R^2
TVOC	0.008	36.9	0.53	0.956
Acetic acid	0.012	1.6	0.03	0.954
Acetoxy propanol	0.032	1.3	0.005	0.950
Propylene glycol	0.009	18.9	0.04	0.935
Propanoic acid	0.006	5.6	0.04	0.891
BEE	0.008	6.6	0.16	0.953
BEEA	0.007	3.4	0.25	0.945

Table 4 Curve fitted parameters for the empirical sink model (eq.(11)), with data from the experiment with carpet (experiment 1.b.)

	f (-)	K_a (mg/m^2h)	K_d (mg/m^2h)	R^2
TVOC	2.5	11.1	0.54	0.970
Acetic acid	4.4	0.6	0.003	0.928
Acetoxy propanol	1.2	0.3	0.002	0.896
Propylene glycol	2.1	5.7	0.19	0.973
Propanoic acid	6.9	2.3	0.13	0.914
BEE	1.6	1.7	0.14	0.953
BEEA	2.6	0.9	0.08	0.931

Another important quantity is the total emitted mass (m_{em}) during the experimental period. Using the measured concentrations, the emitted mass can be calculated by the trapezoid method:

$$m_{em}(t) = V \cdot n \int_0^t C(t)dt \approx \frac{V \cdot n}{2} \sum_{i=0}^{i=n-1} (C_i + C_{i+1})(t_{i+1} - t_i) \qquad (15)$$

The total emitted mass, both with and without the carpet present in the chamber, during the experimental period of 700 hours is shown in Table 5. The difference in emitted mass between the experiments with and without the carpet is an estimate of the remaining mass in the sink (the carpet). Table 6 shows that the remaining mass in the sink after 700 hours is

considerable, and amounts to 78% for the compound with the strongest sink effect (propanoic acid), and an average of 47% for TVOC. This means that, on average, half of the emitted mass is still remaining in the sink after 700 hours. If we use the calculated remaining mass in the sink after 700 hours (Table 6), and the steady state desorption rate from the carpet (Table 5), an estimate of the time when all the mass in the sink is re-emitted can be calculated. This extrapolation of the empirical sink model indicates that the carpet is free of the dominating VOC (propylene glycol) after 7 months, and free of TVOC after approximately 8 months. This estimation assumes a constant desorption rate. In a real situation, the desorption rate will most likely decrease with time, and the desorption time will probably be even longer than those estimated. To investigate this slow desorption effect further, long term sink experiments are needed.

Table 5 Emitted mass from paint A, with and without carpet, and remaining mass in the sink. Calculated from experimental data (with eq. (15)), for the experimental period of 700 hours.

	m_{em} (mg)		Δm_{em} (mg)
Compound	Without carpet	With carpet	Remaining mass in sink
Acetic acid (mg)	15	5	10 (68 %)
Acetoxy propanol (mg)	5	3	2 (31 %)
Propylene glycol (mg)	202	108	94 (46 %)
Propanoic acid (mg)	92	20	71 (78 %)
BEE (mg)	95	70	25 (26 %)
BEEA (mg)	70	46	24 (35 %)
TVOC (mg)	476	253	314 (47%)

Substrate experiments in chambers

The five major VOCs emitted from paint B are: 2-butoxy-ethanol (butoxy ethanol), propylene glycol, 1-1-methyl-2-(2-propenyloxy)ethoxy-2 propanol (MPEP), 1-1-methyl-2-(2-propenyloxy)ethoxy-2 propanol (MPEP*)[1] and butan, 1-(1-methylpropoxy) (BMP). The four compounds: butoxy ethanol, propylene glycol, MPEP and MPEP*, are the most dominant

[1] Two peaks are identified as the same compound (MPEP) in the mass spectrometer (NIST library), even if they are two distinct peaks with different retention time in the gas chromatogram. A possible explanation can be that the two compounds are isomers.

VOCs emitted from paint B, and amount to approximately 96% of the emitted mass (after 1900 hours, see Table 8).

Fig. 9-13 show the emission of TVOC and the four dominating VOC compounds from paint B, with both aluminium and spruce as substrate. As one would expect, the emissions from the paint are lower with spruce as substrate compared to aluminium as substrate. This substrate effect is, however, very different for different compounds in the paint. The compound butoxy ethanol has no significant substrate effect, i.e. the emissions from the two substrates are practically equal. In contrast to this, propylene glycol (dominant VOC emitted from the aluminium substrate) has a very strong substrate effect. In fact, with spruce as substrate propylene glycol is no longer the dominant emitted VOC (Table 6).

The most important effect of the substrate seems to be that the initial emission is reduced. For TVOC and most of the compounds, the steady state emissions level from the two substrates are approximately equal. However, propylene glycol, the compound with the strongest substrate effect, has a somewhat higher steady state emission level from the spruce substrate.

Fig. 9-13 and the regression coefficients in Table 6 show that the source model (eq. (3)) describes the emissions from the aluminium substrate adequately. The simple substrate model (eq. (14)), also seems to describe the main effect of the spruce substrate acceptably. Even if the regression coefficient for propylene glycol is somewhat low (Table 7), it describes the large effect of the spruce substrate on this compound acceptably.

Table 6 Curve fitted parameters for the source model (eq. (3)), fitted to the data from the aluminium substrate experiment (3.a.)

	a (h^{-1})	g''_0 (mg/m^2h)	g''_∞ (mg/m^2h)	R^2
TVOC	0.034	86.2	0.22	0.935
Butoxy ethanol	0.150	9.6	0.03	0.984
Propylene glycol	0.032	48.9	0.01	0.905
MPEP	0.033	15.2	0.08	0.968
MPEP*	0.031	13.3	0.09	0.963
BMP	0.030	1.5	0.02	0.970

Table 7 Curve fitted parameters for the substrate model (eq. (14)), fitted to the data from the spruce substrate experiment (3.b.)

	F_{sub}	R^2
TVOC	0.37	0.864
Butoxy ethanol	0.76	0.942
Propylene glycol	0.15	0.600
MPEP	0.64	0.941
MPEP*	0.67	0.933
BMP	0.75	0.952

The total emitted mass for both the aluminium substrate and the spruce substrate during the experimental period of 1917 hours is shown in Table 8. The difference in emitted mass between the aluminium and spruce substrates, is an estimate of the remaining mass in the spruce substrate. Table 8 shows that the remaining mass in the spruce substrate amounts to 73% for propylene glycol, and an average of 48% for TVOC. These figures are similar to the sink effect of the carpet, i.e. approximately half the emitted mass (TVOC) is still remaining in the spruce substrate. Since the experimental period for the substrate experiment is longer than the sink experiment, it is more likely that the spruce substrate acts as an irreversible sink., i.e. that a considerable amount of VOCs are permanently bound in the wood substrate.

Table 8 Emitted mass from paint B, with both aluminium and spruce panel as substrate, together with remaining mass in the substrate after 1900 hours.

	m_{em} (mg)		Δm_{em} (mg)
Compound	Aluminium substrate	Wood substrate	Remaining mass in sink
Butoxy ethanol (mg)	11	12	-1 (-6 %)
Propylene glycol (mg)	169	46	123 (73 %)
MPEP 1 (mg)	68	52	15 (23 %)
MPEP 2 (mg)	70	54	16 (22 %)
BMP (mg)	9	7	2 (19 %)
TVOC (mg)	326	171	155 (48%)

Field experiments

With the new data from the sink and substrate experiments, a new and more accurate comparison of prediction and measured concentrations in the field experiment (bedroom) is possible. The proposed empirical sink model and the proposed substrate model are used in the

predictions. Data from different emission, sink and substrate experiments used in the prediction are shown in Table 9.

Table 9 Emission-, sink- and substrate data used in the model prediction of the bedroom.

Data for prediction	Value for TVOC	Value for prop. glycol	Taken from
Emission rate constant, a	0.0079 h^{-1}	0.009 h^{-1}	Emission experiment, Table 3.
Initial emission factor, g''_0	36.9 mg/hm²	18.9 mg/m²h	Emission experiment, Table 3.
Steady state emission factor, g''_0	0.53 mg/m²h	0.04 mg/m²h	Emission experiment, Table 3.
Adsorption rate factor, K_a	11.1 mg/m²h	5.7 mg/m²h	Sink experiment, Table 4.
Steady state desorption rate, K_d	0.54 mg/m²h	0.19 mg/m²h	Sink experiment, Table 4.
Emission decay factor, f	2.5	2.1	Sink experiment, Table 4.
Substrate factor, F_{sub}	0.685*	0.575*	Substrate experiment, Table 7.

* Calculated as : $F_{sub,TVOC} = (F_{sub,alum} + F_{sub,spruce})/2 = (1.0+0.37)/2 = 0.69$, $F_{sub,pr.glycol.} = (F_{sub,alum} + F_{sub,spruce})/2 = (0.15 + 1.0)/2 = 0.58$

Emission and sink rate data for the field prediction is quite easy to choose since the emission experiments are done with the same paint as used in the field experiment (paint A), and the sink experiments with a carpet similar to the carpet in the bedroom (field experiment). The substrate data are, however, more difficult to estimate, since the substrate experiments are done with paint B and a different substrate. The substrate in the bedroom is a hard particle board with a glass fibre wall covering with "old" paint. The substrate effect of the hard particle board will likely be substantially lower than the substrate effect of the spruce used in the substrate experiment. As a first approximation, we have estimated the substrate factor for the particle board to be the mean between the values of the spruce and the aluminium (no substrate effect). This yields the values in Table 9. Other physical data for prediction in the bedroom are given in Table 1.

Fig.14 and Fig.15 show the comparison between model prediction and measured concentration in the bedroom, for TVOC and the dominant VOC (propylene glycol). The predicted TVOC concentration profile are close to the measured concentrations. The steady state concentration level after the experimental period of 700 hours are, however, higher than the measured concentration level. The predicted concentration of propylene glycol are also acceptably close to the measured one, even if the prediction is somewhat low in the first part

of the experiment. The steady state concentration level is predicted well for propylene glycol. A substrate factor for propylene glycol of approximately 0.7 gives a much better prediction than the value of 0.58. This is in the range where the "real" substrate factor for the hard particle board can lie.

Overall, the concordance between prediction and measurement is good when both sink effects and substrate effects are taken into account. The TVOC predictions with the proposed empirical sink model and the substrate model (Fig.14) are much better than the earlier prediction (Fig. 1) where Tichenor's sink model was used.

Conclusion

The conclusions of this study are:

- The presence of a carpet, representing a common sink surface in real indoor environment, decrease the measured emissions from a water-based paint significantly (chamber experiments).
- The influence of the carpet cannot be described with linear and reversible adsorption kinetics, like the commonly used model of Tichenor. The measured data indicate a rather strong irreversible sink effect, or a very slow re-emission from the carpet, taking several months. The sink effect of the carpet varies considerably for different VOC compounds emitted from the paint.
- The substrate, in this study represented by an aluminium plate and a spruce panel, strongly influences the emissions from a water-based paint. The emissions from the spruce substrate are substantially lower than the emissions from the aluminium substrate. An irreversible substrate factor has been proposed to take this phenomena into account when

modelling emissions from paints on permeable substrates (e.g. wood). The substrate factor varies considerably for the different VOCs emitted from the paint.

- When taking into account sink effects of carpets and substrate effects of painted wall boards, the modelled concentrations and measured concentrations in a refurbished bedroom are close.
- New models are proposed to describe the strong sink and substrate effects found. These models can also be used to predict VOC concentrations in real rooms, based on data from small chambers experiments (emission, sink and substrate experiments).
- Strong and maybe irreversible sink and substrate effects can probably explain the substantial difference in concentrations between chamber experiments and field experiments found in earlier studies.
- To investigate if the sink and substrate effects found are irreversible, or only if the desorption is extremely slow, long-term sink and substrate experiments are needed.

Acknowledgement

This work has been financially supported by the Norwegian Research Council, Project no. 111372\330.

References

Chang J.C.S. (1997.a) "VOC emissions from latex paint: Sink effects" In : *Inside IAQ, EPA's Indoor Air Quality Research Update*, spring /summer 1997, pp. 1-4.

Chang, J.C.S., Tichenor, B.A., Guo, Z., Krebs, K.A. (1997.b) "Substrate effects on VOC emissions from a latex paint", *Indoor Air,* 7 : 241 – 247.

Chang, J.C.S., Guo, Z. (1993); "Modelling of alkane emissions from a wood stain", *Proceedings of Indoor Air '93*, Helsinki, International conference on Indoor Air Quality and Climate, Vol. 2, pp. 561–566.

Dokka, T.H., Jørgensen, R.B., Bjørseth, O., Malvik, B.(1999), "Comparison of field experiments in a refurbished bedroom with small chamber experiments." *Proceedings of Indoor Air '99*, Edinburgh, International conference on Indoor Air Quality and Climate, Vol. 5, pp. 93–95.

Gustafsson, H., Johnson, B. (1993), "Trade standards for testing chemical emissions from building materials. Part 1. Measurements of flooring materials." *Proceedings of Indoor Air '93*, Helsinki, International conference on Indoor Air Quality and Climate, Vol. 2, pp. 437–442.

Jørgensen, R., Bjørseth, O. (1995), "Emission from wall paint - The influence of the wall material", *Proceedings Healthy Building '95, Milan*, Vol. 2, pp. 977-982.

Jørgensen, R.B. and Bjørseth, O. (1999) "Sorption behaviour of volatile organic compounds on material surfaces - the influence of combinations of compounds and materials compared to sorption of single compounds on single materials.", *Environment International*, Volume 25 (1) : 17-27.

Wolkoff, P., Nielsen, P.A. (1993), "Indoor climate labelling of building materials – chemical emission testing , modelling and indoor relevant odour thresholds." National Institute of Occupational Health, Copenhagen, Denmark.

Zellweger, C., Gehrig, R., Hill, Hofer, P. (1995), "VOC Emissions from Building Materials: Comparison of Chamber Emission Data with Concentrations in Real Rooms", *Proceedings of Healthy Buildings '95,* Milan, Vol. 2, pp. 845-850.

Tichenor, B.A., Guo, Z., Dunn, J.E., Sparks, L.E., Mason, M.A.(1991), "The Interaction of Vapour phase Organic Compounds with Indoor Sinks.", *Indoor Air*, Vol. 1 : 23-35.

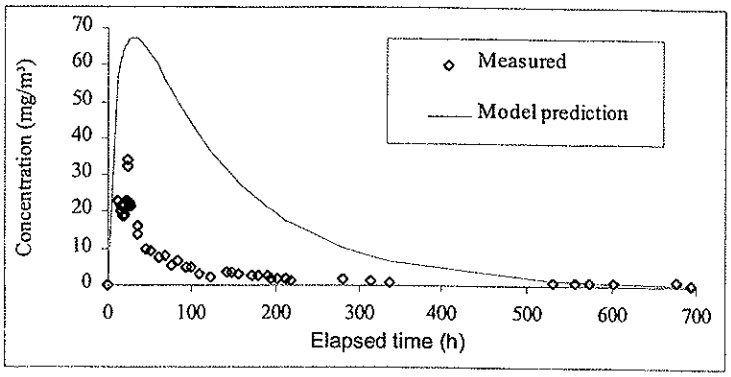

Fig. 1 Predicted and measured concentration in the bedroom. Taken from Dokka et al. (1999)[1]

[1]In this paper (Dokka et al., 1999) the predicted concentration in the bedroom, was based on data from chamber experiments where the air change rate was set at 1.0. The real air change rate was only 0.5 ach, resulting in a lower predicted concentration in the bedroom. The prediction based on the correct air change rate (0.5 ach) is shown in Fig.1

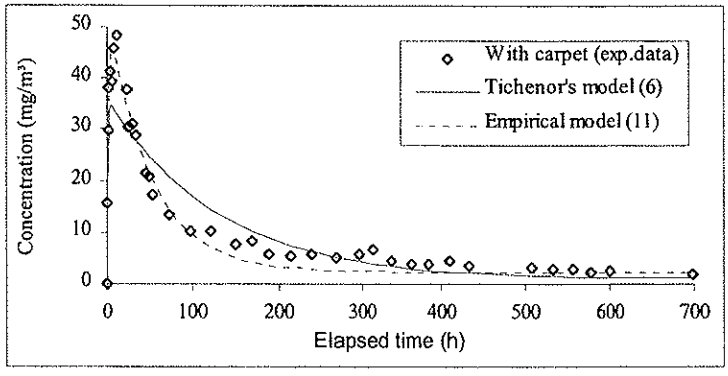

Fig. 2 Comparison of Tichenor's theoretical sink model (eq. (6)), and the proposed empirical sink model (eq. (11)) to describe the sink effect of carpet on the emission of TVOC from paint A.

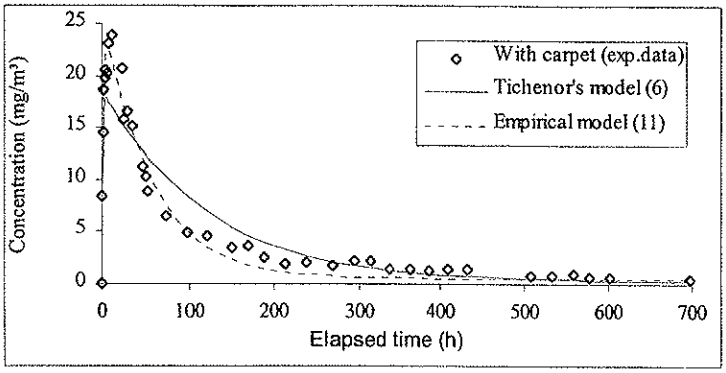

Fig. 3. Comparison of Tichenor's theoretical sink model (eq. (6)), and the proposed empirical sink model (eq. (11)) to describe the sink effect of carpet on the emission of propylene glycol from paint A.

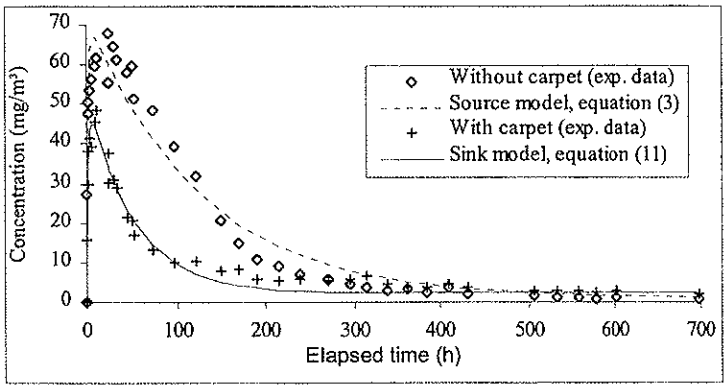

Fig. 4 Effect of the carpet on the emission of TVOC from paint A

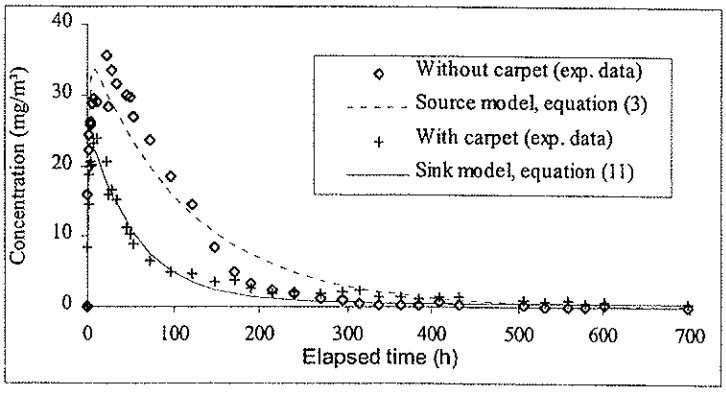

Fig. 5 Effect of the carpet on the emission of propylene glycol from paint A

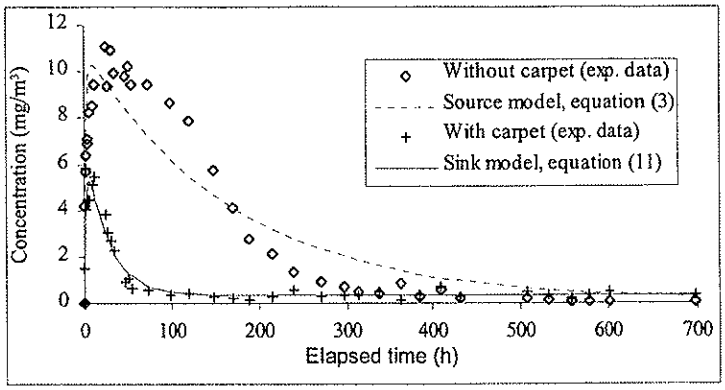

Fig. 6 Effect of the carpet on the emission of propanoic acid on emission from paint A

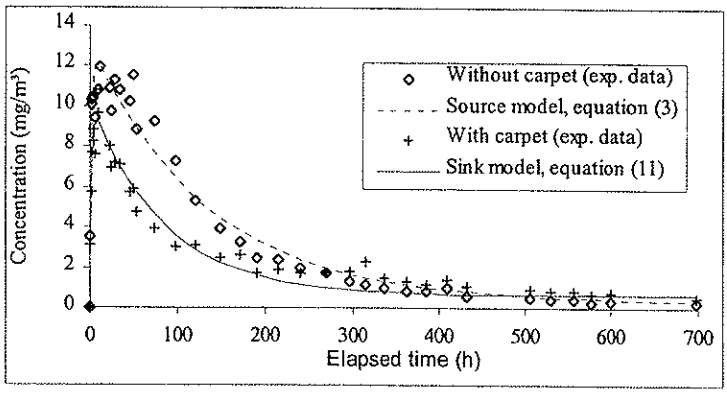

Fig. 7 Effect of the carpet on the emission of BEE from paint A

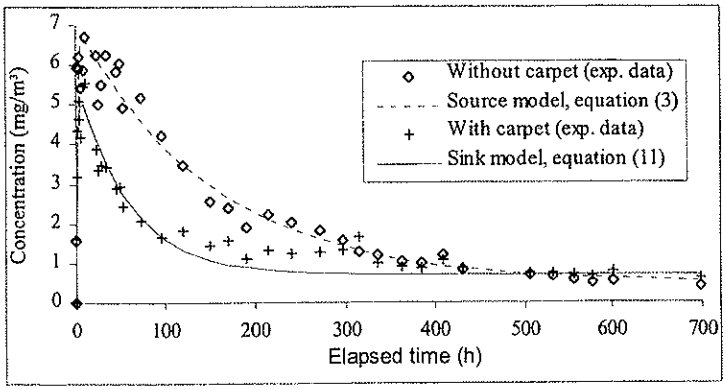

Fig. 8 Effect of the carpet on the emission of BEEA from paint A

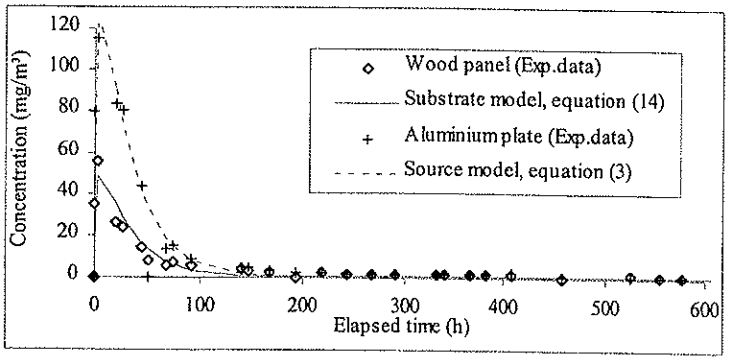

Fig.9 Effect of the substrate on the emission of TVOC from paint B

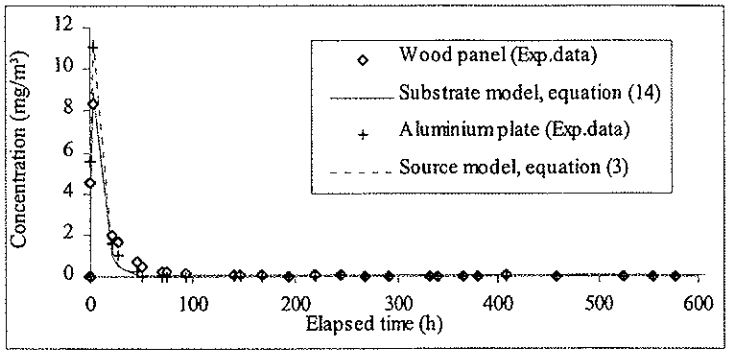

Fig. 10 Effect of the substrate on the emission of butoxy ethanol from paint B

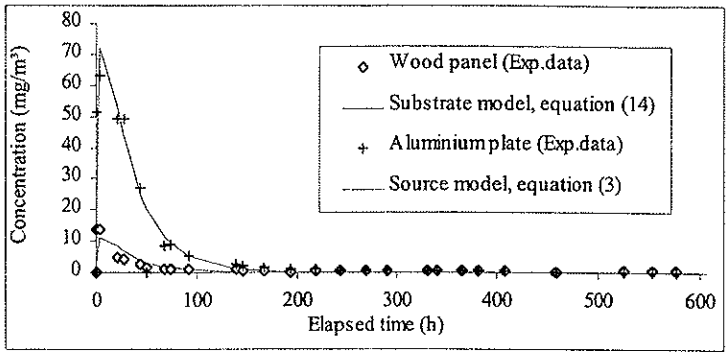

Fig. 11 Effect of substrate on the emission of propylene glycol from paint B

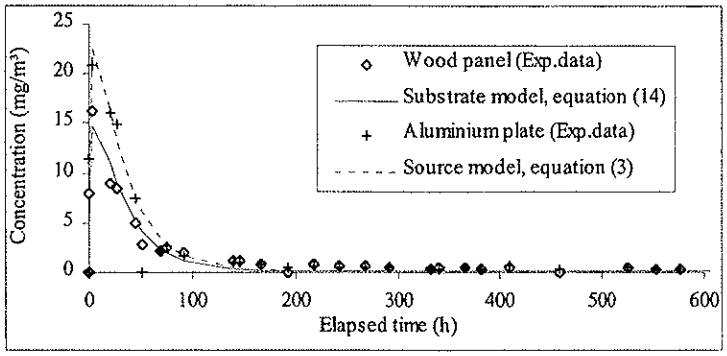

Fig. 12 Effect of substrate on the emission of MPEP from paint B

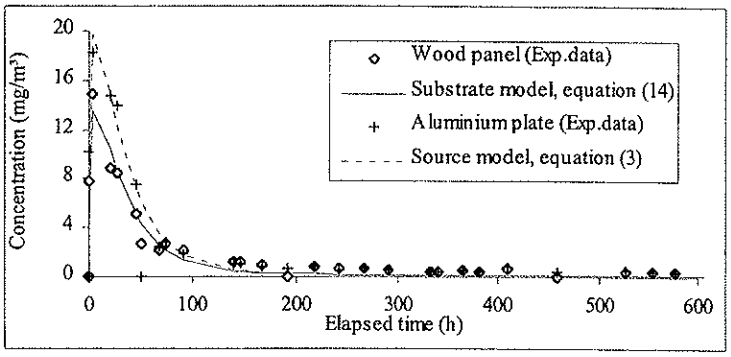

Fig. 13 Effect of substrate on the emission of MPEP* from paint B

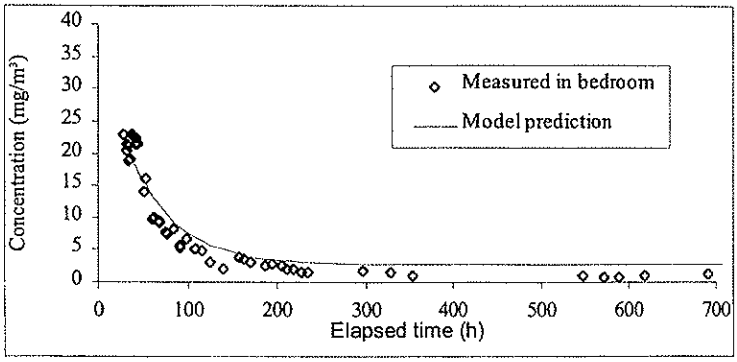

Fig.14 Comparison between measured TVOC concentration in the bedroom and model prediction.

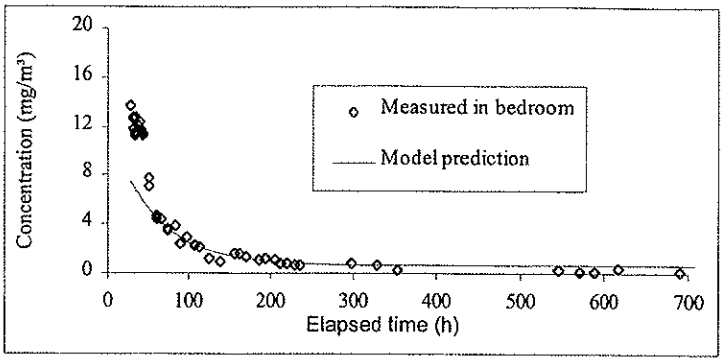

Fig.15 Comparison between measured propylene glycol (dominant VOC) concentration in the bedroom and model prediction.

Simplified models for prediction of vertical contaminant and temperature stratification in displacement ventilated rooms.
Part 2: Validation

Tor Helge Dokka[1]

Per Olaf Tjelflaat[2]

[1] Department of Industrial Economics and Technology Management

[2] Department of Refrigeration and Air Conditioning,

Norwegian University of Science and Technology

Correspondence to

Tor Helge Dokka, Dep. of Industrial Economics and Technology Management, Norwegian University of Science and Technology, N-7491 Trondheim, Norway.
FAX: +47 73593107
e-mail: tor.dokka@iot.ntnu.no

Computer system: Windows/Word version 97

Abstract

Several models for prediction of temperature and contaminant stratification in displacement ventilated rooms has been proposed in an accompanying paper, part 1. These models both cover steady state and transient conditions.

In this paper, part 2, these models are validated and evaluated against empirical data sets taken from the literature. The steady state temperature stratification model is also compared to three other simplified models for temperature stratification. The steady state thermal model predictions comes close to the measured values, and are superior to the other three models for temperature stratification.

The prediction of the transient thermal model is very promising, but should be compared to more transient empirical cases before a final conclusion can be drawn about the validity of the model.

The evaluation of the contaminant models is also very promising, for most of the compared parameters. However, the model is under-predicting the indices related to the air quality in the inhalation zone. This under-prediction is, however, conservative when the models are used to determine ventilation air flow rates.

Keywords: Displacement ventilation, Models, Stratification, Contaminants, Inter-model comparison, Validation

1. Introduction

There are basically two ventilation principles that can be utilised in a room: mixing ventilation and displacement ventilation. In mixing ventilation, air with high velocity is supplied outside the zone of occupancy, which ideally gives uniform temperature and concentration in the room. Mixing ventilation is the most used ventilation principle in comfort ventilation. In displacement ventilation, cool air with low velocity is supplied in the lower part of the room. Contaminated air and heat is transported towards the ceiling by the convection currents set up by heat sources, where it is extracted[1]. This ventilation principle has the potential to provide clean air to the occupants, give energy efficient cooling and lower noise and turbulence level due to the low air supply velocity. Displacement ventilation has grown popular in industrial and-non industrial buildings during recent decades, especially in the Nordic countries.

When designing displacement ventilation it is important to use models predicting vertical temperature and concentration gradients in the room. Such models can be used to predict and evaluate thermal comfort, IAQ and energy use for different design alternatives under varying climatic conditions.

Figure 1: The working principles in displacement ventilation

In an accompanying paper [1], part 1, the authors have proposed several simplified models for prediction of temperature and contaminant stratification in displacement ventilated rooms. These models cover both steady and transient conditions, and can be used for hand calculation or implemented in computerised building simulation tools. In this paper, these models are validated against experimental data sets found in the literature. The steady state thermal model is also compared to other simplified models [2, 3, 4] for vertical temperature stratification in displacement ventilated rooms.

2. Thermal models used for inter-model comparison

Three different models for prediction of temperature stratification in displacement ventilated rooms under steady conditions have been chosen for the inter-model comparison. They are:

- the "rule of thumb" model proposed by Skistad [2]
- the simplified model by Mundt [3], where the floor temperature is deduced from the specific ventilation air flow
- the simplified model by Nielsen [4], where the floor temperature is deduced from the Archimedes number

These models are briefly described below.

2.1. Skistad's vertical temperature gradient model

Skistad [2] has proposed a very simplified "rule of thumb" model where half the temperature difference between the supply and extract air is evened out at floor level, and the other half is given as a linear gradient from floor to ceiling, see Fig. 1. This is equal to saying that the normalised floor temperature has a value of 0.5:

[1] There are also other types of displacement ventilation systems, for example air supply through a perforated floor or ceiling, but these systems are not dealt with in this paper.

$$\kappa \equiv \frac{T_{fl} - T_s}{T_e - T_s} = 0.5 \tag{1}$$

T_{fl} is the floor air temperature (10 cm above the floor), T_s the supply temperature and T_e the extract temperature.

Figure 2: The principles in Skistad's "rule of thumb" model.

Assuming that infiltration is negligible, the heat load(q_{tot}) in the room is removed by ventilation and transmission (q_{tr}). The temperature at the ceiling (T_{ceil}) is assumed equal to the extract temperature (T_e), which from a steady state heat balance can be calculated by:

$$T_e = T_{ceil} = T_s + \frac{q_{tot} - q_{tr}}{C_{air}\dot{V}_v} \tag{2}$$

If the extract temperature (T_e) is given, which is the case for the empirical test cases used in this paper, the transmission loss can be calculated by rearranging (2):

$$q_{tr} = q_{tot} - C_{air}\dot{V}_v(T_e - T_s) \tag{3}$$

From definition (1), the floor temperature can be calculated as:

$$T_{fl} = 0.5 \cdot (T_s + T_{ceil}) \tag{4}$$

The temperature gradient (dT/dz) and the mean room temperature ($<T>$) are then:

$$\frac{dT}{dz} = \frac{T_{ceil} - T_{fl}}{h_{ceil}} \tag{5}$$

$$<T> = 0.5 \cdot (T_{fl} + T_{ceil}) \tag{6}$$

h_{ceil} is the ceiling height. Given the height of the occupation zone (h_{occ}), the mean temperatures in the occupation zone (T_{occ}) and the upper non-occupied zone (T_{nocc}) can be calculated as:

$$T_{occ} = T_{fl} + 0.5 \cdot \frac{dT}{dz} h_{occ} \tag{7}$$

$$T_{nocc} = T_{fl} + 0.5 \cdot \frac{dT}{dz}(h_{ceil} + h_{occ}) \tag{8}$$

The temperature effectiveness for the occupation zone(η_{occ}) is then (see [1]):

$$\eta_{occ} = \frac{T_{ceil} - T_s}{T_{occ} - T_s} \tag{9}$$

2.2. Mundt's vertical temperature gradient model

In Mundt's model [3], the normalised floor temperature(κ) is given as a function of the specific air flow ($\dot{V}_v / A_{fl}$):

$$\kappa = \frac{1}{\frac{C_{air}\dot{V}_v}{A_{fl}}\left(\frac{1}{\alpha_r}+\frac{1}{\alpha_c}\right)+1} \tag{10}$$

C_{air} is the volumetric heat capacity of air, $\dot{V}_v$ is the ventilation air flow rate and A_{fl} is the floor area. The linearized radiation heat transfer coefficient is assumed to be constant: $\alpha_r = 5$ W/m²K and the convective heat transfer coefficients are in the range: α_c : 3-5 W/m²K (we have used 4 W/m²K in the comparison below). The transmission loss (q_{tr}), the temperatures in the room (T_{ceil}, T_{fl}, T_{mean}, T_{occ}, T_{nocc}), the temperature gradient (dT/dz) and the temperature effectiveness in the occupation zone (η_{occ}) are calculated the same way as in the Skistad model (equations 2-9).

Figure 3: The vertical temperature gradient model of Mundt [3], and the normalised floor temperature as a function of the specific air flow.

2.3. Nielsen's vertical temperature gradient model

In Nielsen's model [4], the normalised floor temperature (κ) is a function of the Archimedes number (Ar) and type of heat source. The Archimedes number is defined here as:

$$Ar = \frac{\beta \cdot g \cdot h_{ceil} \cdot (T_e - T_s)}{\left(\dot{V}_v / A_{fl}\right)^2} \tag{11}$$

Where β and g are respectively the volumetric expansion factor and the acceleration of gravity. The normalised floor temperature (κ) as a function of the Archimedes number for different types of heat sources is shown in Fig. 4.

Figure 4: The normalised floor temperature versus the Archimedes number for different types of heat sources (design chart adapted from Nielsen [4]), and the principles in Nielsen's vertical temperature gradient model.

The transmission loss (q_{tr}), the temperatures in the room (T_{ceil}, T_{fl}, T_{mean}, T_{occ}, T_{nocc}), the temperature gradient (dT/dz) and temperature effectiveness in the occupation zone (η_{occ}) are all calculated the same way as in Skistad's model (equations 2-9)

3. Empirical validation and inter-model comparison of the thermal models

In this section, the thermal models presented in the accompanying paper [1] are compared to experimental data sets, and the three simplified models presented in the preceding section.

3.1 Description of test cases

Empirical data sets for validation and comparison of the models have been taken from the literature on displacement ventilation. There exist a lot of experimental investigations on temperature stratification in displacement ventilated rooms. Many of them, however, ignore, or fail to report, important parameters that influence thermal stratification. The cases chosen for validation of the models have detailed temperature measurements and most of the data needed for prediction. But even here some of the input data for the model predictions has to be assumed. This will be discussed in more detail below.

Data sets for the empirical validation and inter-model comparison of the steady state thermal model have been taken from Mattson [5] (two offices and two classroom cases), Li et.al. [6,7] (two office cases) and Brohus & Nielsen [8] (one meeting room case). These rooms differ in size from 15 m² to 60 m² and in ceiling height from 2.5 m to 4.2 m. The heat load varies from 8 W/m² to 48 W/m², and the specific air flow rates are in the range : 1.38 l/sm² to 3.16 l/sm². This is fairly representative for rooms in office and educational buildings. Reliable data sets for larger rooms such as shopping centres, theatres and concert halls, have not been found. A description of the data sets used for testing the steady state thermal model is given in table 1.

Table 1: Description of the different test cases used in the validation and inter-model comparison of the steady state thermal model

Case no	Author(s)	Heat sources (total heat output/convective part heat output**/height to top heat source from floor/cross sectional dimension heat source)	Type of room	Air flow rate/ supply temp./ extract temp.	Tot. heat load/ Trans.heat loss	Floor area/ Ceiling height
1	Mattson	Thermal manikin (100 W/0.5/1.71 m/0.33 m), Cylind. person simulat. (100 W/0.5/1.2 m/0.26 m), PC-simulator (50 W/0.67/1.11 m/0.42 m), Ceiling light (145 W/0.3/2.2 m/0.1 m)	Office	20.9 l/s 16.4 °C 25.9 °C	395 W/ 152 W*	15.1 m²/ 2.5 m
2	Mattson	Thermal manikin (100 W/0.5/1.71 m/0.33 m), Cylind. person simulat. (100 W/0.5/1.2m/0.26 m), PC-simulator (50 W/0.67/1.11 m/0.42 m), Ceiling light (145 W/0.3/2.2 m/0.1 m)	Office	36.6 l/s 16.4 °C 23.6 °C	395 W/ 72 W*	15.1 m²/ 2.5 m
3	Li et.al.	Point heat source (300 W/0.9/0.4 m/ 0.35 m)	Office	23.1 l/s 19.2 °C 26.7 °C	300 W/ 88 W*	15.1 m²/ 2.75 m
4	Li et.al.	Point heat source (300 W/0.9/0.4 m/0.35 m)	Office	34.7 l/s 18.0 °C 24.8 °C	300 W/ 12 W*	15.1 m²/ 2.75 m
5	Brohus & Nielsen	Therrmal manikin (75 W/0.5/1.7 m/0.26 m), 2 cylind. person simul. (100 W/0.5/1.0 m/0.4 m), Point heat source (101 W/0.5/0.2 m/0.15 m)	Meeting room	80.6 l/s 17.6 °C 22.6 °C	376 W/ -117 W*	48 m²/ 4.0 m
6	Mattson	25 cylind. person simul. (95W/0.5/1.32 m/0.38 m), Ceiling light (525 W/0.3/2.5 m/0.1 m)	Class-room	191 l/s 14.5 °C 26.5 °C	2900 W/ 100 W*	60.5 m²/ 3.0 m
7	Mattson	25 cylind. person simul. (95W/0.5/1.32 m/0.38 m), Ceiling light (525 W/0.3/3.7 m/0.1 m)	Class-room	191 l/s 14.5 °C 26.5 °C	2900 W/ 100 W*	60.5 m²/ 4.2 m

* The transmission heat loss is calculated according to expression (3) in the preceding section. ** The convective part of the heat output from thermal manikins and person simulators is set at 50%,, as deduced by Mattson [5]. The PC simulators in the Mattson cases are made of aluminium (low emissivity) , and the convective part is estimated at 67%. The point sources in the cases of Li et.al. is reported to be designed to emit minimum radiation, and the convective part is set at 90%. The emissive properties for the point source in the case of Brohus & Nielsen are not given, and the convective part is estimated at 50%. The fluorescent ceiling light in the cases of Mattson presumably gives most of its heat output in the form of radiation, and the convective part is set at 30%.

In the accompanying paper [1], the authors have proposed two models for the vertical temperature gradient: one linear gradient model for rooms with few to normal number of heat sources/occupants (for example offices), and one non-linear gradient model for rooms with high occupancy/many heat sources (for example classrooms). Table 2 shows the model that has been used for the different cases. Table 2 also shows which curve in the design chart has been applied for Nielsen's model for the different cases, and lastly which value of the convective heat transfer coefficients has been used in Mundt's model.

Table 2:Temperature gradient model (linear or non-linear) used by the authors, curves used for Nielsen's model and radiation heat transfer coefficient used in Mundt's model.

Case no. :	1	2	3	4	5	6	7
Model used by the authors	Linear grad. model	Linear grad. model	Linear grad. model	Linear grad. model	Linear grad. model	Non-linear grad. model	Non-linear grad. model
Curve used in Nielsen's design chart	B (Sedentary persons)	B (Sedentary persons)	D (Point heat source)	D (Point heat source)	B (Sedentary persons)	B (Sedentary persons)	B (Sedentary persons)
Convective coefficient used in Mundt's model	4 W/m²K	4 W/m²K	4 W/m²K	4 W/m²K	4 W/m²K	4 W/m²K	4 W/m²K

Very few data sets for testing transient cases are reported in the literature, even if transient conditions are more likely than steady state conditions in a real room [1, 5]. The only reliable transient thermal case found is that of Mattson [5]. A description of this case is given in table 3.

Table 3: Description of the test case used in the empirical validation of the transient thermal model

Author	Heat sources (total heat output/convective part heat output/height to top heat source from floor/cross sectional dimension heat source)	Room type	Air flow rate/ supply temp./ Initial temp.	Heat capacity (wall/floor/ roof)	Tot. heat load/ U-values(walls/ floor/roof)	Floor area/ Ceiling height
Mattson	Cyl. person simul. (100 W/0.5/1.21 m/0.26 m), Ceiling light (145 W/0.3/2.2 m/0.1 m)	Office	20.9 l/s 16.9 °C 19.0 °C	2.4 Wh/m²K 12 Wh/m²K 4.4 Wh/m²K	245 W U_w = 0.5 W/m²K U_f = 0.4 W/m²K U_c = 0.2 W/m²K	15.1 m²/ 2.5 m

Comment: Based on reported surface temperatures in [5] the down draft air flow in the transient case has been estimated to be small (1 l/s).

3.2 Compared quantities and proposed tolerance

To compare the models with measurements and the other three simplified models, the following eight temperatures and temperature efficiency indices are computed for the steady state thermal models:

- T_{occ} - the temperature in the occupied zone. In all cases set to 1.2 meters above the floor, assuming seated activities
- T_{nocc} - the temperature in the non occupied zone (above 1.2 meters)
- η_{occ} - the temperature effectiveness in the occupation zone, as defined in the accompanying paper [1]
- T_{floor} - the air temperature at floor level (~10 cm above the floor)
- T_{ceil} - the air temperature near the ceiling (~10 cm below the ceiling)
- κ - the normalised floor temperature, as defined in the accompanying paper [1]
- dT/dz - the mean temperature gradient, defined as the difference between the temperature in the upper polluted zone and the temperature in the lower clean zone, divided by half the ceiling height.
- T_{mean} - the mean air temperature in the room.

The quantities above may have influence on the thermal comfort and energy use in a displacement ventilated room. To evaluate and compare the models, the following allowed tolerances for the different computed quantities are proposed:

- Temperature T: ± 1 °C
- Normalised floor temperature κ: ± 0.10
- Temperature effectiveness η_{occ}: ± 0.15
- Temperature gradient dT/dz: ± 0.25 K/m.

3.3 Results and discussion

In table 4 the linearized and by floor area normalised radiation heat transfer coefficient is shown, together with the calculated height of zone 1 and the estimated down draught air flow rate. The heat transfer coefficient and the height of zone 1 (clean zone) are calculated with models given in the accompanying paper [1]. The radiation coefficient is quite close to the "rule of thumb" value of 4 W/m²K, as proposed by the authors [1]. Table 4 also reveals that the radiation coefficient increases when the height of zone 1 is reduced, when the other variables are similar. The down draught air flow is estimated from reported surface temperatures, from U-values and temperatures in the surrounding air, or from reported smoke tests (visual tests). In most of the cases the down draught air flow is reported to be negligible (cases 1-4 and 6). In the meeting room case (case 5), the down draught air flow is considerable, as indicated by the reported concentration in and height of zone 1. Also in the classroom case (case 7) with the 4.2 m high ceiling, the down draught air flow is reported to be significant. In these two cases the down draught air flow is adjusted so the reported (measured) and calculated height of zone 1 are equal.

Table 4: By floor area normalised radiation heat transfer coefficient, height of zone 1, and estimated down draught air flow. Calculated with models from the accompanying paper [1]

Case no.	1	2	3	4	5	6	7
Normalised radiation heat transfer coefficient (W/m2K)	3.95	3.93	4.18	3.99	3.85	3.97	3.9
Height zone 1 (m)	0.94	1.29	0.51	0.71	1.36	0.88	0.95
Estimated down draught air flow (l/s)	1	1	0	0	20	1	19

Figure 5: Comparison of measured and predicted temperature in the occupation zone

Fig. 5 shows the measured and predicted mean air temperature in the occupation zone (1.2 m high). Our model predicts temperatures higher than those measured, but all are within the proposed tolerance (± 1 °C). The models of Skistad, Mundt and Nielsen are in all cases low compared to the measured temperatures. Mundt's model in particular predicts very low temperatures for the classroom cases. This can partly be explained by the fact that the gradient is very non-linear (steep in the lower part of the room) in the classrooms, while Mundt's model assumes a linear gradient. However, Nielsen's model also assumes a linear gradient but is much closer to the measured temperatures.

Figure 6: Comparison of measured and predicted temperature in the non-occupied zone

Fig. 6 shows the air temperature in the non-occupied zone. Our model predicts temperatures that are very close to the measured temperatures, and well within the proposed tolerance limit (± 1°C). The models by Skistad, Mundt and Nielsen all under-predict compared to the measured temperatures, for all the cases. The under-prediction is especially large for the classroom cases (cases 6 and 7).

Fig. 7 shows the floor air temperature (10 cm above the floor). Our model over-predicts for the office and meeting room cases (cases 1-5), but under-predicts for the classroom cases, but is for all cases within the proposed tolerance limit. Skistad's model is also within the tolerance limit in all cases. Mundt's model predicts well for the office and meeting room cases, but under-predicts for the classroom cases (6 and 7). Nielsen's model is within the tolerance for the office and meeting room cases, but over-predicts the floor temperature in the classroom cases (6 and 7).

Figure 7: Comparison of measured and predicted air temperature at floor level

Fig. 8 shows the measured and predicted ceiling air temperature (10 cm below the ceiling). Except for case 4 (office case) our model is within the tolerance limit. The models of Skistad, Mundt and Nielsen predict within the tolerance limit for all except cases 2 and 3 (office cases), where they under-predict the ceiling temperature. The models of Skistad, Mundt and Nielsen give the same value for all the cases, because the ceiling temperature is assumed to be equal to the extract temperature (given) for all three models. In the classroom cases (6 and 7), the non-linear gradient model used by the authors predicts equal to the three other models. This is due to the fact that the temperature in the upper zone (zone 2) is assumed constant, and therefore equal to the extract temperature (as the other models).

Figure 8: Comparison of measured and predicted air temperature at ceiling level

Fig. 9 shows the mean room air temperature. Our model is very close to the measured temperatures. The models of Skistad and Mundt under-predict the temperature in all cases, and only cases 4 and 5 (office and meeting room) are within the proposed tolerance. Nielsen' model also under-predicts the temperature, but only cases 3 and 7 are outside the tolerance limit.

Figure 9: Comparison of measured and predicted mean room air temperature

Fig. 10 shows the measured and predicted temperature effectiveness in the occupation zone (at 1.2 meters). Our model under-predicts the temperature effectiveness for cases 3 and 4 (office cases), but predicts within the limits (± 0.15) for the other cases. The models of Skistad, Mundt and Nielsen all over-predict the temperature effectiveness for all the cases. Mundt's model well over-predicts the temperature effectiveness for many of the cases. Nielsen's model also considerably over-predicts for cases 3 and 4 (offices), but is quite close for the classroom cases (6 and 7). The over-prediction of the temperature effectiveness for the models of Skistad, Mundt and Nielsen can be explained by the fact that these models under-predict the temperature in the occupation zone (see Fig. 5).

Figure 10: Comparison of measured and predicted temperature effectiveness in the occupied zone

Fig. 11 shows the normalised floor temperature. Our model under-predicts the normalised floor temperature in the office and meeting room cases (1-5), while it over-predicts for the classroom cases (6 and 7). However, the prediction lies within the proposed tolerance limits (± 0.1). Skistad's model predicts within the tolerance for all cases except the meeting room (case 5). Mundt's model predicts outside the tolerance for cases 5 and 7. Nielsen's model predicts within the tolerance for the office and meeting room cases (1-5), while it over-predicts the normalised floor temperature in the classroom cases (6 and 7). The measured normalised floor temperature for the classroom cases are surprisingly close to the 0.5 value for offices, as proposed by Skistad, while some of the office cases (1 and 4) and the meeting room case is a long way from 0.5

Figure11: Comparison of measured and predicted normalized floor temperature

Fig. 12 shows the measured and predicted mean temperature gradient. This value is calculated as the difference between the mean temperature in zone one and two, divided by half the ceiling height (see [1] for mathematical definition). Our model predicts close to the measured value for all except case 3 where it under-predicts the gradient. Skistad's model predicts the gradient poorly, and only case 5 (meeting room) is within the proposed tolerance (± 0.25 K/m). Mundt's model predicts the gradient acceptably for most cases, but under-predicts it considerably for cases 3 and 4 (offices). Nielsen's model strongly under-predicts the gradient for all cases except the meeting room case (case 5).

Figure 12: Comparison of measured and predicted mean temperature gradient

Figure 13: Percent prediction within the proposed tolerance for the steady state thermal models

Fig. 13 summarise the predictive ability of the steady state thermal models for all seven cases and for the eight compared quantities (total 56). Both Skistad's and Mundt's model predict approximately 50 % within the proposed tolerance limits, while Nielsen's model predicts somewhat better with 57 %. Our model predicts considerably better than the three other models, with 93 % of the predictions within the proposed tolerance limits. Although our model is more complex than the other three models, this can be defended by its superior predictive capability. The reasons for the rather low predictive capability of the other models can be:

- The ceiling temperature is not equal to the extract temperature (as assumed in the three models) due to the location of the extraction unit[2]
- The assumption of a linear vertical temperature gradient is not fulfilled in many cases, especially in cases with high occupancy (for example the classroom cases)
- The estimation of the floor temperature or the normalised floor temperature in these models is inaccurate, or not representative for many of the cases.
- The models of Skistad and Mundt does not take into consideration the convective air flow around heat sources, which strongly influence the mass and heat transfer in the room.
- Nielsen's model does indirectly take into consideration the convective transport for different heat sources, by having different curves for different heat source types, but the different curves do not always reflect the heat loads in real rooms, since they are often a mixture of ceiling light, sedentary persons and point heat sources (for example computers).

In Fig. 14 and 15, predictions with the transient thermal model presented in the accompanying paper [1] are compared to measured temperatures 1.2 meters above the floor and in the extract air. This case is described in table 3. Predicted and measured temperatures agree well, with a maximum difference of 0.6 °C between prediction and measurement. Even if the results are promising for the transient thermal model, it should be compared to more well documented transient experiments before conclusions on the validity of the model can be drawn.

Figure 14: Measured and predicted temperatures in the extract air, during a thermal step up experiment (ceiling light and a person simulator switched on at time: t = 0).

Figure 15: Measured and predicted air temperatures 1.2 meters above the floor, during a thermal step up experiment (ceiling light and a person simulator switched on at time: t = 0).

4. Empirical evaluation of the contaminant gradient model

In this section the contaminant gradient models presented in the accompanying paper [1] are applied and results are compared to experimental data found in the literature. The reason for using the phrase "evaluation" instead of "validation", is because some of the parameters in the contaminant model are adjusted to fit the measured concentration data, i.e. this is not a strict and independent comparison of the prediction and measurements, as implemented for the thermal models. The adjusted parameters are discussed below.

4.1 Description of test cases

A relatively large number of cases (14) have been taken from the literature to evaluate the contaminant models. These cases contain both steady state results (for example contaminant removal efficiencies) and/or transient results (air exchange efficiencies or age of air). However, for many of these cases there has only been reported a few results that can be compared to the output of the models presented.

Data sets for evaluation of the contaminant models have been taken from Mattson [5] (three office cases and two classroom cases), Heiselberg & Sandberg [9] (five office cases) and from Brohus & Nielsen [8] (four meeting room cases). The different cases are descried in table 5. In table 6, the compared quantities chosen to evaluate the contaminant models are shown together with cases that provided results for these outputs.

[2] Mundt has also proposed an extended model for cases where the extract is located below the ceiling level. This model also take into consideration heat conduction through the roof and the floor, but is considerably more complex than the simplified model used here (mathematically complex).

Table 5: Description of the test cases used in the evaluation of the contaminant model

Case no	First author	Heat sources (total heat output/convective part heat output**/height to top heat source from floor/cross sectional dimension heat source)	Type of room	Vent.air flow	Total heat load	Height occup. zone	Floor area/ Ceiling height
1	Mattson	Thermal manikin (100 W/0.5/1.71 m/0.33 m), PC-simulator (50 W/0.67/1.11 m/0.42 m), Ceiling light (145 W/0.3/2.2 m/0.1 m)	Office	20.9 l/s	295 W	1.7 m	15.1 m²/2.5 m
2	Mattson	Thermal manikin (100 W/0.5/1.71 m/0.33 m), Cylind. person simulat. (100 W/0.5/1.2 m/0.26 m), PC-simulator (50 W/0.67/1.11 m/0.42 m), Ceiling light (145 W/0.3/2.2 m/0.1 m)	Office	20.9 l/s	395 W	1.7 m	15.1 m²/2.5 m
3	Mattson	Thermal manikin (100 W/0.5/1.71 m/0.33 m), Cylind. person simulat. (100 W/0.5/1.2 m/0.26 m), PC-simulator (50 W/0.67/1.11 m/0.42 m), Ceiling light (145 W/0.3/2.2 m/0.1 m)	Office	36.6 l/s	395 W	1.7 m	15.1 m²/2.5 m
4	Heiselberg	Heated slender cylinder (600 W/0.89/2.5 m/0.1 m)	Office	10.6 l/s	600 W	1.8 m	15.1 m²/2.5 m
5	Heiselberg	Heated slender cylinder (600 W/0.89/2.5 m/0.1 m)	Office	21.1 l/s	600 W	1.8 m	15.1 m²/2.5 m
6	Heiselberg	Heated slender cylinder (600 W/0.89/2.5 m/0.1 m)	Office	31.4 l/s	600 W	1.8 m	15.1 m²/2.5 m
7	Heiselberg	Heated slender cylinder (600 W/0.89/2.5 m/0.1 m)	Office	41.9 l/s	600 W	1.8 m	15.1 m²/2.5 m
8	Heiselberg	Heated slender cylinder (600 W/0.89/2.5 m/0.1 m)	Office	52.5 l/s	600 W	1.8 m	15.1 m²/2.5 m
9	Brohus	Seated thermal manikin (75 W/0.5/1.2 m/0.35 m), 2 cylind. person simul. (100 W/0.5/1.0 m/0.4 m), Point heat source (500 W/0.5/0.2 m/0.15 m)	Meeting-room	40.3 l/s	771 W	1.8 m	48 m²/4.0 m
10	Brohus	Stand. therm. manikin (75 W/0.5/1.2 m/0.26 m), 2 cylind. person simul. (100 W/0.5/1.0 m/0.4 m), Point heat source (500 W/0.5/0.2 m/0.15 m)	Meeting-room	40.3 l/s	771 W	1.8 m	48 m²/4.0 m
11	Brohus	Seated thermal manikin (81 W/0.5/1.2 m/0.35 m), 2 cylind. person simul. (100 W/0.5/1.0 m/0.4 m), Point heat source (100 W/0.5/0.2 m/0.15 m)	Meeting-room	80.6 l/s	381 W	1.8 m	48 m²/4.0 m
12	Brohus	Stand. therm. manikin (81 W/0.5/1.2 m/0.26 m), 2 cylind. person simul. (100 W/0.5/1.0 m/0.4 m), Point heat source (100 W/0.5/0.2 m/0.15 m)	Meeting-room	80.6 l/s	381 W	1.8 m	48 m²/4.0 m
13	Mattson	25 cylind. person simul. (95W/0.5/1.32 m/0.38 m), Ceiling light (525 W/0.3/2.5 m/0.1 m)	Class-room	191 l/s	2900 W	1.2 m	60.5 m²/3.0 m
14	Mattson	25 cylind. person simul. (95W/0.5/1.32 m/0.38 m), Ceiling light (525 W/0.3/2.5 m/0.1 m)	Class-room	117 l/s	2900 W	1.2 m	60.5 m²/3.0 m

COMMENT: In the cases of Heiselberg & Sandberg (cases 4-8), the convective air flow rates around the heated cylinder are measured and not calculated values. For all other cases the convective air flow induced by heat sources are calculated by models given in the accompanying paper [1].

Table 6: Compared quantities for the contaminant models, and the cases with which they are compared.

Compared quantities	Cases that have reported these quantities
Height zone 1 (clean zone) (m)	1 – 13
Contaminant removal efficiency complete room	1 – 8, 13
Contaminant removal efficiency occupation zone	1 – 12
Contaminant removal efficiency inhalation zone, seated person	2, 3, 9, 11, 13
Contaminant removal efficiency inhalation zone, standing person	1, 2, 3, 10, 12
Air exchange efficiency complete room	1, 2, 3, 13, 14
Air exchange efficiency inhalation zone	1, 12, 14
Effectiveness of entrainment, seated person	1, 2, 3, 9, 11, 13
Effectiveness of entrainment, standing person	2, 3, 10, 12

4.2 Results and discussion

Table 7 shows the estimated convective factor and the estimated down draught air flow for all the cases. The convective factor is the part of the pollution generated around heat sources following the plume (the convective air flow) above the sources into zone 2. A convective factor of 1.0 means that all the contaminants are transported into zone 2. The convective factor, as shown in table 7, has been adjusted to give the best prediction of the concentration in zone 1 and 2. The convective factor is close to 1.0 for many of the cases, the lowest value is 0.8 for cases 11 and 12 (meeting room cases). This means that most of the generated contaminants in the occupation zone are transported into the polluted zone (zone 2). The down draught air flow rate in table 7 is estimated from reported surface temperatures, U-values and temperatures in the surrounding air (surrounding the test room), or from reported smoke tests (visual tests). In most of the cases the down draught air flow is reported to be negligible (cases 1-8, 13 and 14). In the meeting room cases of Brohus & Nielsen, the down draught air flow is considerable, as the reported concentration in zone 1 and the height of zone 1 indicate. In these cases the down draught air flow is adjusted to fit the reported height of zone 1.

Table 7: The estimated convective factor (part of the pollution following the plume into zone 2), and the estimated down draught air flow rate for the different cases.

Case no. :	1	2	3	4	5	6	7	8	9	10	11	12	13	14
Convective factor	0.90	0.90	0.90	1.00	1.00	1.00	0.95	0.85	0.90	0.90	0.80	0.80	0.90	0.90
Estimated down draught	1 l/s	1 l/s	1 l/s	3 l/s	3 l/s	1 l/s	1 l/s	0 l/s	28 l/s	28 l/s	25 l/s	20 l/s	1 l/s	1 l/s

Figure 16: Comparison of predicted and measured height of zone 1

Fig. 16 shows the height of zone 1 (the clean zone), also called the stratification height or the height of the stationary front. The height of zone 1 is entirely determined from the ventilation air flow, the calculated convective air flow, and the estimated down draught air flow. Higher ventilation air flow or down draught air flow raises the height of zone 1, while higher convective air flows induced by heat sources lower the height of zone 1. The measured height of zone 1 is defined as the height where the concentration is 50% of the concentration in the extract, as proposed by Heiselberg & Sandberg [9]. The predicted and measured heights of zone 1 seem to follow each other for the different cases quite well. Only in case 2 (the office case of Mattson [5]) is there a significant under-prediction. But in this case the measured height of zone 1 is uncertain due to few measuring points for the concentration (based on a linear interpolation), and could in reality be much closer to the predicted value. Except for the meeting room cases (9-12) discussed above, the calculated (predicted) height of zone 1 is primarily a function of the calculated convective air flows around and above the heat sources in zone 1. Given the good prediction of the height of zone 1 it is fair to assume that the models of the convective air flow presented in the accompanying paper [1] give acceptable results.

Figure 17: Comparison of predicted and measured contaminated removal efficiency for the complete room

Fig. 17 shows the contaminant removal efficiency for the complete room. This index shows the ability of the ventilation systems to remove contaminants from all points in the room under steady state conditions. For the mathematical definition see [1]. The measurements and predictions are close for all the compared cases.

Fig. 18 shows the contaminant removal efficiency for the occupation zone. This index shows the ability of the ventilation systems to remove contaminants from the occupation zone, for definition see [1]. The height of the occupation zone for the different cases is given in table 5. The predicted efficiency is very close to the measured value in all cases.

Figure 18: Comparison of predicted and measured contaminant removal efficiency in the occupation zone

Figure 19: Comparison of predicted and measured contaminant removal efficiency in the inhalation zone, seated persons

Fig. 19 shows the contaminant removal efficiency in the inhalation zone for the cases with seated persons (persons simulators). This efficiency shows the ventilation systems ability to provide clean air to the occupants. A high efficiency value means that the concentration to which the occupant is exposed is low compared to the concentration in the extract (see [1] for a definition of the efficiency). The figure shows that the model under-predicts the measured efficiency, especially for case 3 (office case). In case 3 the air in the inhalation zone is almost as clean as the supply air, which implies that the air in the boundary layer around the person is entrained from the clean air layer at floor level. In our model [1], which on this point is similar to the model proposed by Brohus & Nielsen [8], it is assumed that the air in the human boundary layer is entrained evenly from all heights up to the height of the inhalation zone. Cases 9, 11 and 13 in Fig. 18, seems to correspond well to this assumption, but also in case 2 (office case) the air in the inhalation zone is substantially better than predicted by the model. However, the model gives in all cases a conservative estimate of the air quality in the inhalation zone. If the contaminant removal efficiency in the inhalation zone is to be used for determining the necessary air flow rates, as proposed in the accompanying paper [1], it is preferable that the model under-predicts the efficiency (conservative).

Fig. 20 shows the contaminant removal efficiency in the inhalation zone for standing persons. Compared to seated persons, the inhalation zone for standing persons is often located high into the polluted zone (zone 2), and one would expect that the efficiency was lower in these cases. This holds true for cases 2 and 3, where both the efficiency for seated and standing persons are measured. The efficiency for the seated persons are much higher than for the standing persons. The model under-predicts the efficiency substantially for cases 1 and 3, but predicts quite closely for the other cases (2, 10, 12). The reason for under-prediction in cases 1 and 3, could be

due to the fact that zone 1 is relatively high in these cases, and that the human boundary layer is therefore entraining air to the inhalation zone mostly from the clean zone (zone 1).

Figure 20: Comparison of predicted and measured contaminant removal efficiency in the inhalation zone, standing persons

Figure 21: Comparison of predicted and measured air exchange efficiency in the complete room

Fig. 21 shows the air exchange efficiency for the complete room. The model prediction of the air exchange efficiency is predicted with the transient (time dependent) contaminant stratification model presented in the accompanying paper [1], since the air exchange efficiency is measured with a time dependent experiment (often a step down experiment, see for example Mattson [5]). The predictions and measurements are in good concordance for all cases. As seen, the air exchange efficiency does not vary much for the different cases. In our opinion, it is therefore a poor indication of the effectiveness of a ventilation system in a room. A better indication of how effective the ventilation system is in providing clean air to the occupants, is the air exchange efficiency in the occupation zone or in the inhalation zone.

Fig. 22 shows the air exchange efficiency in the inhalation zone (zone of exposure). Case 1 (office case) involves a standing person, while cases 13 and 14 (classroom cases) have seated persons. As for the contaminant removal efficiency in the inhalation zone, the model under-predicts the efficiency, but the under-prediction is more moderate here. The under-prediction is larger for the seated persons, compared to the standing persons. The under-prediction means that the air to which the occupants are exposed is "younger" than the model predicts.

Figure 22: Comparison of predicted and measured air exchange efficiency in the inhalation zone

Fig. 23 shows the effectiveness of entrainment in the human boundary layer for cases with seated persons. This index, proposed by Brohus & Nielsen [8], measures the ability of the human boundary layer to entrain (supposedly) clean air from the floor level to the inhalation zone (height of exposure). An effectiveness of 1.0 means that all the air in the inhalation zone is entrained from the clean air layer at floor level (see [1] for definition). The model prediction corresponds well with the measured effectiveness, for all the cases. In case 11 (meeting room case), the effectiveness is even better than 1.0, which means that the air quality in the inhalation zone is even better than the air quality in the clean air level at floor level.

Figure 23: Comparison of predicted and measured effectiveness of entrainment, seated persons

Figure 24: Comparison of predicted and measured effectiveness of entrainment, standing persons

Fig. 24 shows the effectiveness of entrainment for standing persons. The predictions in these cases are also acceptable. As one would expect, the effectiveness is lower for standing persons, compared to seated persons.

5. Conclusions

The following conclusions can be drawn from the experimental validation and from the inter-model comparison of the steady state thermal model:

- The model presented by the authors is predicting well for all the seven cases and for the eight compared quantities. The validity of the steady state thermal model can therefore be regarded as good for rooms similar to those tested here (small to medium large rooms).
- Use of the linear temperature gradient assumption for office and "meeting" room cases, and use of the non-linear temperature gradient assumption for the classroom cases give the best results.
- The predictions of our steady state thermal model are closer to the experimental data than the predictions using the models of Skistad , Mundt and Nielsen. However, our model is slightly more complex than the three other models, but can (in the authors opinion) be defended by its superior predictive capability.

The transient thermal model proposed by the authors [1] is in excellent concordance with experimental data. However, the model should be compared to additional transient cases before a conclusion can be drawn about the validity of the model.

The evaluation of the two contaminant models (steady state and transient) is very promising for most of the variables compared. However, predicted values for indices measuring air quality in the inhalation zone under-predict the experimental results. This under-prediction is, however, conservative if the models are to be used for determining necessary ventilation air flow rates. The convective factor (see sub-section 4.2), which is an important factor in the contaminant models, seems to fit the experimental data (concentrations) best with a value of 0.9.

6. Nomenclature

A	Area (m^2)
Ar	Archimedes number (-)
C	Volumetric heat capacity (Wh/m^3K)
g	Acceleration of gravity (m/s^2)
h	Height (m)
q	Heat flow (W)
T	Temperature (°C)
$\dot{V}$	Air flow rate (l/s or m^3/h)
z	Vertical space coordinate (m)

Greek letters

α	Radiation or convective heat transfer coefficient (W/m^2K)
β	Volume expansion coefficient (1/K)
η	Effectiveness
κ	Normalised floor temperature

Subscript

air	Air (heat capacity)
c	Convective
ceil	Ceiling
e	Extract
fl	Floor
nocc	Non-occupation zone
occ	Occupation zone
r	Radiation
s	Supply
tr	Transmission
v	Ventilation

Acknowledgement

This work has been financially supported by the Norwegian Research Council, Project no. 111372\330.

References

[1] Dokka T.H., Tjelflaat P.O, "Simplified models for prediction of vertical contaminant and temperature stratification in displacement ventilated rooms. Part 2 : Derivation". To be published in Energy & Buildings.

[2] Skistad H., "Displacement ventilation", Research Studies Press Ltd, John Wiley & Sons inc., 1994.

[3] Elisabeth Mundt, "The performance of displacement ventilation systems; Experimental and Theoretical studies", Ph.D.thesis, Royal Institute of Technology, Stockholm 1996.

[4] Nielsen P.V., "Temperature distribution in a displacement ventilated room" Proc. ROOMVENT '96, Yokohama, Japan, 1996.

[5] Mattson M.; "On the efficiency of displacement ventilation", Ph.D. thesis, Royal Institute of Technology, Gavle, Sweden 1999.

[6] Li Y., Sandberg M., Fuchs L., "Vertical temperature profiles in Rooms Ventilated by Displacement: Full-Scale Measurement and Nodal Modelling. Indoor Air, 2, 225 – 243 (1992)

[7] Li Y., Sandberg M., Fuchs L., "Effects of thermal radiation on airflow with displacement ventilation: an experimental investigation". Energy and Buildings, 19 (1993) pp. 263 – 274. 1993

[8] Brohus H., Nielsen P.V., " Personal Exposure in Displacement Ventilated Rooms", Indoor Air 6/96, pp. 157-167. Munksgaard 1996.

[9] Heiselberg P., Sandberg M., "Convection from a slender cylinder in a ventilated room", Proceedings Roomvent '90, Oslo Norway. 1990.

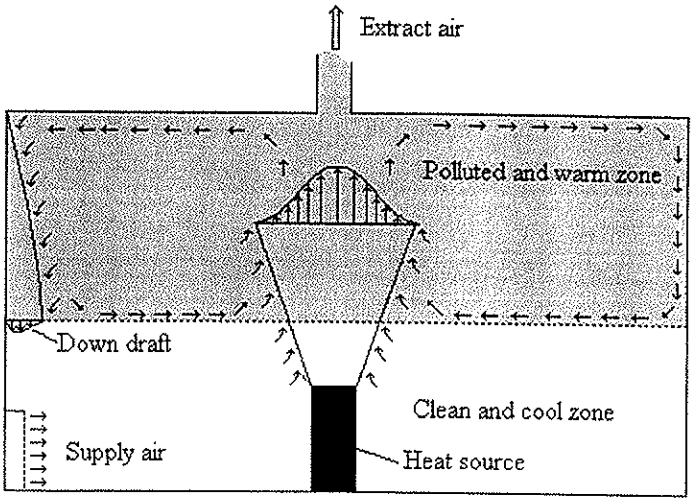

Figure 1: The working principles in displacement ventilation

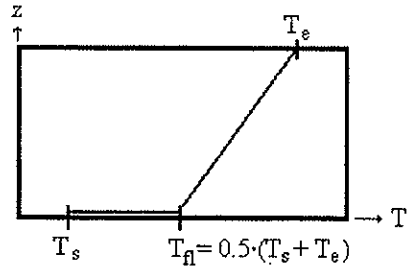

Figure 2: The principles in Skistad's "rule of thumb" model.

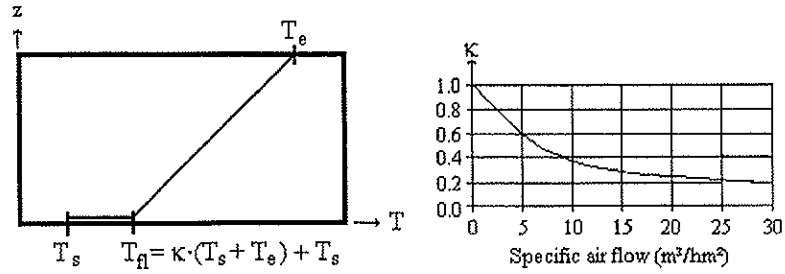

Figure 3: The vertical temperature gradient model of Mundt [3], and the normalised floor temperature as a function of the specific air flow.

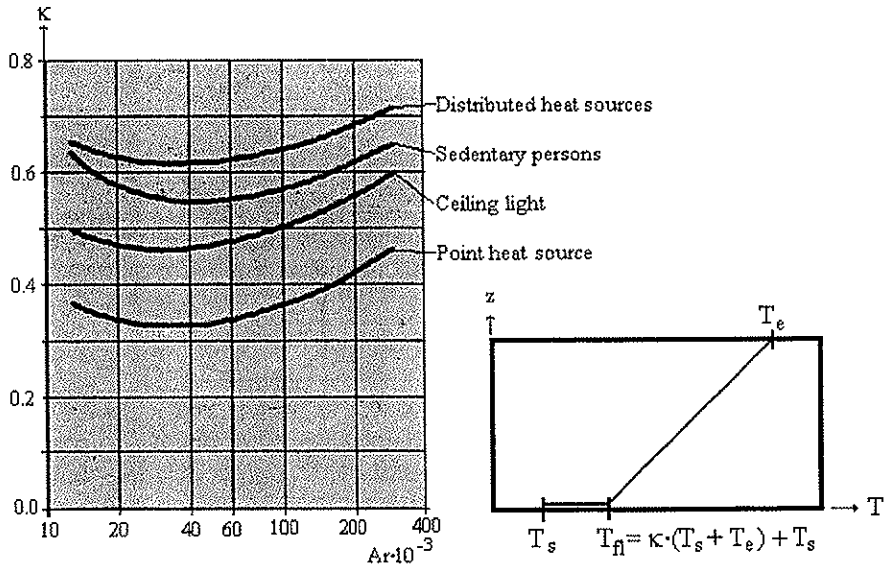

Figure 4: The normalised floor temperature versus the Archimedes number for different types of heat sources (design chart adapted from Nielsen [4]), and the principles in Nielsen's vertical temperature gradient model.

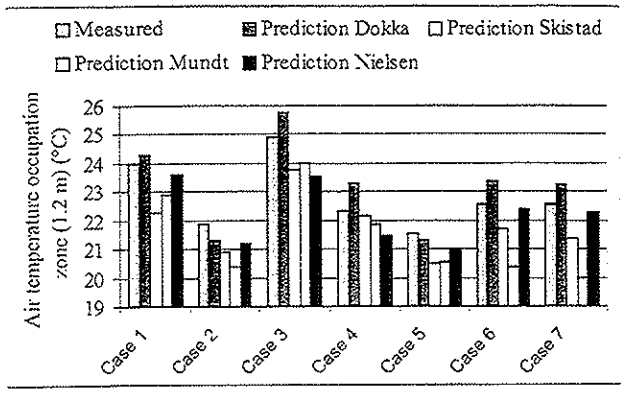

Figure 5: Comparison of measured and predicted temperature in the occupation zone

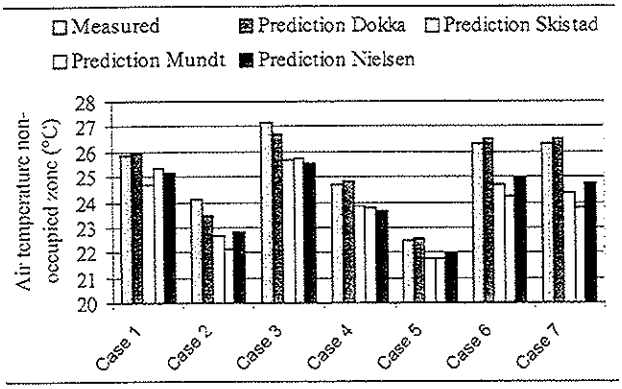

Figure 6: Comparison of measured and predicted temperature in the non-occupied zone

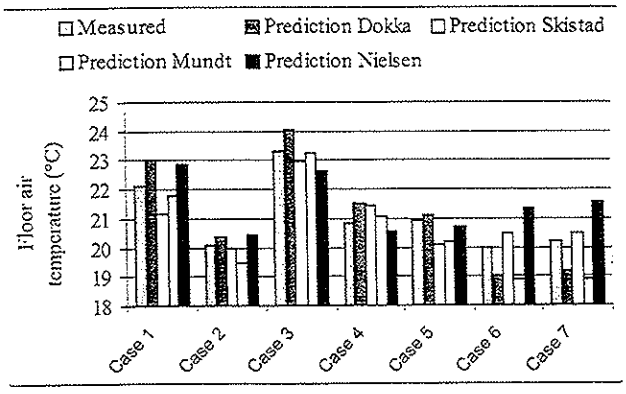

Figure 7: Comparison of measured and predicted air temperature at floor level

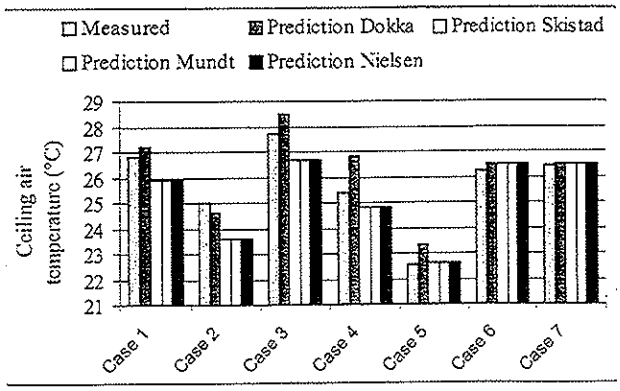

Figure 8: Comparison of measured and predicted air temperature at ceiling level

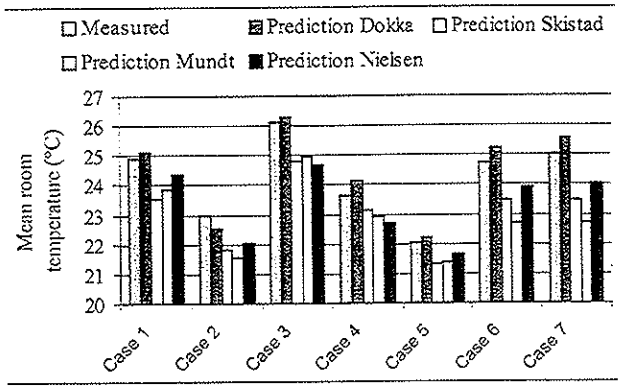

Figure 9: Comparison of measured and predicted mean room air temperature

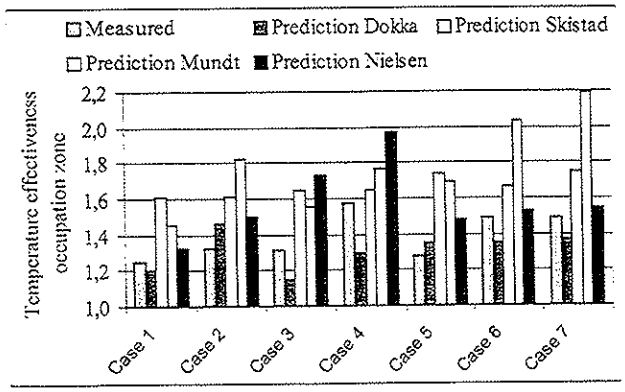

Figure 10: Comparison of measured and predicted temperature effectiveness in the occupied zone

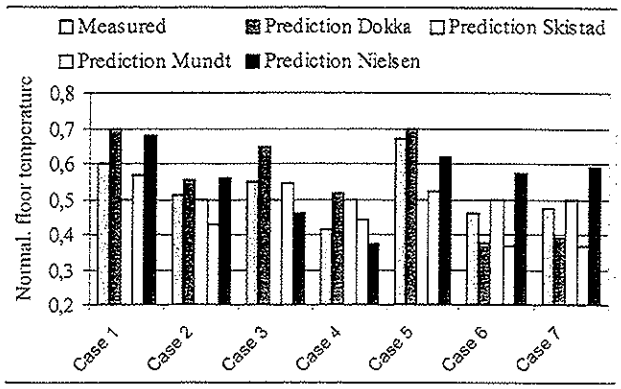

Figure11: Comparison of measured and predicted normalized floor temperature

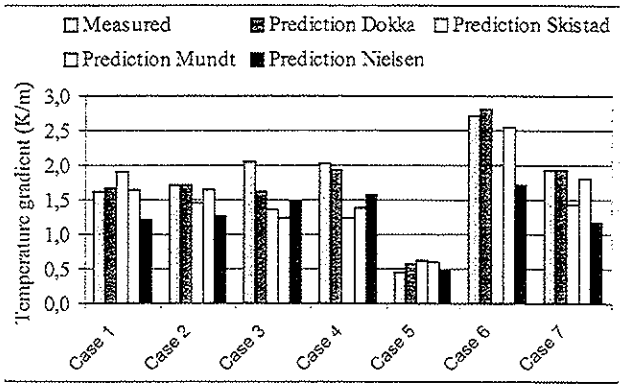

Figure 12: Comparison of measured and predicted mean temperature gradient

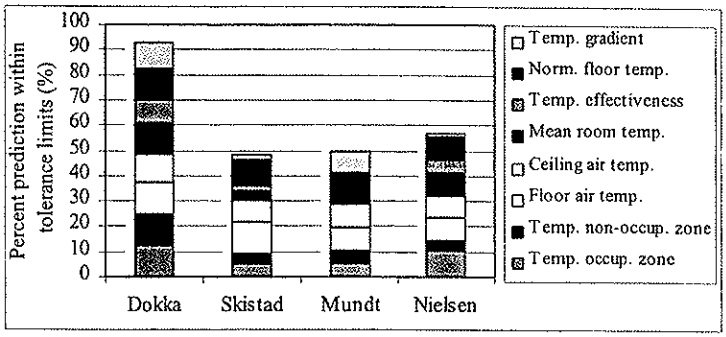

Figure 13: Percent prediction within the proposed tolerance for the steady state thermal models

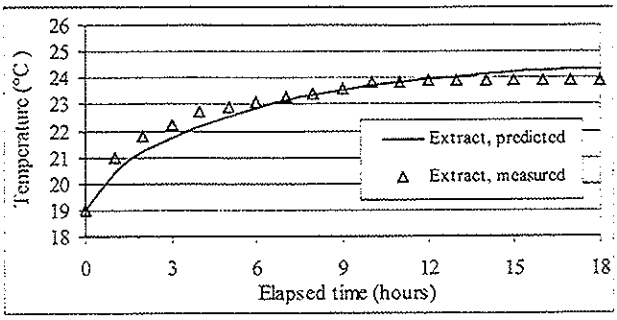

Figure 14: Measured and predicted temperatures in the extract air, during a thermal step up experiment (ceiling light and a person simulator switched on at time: t = 0).

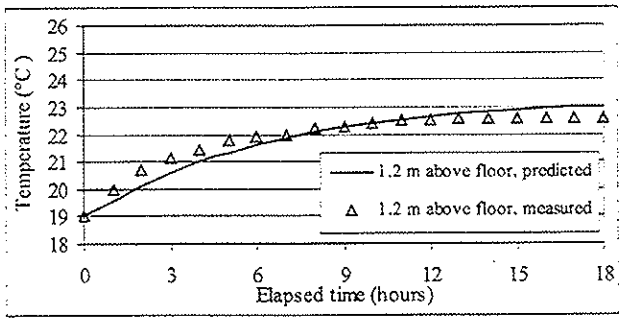

Figure 15: Measured and predicted air temperatures 1.2 meters above the floor, during a thermal step up experiment (ceiling light and a person simulator switched on at time: t = 0).

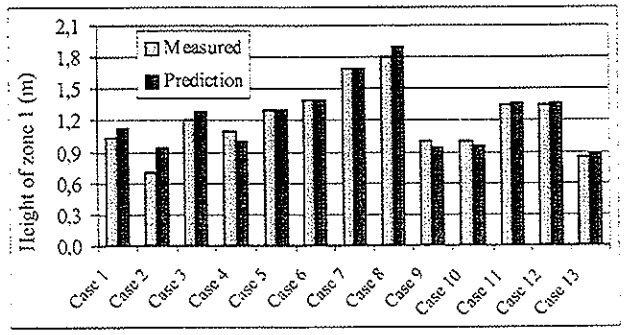

Figure 16: Comparison of predicted and measured height of zone 1

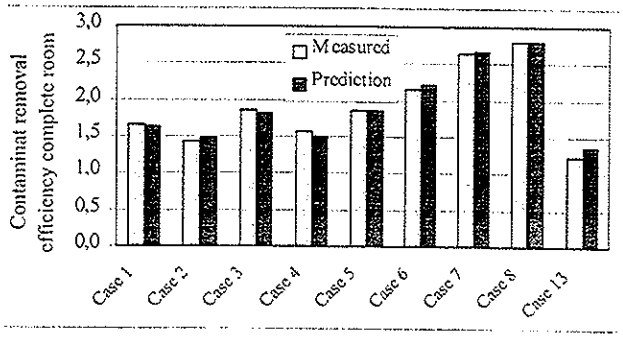

Figure 17: Comparison of predicted and measured contaminated removal efficiency for the complete room

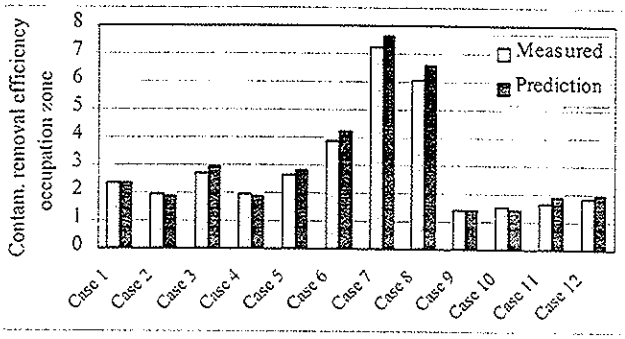

Figure 18: Comparison of predicted and measured contaminant removal efficiency in the occupation zone

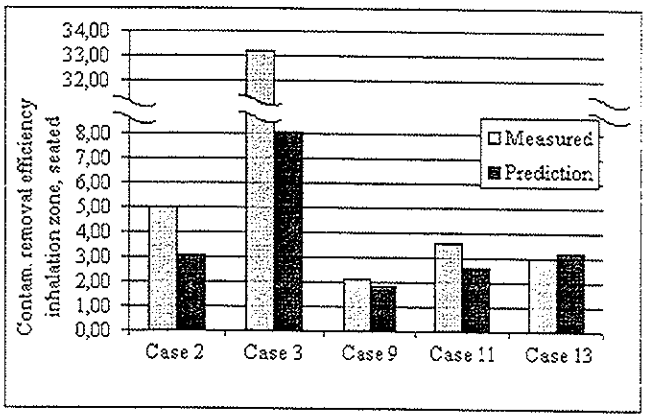

Figure 19: Comparison of predicted and measured contaminant removal efficiency in the inhalation zone, seated persons

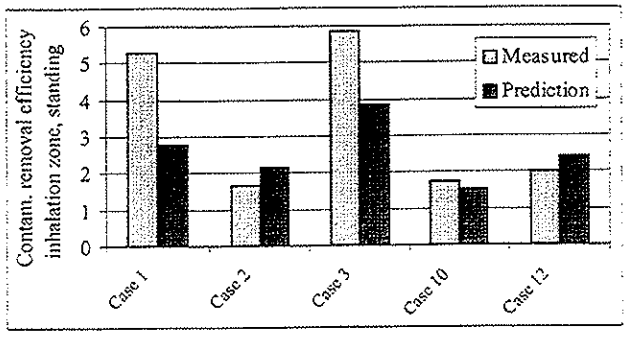

Figure 20: Comparison of predicted and measured contaminant removal efficiency in the inhalation zone, standing persons

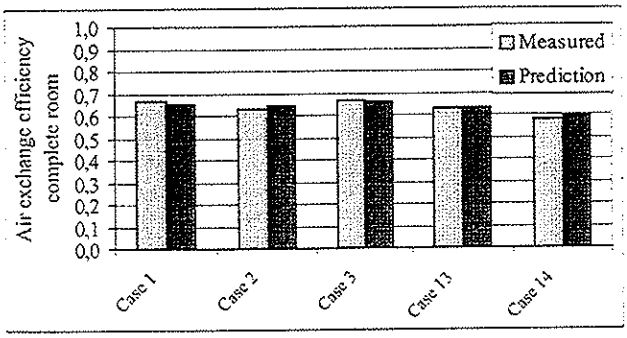

Figure 21: Comparison of predicted and measured air exchange efficiency in the complete room

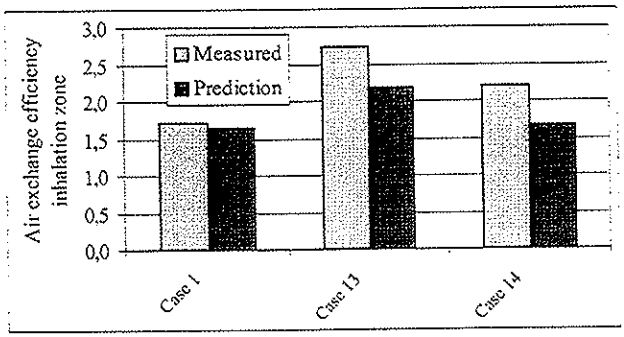

Figure 22: Comparison of predicted and measured air exchange efficiency in the inhalation zone

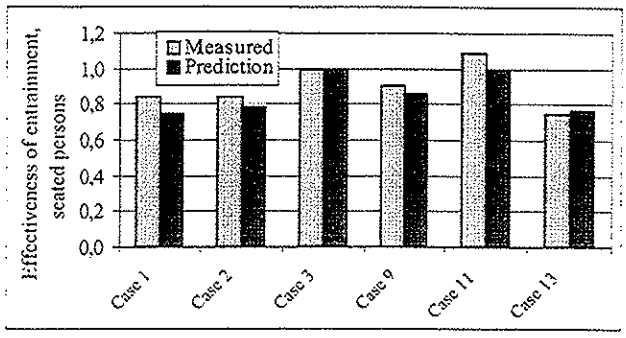

Figure 23: Comparison of predicted and measured effectiveness of entrainment, seated persons

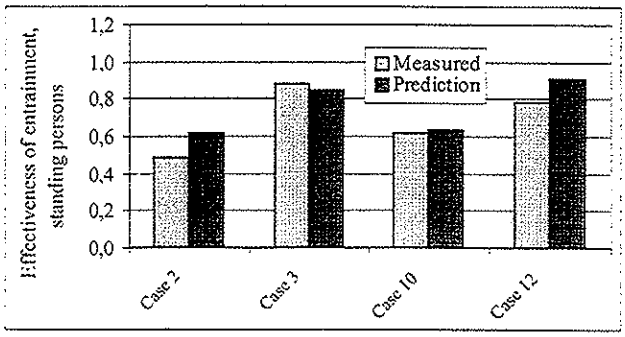

Figure 24: Comparison of predicted and measured effectiveness of entrainment, standing persons